THE EFFECT OF SIMULATED GASTRIC FLUID, SMECTITE LAYER CHARGE AND BENTONITE CHARACTERISTICS ON AFLATOXIN ADSORPTION

A Dissertation

by

ANA LUISA BARRIENTOS VELAZQUEZ

Submitted to the Office of Graduate and Professional Studies of
Texas A&M University
in partial fulfillment of the requirements for the degree of

DOCTOR OF PHILOSOPHY

Chair of Committee,	Youjun Deng
Co-Chair of Committee,	Joe B. Dixon
Committee Members,	Christopher A. Bailey
	Timothy Phillips
	Brandon Lafferty
Head of Department,	David Baltensperger

December 2015

Major Subject: Soil Science

ABSTRACT

Aflatoxins are toxic secondary fungal metabolites that are present in a variety of crops. Numerous animal experiments have demonstrated the effectiveness of smectite clay in adsorbing aflatoxin and in reducing the toxicity of the aflatoxin to animals, yet a 100% recovery from toxicity has not been achieved. The incomplete protection from toxicity can be due to competition of nutrients with aflatoxin molecules for adsorption sites in smectite. Furthermore, many physical and chemical properties of the smectite samples can affect the adsorption of aflatoxin. The present study was divided in three sections: 1) To address the effect of pH, proteins and vitamins present in simulated gastric fluid on the aflatoxin adsorption capacity by smectites. Aflatoxin adsorption isotherms were performed in water and simulated gastric fluid for smectites saturated with Na, Ca and Ba. The interaction of smectite and vitamins (B1, D and E) was also analyzed using adsorption isotherms. Both pepsin and vitamin B1 competed with aflatoxin molecules for adsorption sites on smectite. In the interlayer space of smectite, large molecules such as pepsin can block the hydrophobic sites required for aflatoxin adsorption. Vitamin B1 was absorbed in the interlayer space of smectite, too. Vitamin B1 competed with pepsin for adsorption sites, and it enhanced the adsorption of aflatoxin by increasing the accessibility to the hydrophobic domains on smectite surface. 2) To determine the effects of the layer charge origin and octahedral cations on the selectivity and adsorption capacity for aflatoxin. Six smectite samples with different layer charge density and octahedral cation composition were evaluated for aflatoxin adsorption. Adsorption and binding affinity for aflatoxin of high charge density smectites was improved by reducing the layer charge density. Octahedral charged smectites increased the interlayer accessibil-

ity of aflatoxin molecules. The octahedral cation composition had a negligible effect on the aflatoxin adsorption capacity of smectites. 3) To analyze the mineralogical properties of natural Texas bentonites for the selection of aflatoxin binders. Bentonite and partially altered volcanic ash samples were collected from six locations and characterized with XRD, FTIR, SEM and TEM. All the samples contained montmorillonite as the dominant clay mineral. The major mineralogical differences were in the sand and silt composition. The octahedral structural composition indicated some isomorphic substitutions of Al by Mg, indicating a high layer charge density in some montmorillonite samples that may reduce the aflatoxin adsorption effectiveness. The presence of octahedral Fe in some montmorillonite samples has negligible effect on their aflatoxin adsorption. The majority of the Texas bentonites samples collected are potentially good aflatoxin adsorbents due to high dioctahedral charge origin smectite and moderate content of Mg in the octahedral sheet.

DEDICATION

To my mom Dolores, dad J. Miguel, and brother Miguel for their love and encouragement.

To Luke, for his patience and understanding.

ACKNOWLEDGEMENTS

My sincere gratitude and respect to my advisor Dr. Youjun Deng for the support, encouragement, and patience during my doctorate research. His enthusiasm for research was always a motivation. His guidance during research and writing was very important for the completion of this work.

My deepest gratitude to Dr. Joe B. Dixon for giving me the opportunity to work with him and for supporting the beginning of my graduate education.

My sincere thanks also to my graduate committee: Dr. Timothy Phillips, Dr. Christopher Bailey, and Dr. Brandon Lafferty for their helpful comments.

Thank you to BYK additives (former Southern Clay Products) for allowed us to collect the bentonite samples, and in particular many thanks to geologist Charlie Smith for the numerous trips to the bentonite pits.

Thank you to Dr. Thomas Yancey for his helpful comments and suggestions on the mineralogical study of the bentonite deposits.

Special thanks to the Texas Corn Producers Board, Aflatoxin Mitigation Center of Excellence and TAMU-CONACYT for the financial support of the aflatoxin research.

Many thanks to Stacy Arteaga and Stephanie Oliver for their help while working as student workers in our lab. I also want to thank all the Soil Mineralogy Lab colleagues I met during grad school for their help and friendship.

TABLE OF CONTENTS

Page

LIST OF FIGURES

FIGURE Page

LIST OF TABLES

TABLE Page

1. INTRODUCTION AND LITERATURE REVIEW

1.1 Aflatoxins

A fatal disease that caused the death of about 100 000 turkeys in England in 1960 along with other mortality cases reported in dogs, guinea pigs, swine and cattle was denominated as Turkey X disease (Heathcote and Hibbert, 1978). The common pathological effect in all animals was liver damage. It was soon recognized that ingredients used in animal feed such as corn, peanut and other grains and nuts were contaminated with fungi *Aspergillus flavus*. A toxic blue fluorescent organic compound was extracted from contaminated peanut meal and designated as aflatoxin B1. Fungi *Aspergillus flavus* and *Aspergullis parasiticus* produce aflatoxins as secondary metabolites. The first identified compounds and the most commonly found in contaminated crops are aflatoxin B1 (AfB1) and aflatoxin G1 (AfG1) (Figure 1.1), and AfB1 is the most toxic and carcinogenic. In the aflatoxin group, up to 20 compounds have been identified. The chemical structures of aflatoxins are composed of difurocoumarins with some having a cyclopentenone end such as in AfB1 and others having a lactone ring such as in AfG1 (Bbosa et al., 2013).

The International Agency for Research on Cancer (IARC) has classified aflatoxins as potent human carcinogens (IARC, 2002). Once ingested, aflatoxin molecules are absorbed and metabolized through different pathways producing several metabolites. The AfB1-8,9-epoxide is the active metabolite capable of binding DNA (Eaton et al., 1994). Exposure to aflatoxin can also occur by the presence of intermediate products of metabolic reactions in animal products such ash the common occurrence of aflatoxin M1 in milk. The U.S Food and Drug Administration (FDA) has set regulatory levels to reduce aflatoxin exposure. In corn directed to human consumption, the

action level is less than 20 ppb, and 0.5 ppb is the maximum allowed concentration in milk. Corn containing aflatoxin concentrations between 20 to 300 ppb can be used as animal feed depending on animal and maturity, but even at these concentrations some negative effects have been observed. Feed intake was reduced in dairy cows in the presence of 10 ppb aflatoxin in feed (Iheshiulor et al., 2011), and there were significant reductions of plasma lysine and histidine in broiler chickens at a feeding concentration of 500 ppb aflatoxin (Maurice et al., 1983).

Since the discovery of aflatoxins, numerous animal experiments have demonstrated the toxic effects of this mycotoxin group to animals (Hendricks, 1994; Hussein and Brasel, 2001). In broiler chickens, aflatoxicosis is characterized by an increase in the relative organ weight (Bailey et al., 1998), visible change in coloration of the livers (Phillips et al., 1988; Barrientos Velazquez, 2011), and histological changes in liver tissue (Magnoli et al., 2011b).

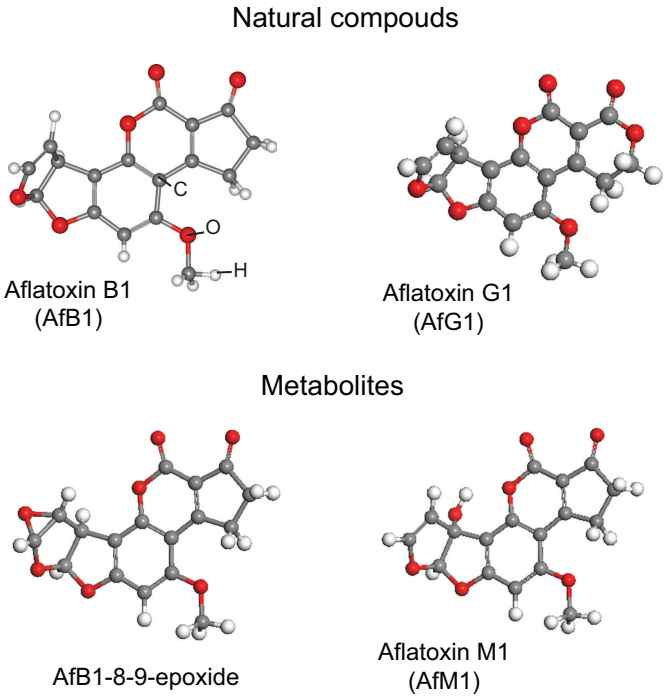

Figure 1.1: Structures of common natural aflatoxins and metabolites.

Several aflatoxin decontamination techniques have been developed to eliminate or to reduce the concentration of aflatoxins or to reduce the bioavailability of aflatoxins to animals. Among the aflatoxin decontamination techniques, incorporation of clays in animal diets is an economic and practical approach capable of reducing the bioavailability of the toxins. Several natural and man-made materials such as yeast, bentonite, modified clays, activated carbon and zeolites have been investigated as aflatoxin adsorbents (Huwig et al., 2001). Bentonite clays are the most effective and commonly used due to their high binding capacity and selectivity. Several in vitro studies have demonstrated the aflatoxin binding capacity of bentonites (Grant and Phillips, 1998; Kannewischer et al., 2006; Phillips et al., 1988, 1995; Vekiru et al., 2007). Numerous animal trials in ducks (Wan et al., 2013), broilers (Bailey et al.,

1998; Magnoli et al., 2008a,b; Pappas et al., 2014; Pasha et al., 2007; Pimpukdee et al., 2004; Rosa et al., 2001), rats (Abdel-Wahhab et al., 1999), and pigs (Lindemann et al., 1993; Shi et al., 2005; Thieu and Pettersson, 2008) had demonstrated the protective effect of smectite-type clays against aflatoxin toxicity. Animals fed an aflatoxin contaminated diet amended with bentonite showed higher weight gain than animals in the no-clay group. The incorporation of clay in the aflatoxin diet has also been shown to reduce the hepatic lesions in broilers (Vekiru et al., 2015). A recent study by Fowler et al. (2015) showed that adding 0.2% of bentonite significantly reduced the aflatoxin residues in the liver during the first week of aflatoxin exposure.

In addition to prevent aflatoxicosis in the gastrointestinal tract, recent studies have been focused on the use of binders to remove aflatoxins during food processing. Seifert et al. (2010) investigated the efficacy of a commercial bentonite to adsorb aflatoxins from peanut meal. The peanut oil extraction process does not remove or destroy aflatoxins, rather the toxins accumulate in the by-product. A commercial bentonite (Astra-Ben 20A) that had shown to be effective in preventing aflatoxicosis was used to remove aflatoxins during the protein extraction from peanut meal. Seifert et al. (2010) observed a significant reduction on the aflatoxin concentration in soluble and insoluble peanut meal fractions when 0.2% of bentonite was added. Approximately 70% of the initial aflatoxin was removed from the soluble fraction, and 51% removed from the insoluble fraction. There were no significant differences in the aflatoxin adsorption at pH2 and pH8. Aflatoxin adsorption was still significant after increasing the water soluble proteins in the corn meal by enzymatic hydrolysis with pepsin and Alcalase (Seifert et al., 2010).

1.2 Bentonites as adsorbents of aflatoxins

Bentonites are natural materials that are composed primarily of the clay mineral montmorillonite (Eisenhour and Brown, 2009). The special physical and chemical properties of bentonites such as expandability, surface area, and cation exchange capacity make them suitable for diverse industrial applications. Bentonites were used in ancient civilizations as cleaning agents and medical purposes. Nowadays the uses of bentonites extent as adsorbents (oils, animal waste, toxins, organic compounds), desiccants, sealants, drilling fluids, anticaking agents in animal feed, and many others (Eisenhour and Brown, 2009).

1.2.1 Smectite mineral group

Smectites are clay minerals with a 2:1 layered structure. Each smectite layer is formed by an octahedral sheet sandwiched between two tetrahedral sheets (Figure 1.2). In the smectite group, the most common minerals are montmorillonite, beidellite, hectorite, saponite, and nontronite. These phyllosilicate minerals are characterized by low layer charge (0.2 to 0.66 per half unit cell) (Reid-Soukup and Ulery, 2002), but differ from each other mainly on the cation composition of the tetrahedral and octahedral structural sheets (Table 1.1).

Montmorillonite, beidellite and nontronite are dioctahedral smectites meaning that two out of three sites in the octahedral sheet are occupied. In montmorillonite, Al^{3+} dominates the octahedral sites with some isomorphic substitutions from Fe^{3+} and Mg^{2+}. On the contrary, the octahedral sheet in beidellite is occupied mainly by Al^{3+} and in nontronite by Fe^{3+}. In trioctahedral smectites such as hectorite and saponite, Mg^{2+} is the dominant cation in the octahedral sheet. The main difference between hectorite and saponite is the occurrence of isomorphic substitution of Mg^{2+} by Li^{+} in hectorite. For those smectites with no isomorphic substitution in the

octahedral sheet, the negative charge arises from the substitutions of Al^{3+} for Si^{4+} in the tetrahedral sheet.

Table 1.1: Structural composition of smectites

Mineral	Ideal structural formula *
Beidellite	$(Na)_{0.5}(Al)_2[Si_{3.5},Al_{0.5}]O_{10}(OH)_2 \cdot nH_2O$
Hectorite	$(Na)_{0.3}(Mg,Li)_3[(Si,Al)_4O_{10}](OH)_2 \cdot nH_2O$
Montmorillonite	$(Na,Ca)_{0.33}(Al,Mg)_2[Si_4O_{10}](OH)_2 \cdot nH_2O$
Nontronite	$(Na)_{0.3}(Fe^{3+})_2[(Si,Al)_4O_{10}](OH)_2 \cdot nH_2O$
Saponite	$(Ca,Na)_{0.3}(Mg,Fe^{2+})_3[(Si,Al)_4O_{10}](OH)_2 \cdot nH_2O$

*Wilson (2013)

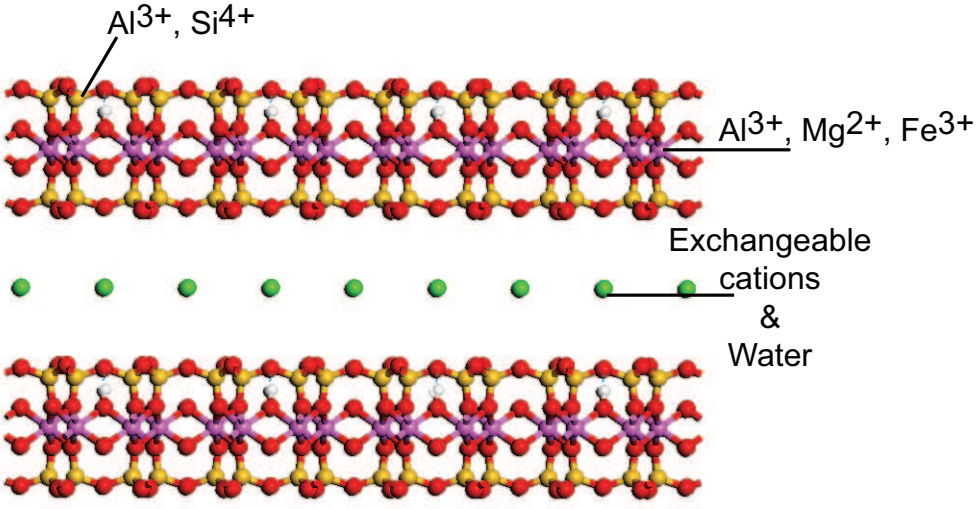

Figure 1.2: Dioctahedral smectite structural model showing the 2:1 layer structure.

1.3 Modification of smectites to enhance aflatoxin B1 adsorption

1.3.1 Exchangeable cations

The negative structural charge deficiency in smectites is originated from the isomorphic substitution in the octahedral or tetrahedral sheets, and the negative charge is compensated by exchange cations in the interlayer. Most bentonites occur naturally as Ca- or Na-saturated. The exchangeable cation can be replaced to modify the interlayer space.

An early study by Tomasevic-Canovic et al. (2001) showed the difference in the aflatoxin sequestration of Ca^{2+}, Co^{2+}, Zn^{2+}, and Cu^{2+}-saturated smectites. The single aflatoxin concentration adsorption showed higher chemisorption index for Co- and Zn-exchanged clays (0.93 and 0.90, respectively) in comparison to Ca- and Cu-exchanged clays (0.89 and 0.75, respectively). In the same study, Tomasevic-Canovic et al. (2001) investigated the potential of montmorillonite to adsorb essential micronutriens such as Cu, Co, Mn and Zn. The adsorption experiments demonstrated high retention of Cu and Co by the clays. The authors concluded that the high adsorption index observed in solution may reduce the bioavailability of these micronutrients. A similar study comparing the adsorption capacities of natural Ca-montmorillonite and Cu-exchanged montmorillonite was performed by Dakovic et al. (2008). Their results were in agreement with previous studies and demonstrated higher adsorption of aflatoxin by Cu-montmorillonite. Furthermore, aflatoxin adsorption was not pH dependent as similar adsorption was reached at pH 3, 7 and 9.

Later studies by Deng et al. (2010) demonstrated that the adsorption of a non-polar compound such as aflatoxin interacted with the interlayer cations. The exchangeable cation interacted with aflatoxin molecules by ion-dipole interaction with

the carbonyl oxygen under low humidity conditions, and H-bonding occurred between the hydration shell of the cation and the carbonyl groups at high moisture conditions. The aflatoxin adsorption experiments demonstrated that higher interaction occurs between cations with di- or -tri valences, small ionic radius, or vacant d-orbitals. The same research group later proposed that the adsorption of aflatoxin molecules can be enhanced by the presence of an interlayer cation with low hydration energy (Deng et al., 2012). Divalent cations having lower hydration energies allowed more of the non-polar sites on the basal surface of the smectite to be available for aflatoxin molecules.

A recent study by Dakovic et al. (2012) compared the aflatoxin adsorption of natural Ca-montmorillonite and Zn-exchanged montmorillonite. The aflatoxin adsorption isotherms showed an increase in AfB1 adsorption from 40.98 mg/g for Ca-montmorillonite to 60.17 mg/g for the Zn-montmorillonite (Dakovic et al., 2012). Zn-montmorillonite adsorbed more aflatoxin at low clay concentrations (0.1 and 0.5 mg) but no significant differences were observed when more than 1 mg of adsorbent was added to the solution. At high clay concentrations, almost a 100% aflatoxin removal was observed. The AfB1-montmorillonite complexes were very stable and desorption was not observed. To explain the influence of the exchangeable cation, quantum chemical calculations were performed for hydrated Ca, Mg, and Zn with aflatoxin B1 molecules. The interaction energy was the lowest for Ca (-62.91 kcal/mol) than for Zn and Mg (-70.19 and -68.84 kcal/mol). The calculations showed a stronger interaction between aflatoxin and hydrated Mg than between aflatoxin and hydrated Ca, but the experimental data by Deng et al. (2012) showed a higher adsorption capacity of Ca-smectite over Mg-smectite. The larger ionic radius of Ca bring less water to the interlayer of smectite allowing for more adsorption sites available for aflatoxin molecules. The highert binding energy of Zn over Ca was attributed to the

higher hydration energy and lower ionic radius of zinc ion. The slight difference in the interaction energy between Zn and Mg, despite the larger ionic radius of Zn, was attributed to the d-electrons.

1.3.2 Intercalation of organic compounds

The interlayer space of the smectite is the major adsorption site for aflatoxin molecules (Kannewischer et al., 2006; Phillips et al., 2008; Deng et al., 2010). Some have proposed modification of the interlayer space by increasing the expandability or replacing the exchangeable cations with organic ions to reduce the hydration and to increase the adsorption of aflatoxin. Shi et al. (2006) tested the in vitro and in vivo efficiency of a modified montmorillonite nanocomposite. In their experiments, the exchangeable cation of a natural montmorillonite was replaced with a polymer to promote expansion of the clay layers (Ishida et al., 2000). The aflatoxin adsorption isotherm for the nanocomposite showed a chemisorption index of 75.4%, suggesting potential to adsorb aflatoxin in vivo. In the animal trial, chickens fed an aflatoxin diet plus the nanocomposite clay showed body weight gain, feed/gain ratio statistically similar to the non-aflatoxin control group. Furthermore, no mortality was observed in this group while the mortality in the aflatoxin group was 2.5%. The montmorillonite nanocomposite was not toxic to the chickens as the parameters were similar in the no-aflatoxin plus nanocomposite and the control group.

Jaynes and Zartman (2011) tested the aflatoxin adsorption of surface modified montmorillonite with hexadecyltrimethylammonium (HDTMA), phenyltrimethylammonium (PTMA), choline and carnitine. The PTMA-montmorillonite significantly expanded the d-001 value to 1.48 nm and showed a higher aflatoxin adsorption than the non-treated montmorillonite. This organoclay is not suitable for animal use as the PTMA is highly toxic. The montmorillonite treated with choline and carnitine,

which are common nutrients, also showed an increase in aflatoxin adsorption.

1.3.3 Layer charge reduction

The adsorption of aflatoxin strongly depends on unoccupied non-polar sites on the smectite interlayer surface. The number of non-charged sites is determined by the structural charge of the clay. High-charge smectites had shown low aflatoxin adsorption (Deng et al., 2012). Jaynes and Zartman (2011) demonstrated that reducing the layer charge can significantly increase the aflatoxin adsorption capacity of clays.

1.3.4 Thermal treatment

One method to modify the specific surface area of smectites is by exposing the clays to high temperatures. Bojemueller et al. (2001) heated a montmorillonite sample at temperatures from 350 to 550 °C and observed that the adsorption of metolachlor (pesticide) was significantly increased as the calcination temperature was increased. Heating smectites produces structural changes and also alter the expandability. The high adsorption of pesticide by a calcinated smectite was attributed to the formation of mesopores among the collapsed smectite layer, and to the exposed structural Al at the edges. Grant and Phillips (1998) demonstrated that heating a montmorillonite clay up to 800°C significantly reduced the aflatoxin adsorption from 0.461 mol/kg (unheated clay) to 0.0567 mol/kg. Heating collapsed the interlayer space leaving only the external surface for AfB1 adsorption. In a recent experiment, Nones et al. (2015) also investigated the aflatoxin adsorption of a heated bentonite. They tested the effect of heating a bentonite at 125, 250, 500, 750, and 1000 °C on the aflatoxin adsorption in solution and the effectiveness in protecting neural crest (NC) stem cells. The aflatoxin adsorption was similar for the unheated bentonite and to the 125, 250 and 500 °C heated samples, but adsorption was significantly

reduced at higher temperatures as previously observed by Grant and Phillips (1998). Similarly, heated clays (up to 750°C) showed a protection effect on the number of NC stem cells. The low aflatoxin adsorption at high temperatures was due to collapse of the smectite layers. As the interaction between the interlayer cations and aflatoxin molecules is the main adsorption mechanism, preserving the interlayer seem critical for high adsorption capacity.

Several factors can affect the aflatoxin adsorption such as the complexity of the gastrointestinal fluids and the intrinsic properties of the smectite. Extensive studies had reported the adsorption capacity of aflatoxins by smectites in simplified solutions but the competition between proteins and vitamins in the gastrointestinal fluids with aflatoxin molecules for adsorption site on the smectite interlayer has not been fully addressed. Furthermore, an effective bentonite must offer accessibility of aflatoxin molecules to the interlayer space. As the swell/shrink properties of smectites are affected by charge density and charge origin, we expect that the charge origin might influence aflatoxin adsorption.

The present research had three major objectives: 1) to address the effect of pH, proteins and vitamins present in simulated gastric fluid on the aflatoxin adsorption capacity by smectites, 2) to determine the effects of the charge origin and octahedral cations on the selectivity and adsorption capacity for aflatoxin, and 3) To analyze the mineralogical properties of natural Texas bentonites for the selection of aflatoxin binders.

2. THE EFFECTS OF PH, PEPSIN, EXCHANGE CATION, AND VITAMINS ON AFLATOXIN ADSORPTION ON SMECTITE IN SIMULATED GASTRIC FLUIDS

2.1 Introduction

Aflatoxins are carcinogenic mycotoxins produced by fungi *Aspergillus flavus* and *Aspergillus parasiticus*. Among twenty aflatoxin compounds, aflatoxin B1 (AfB1) is the most toxic. The U.S Food and Drug Administration (FDA) has set regulatory levels on aflatoxin exposures. In corn directed for human consumption, the action level is less than 20 ppb. Corn containing aflatoxin concentrations between 20 to 300 ppb can be used as animal feed depending on animal species and maturity. Even with low concentrations of aflatoxin in feed, some adverse effects from aflatoxins have been observed: 1) feed intake was reduced in dairy cows in the presence of 10 ppb aflatoxin in feed (Iheshiulor et al., 2011), and 2) plasma metabolites (lysine and histidine) were significantly reduced in broiler chickens at a feeding concentration of 500 ppb aflatoxin (Maurice et al., 1983).

Adding bentonites to animal feed to inactivate aflatoxin has been extensively investigated (Lindemann et al., 1993; Phillips et al., 1995; Abdel-Wahhab et al., 1999; Rosa et al., 2001; Pimpukdee et al., 2004; Pasha et al., 2007; Magnoli et al., 2008a,b). Bentonites are commonly used as anti-caking agents in animal feed. Little or no adverse effects have been observed in animal performance with up to 3% of clay incorporation in the feed in some studies (EFSA, 2010, 2011). Numerous animal experiments have demonstrated the effectiveness of the clay in adsorbing aflatoxin and in reducing the toxicity of the aflatoxin to animals, yet a 100% toxicity recovery has not been reported in the literature. It is unclear why a full aflatoxicosis protec-

tion cannot be achieved even when relatively high doses of clays are incorporated in the diet. We speculated the following possible reasons for the low recovery 1) competition of nutrients with aflatoxin molecules for adsorbing sites on the smectite, and 2) inhomogeneous distribution of both bentonite and aflatoxin in the feed, which reduced the interaction opportunity between the clay and aflatoxin. The efficiency of a binding agent is usually quantified in vitro using adsorption isotherms, and the procedure is typically done in a simplified solution that may overestimate the binder's aflatoxin adsorption. In the gastrointestinal system, the adsorption can be affected by organic compounds, such as proteins and vitamins. The large pH variations and the presence of nutrients in animal digestive system must be considered in aflatoxin binding efficiency quantification.

2.1.1 Reduced efficiency of bentonite in detoxifying aflatoxin in the presence of biological molecules

In most of the reported studies, the efficiency of a binding agent was tested in simplified aqueous solutions, without considering the effect of biological molecules. The reactions between aflatoxin molecules and clay particles in the gastrointestinal tract should be more complex than most batch adsorption studies reported (Kannewischer et al., 2006). The adsorption of aflatoxin in buffer solutions, simulated gastric solutions, and real gastric fluids has been addressed in limited studies (Spotti et al., 2005; Vekiru et al., 2007; Thieu and Pettersson, 2008; Li et al., 2010; Magnoli et al., 2011a). Lemke et al. (2001) tested a bentonite clay and observed that about 100% aflatoxin binding was achieved in both water and simulated gastric fluid (GF). Spotti et al. (2005) observed that two tested bentonites could adsorb nearly 100% of added aflatoxin in ruminal fluid but only 60% of added aflatoxin in water. The greater adsorption in ruminal fluid was not explained. The high percentage of

aflatoxin adsorption in gastric and ruminal fluids observed in the experiments by Lemke et al. (2001) and Spotti et al. (2005) could be due to the high clay/aflatoxin ratios used in their experiments: 125 mg clay to adsorb 400 μg aflatoxin and 25 mg of clay to adsorb 0.08 μg aflatoxin respectively. In contrast, Magnoli et al. (2011a) showed that at low aflatoxin concentrations, the biological compounds in the ruminal fluid reduced the AfB1 adsorption substantially, resulting in a 74% reduction on the maximun aflatoxin adsorption capacity.

2.1.2 Potential factors in hindering aflatoxin adsorption by smectite

2.1.2.1 Low pH reduces aflatoxin adsorption by smectite

Thieu and Pettersson (2008) performed single concentration adsorption on a bentonite in a simulated gastric fluid, and observed a significant reduction on the aflatoxin binding capacity at low pH. In the simulated intestinal fluid with pH 7, up to 80% of the aflatoxin in solution was adsorbed. However only 30% of the initial aflatoxin was adsorbed when the pH was reduced to pH 3. In their experiments, no pepsin or other proteins were included in the simulated fluids. Spotti et al. (2005) compared the aflatoxin adsorption in a ruminal fluids against in water. The pH of the ruminal solution ranged from 5.7 to 6.5. Among the different binders tested, a bentonite showed nearly a complete removal of the aflatoxin added to the ruminal solution. Magnoli et al. (2011a) also observed higher adsorption of aflatoxin in buffer solutions at pH 6 and 4, but a significant decrease in adsorption at pH 2. Vekiru et al. (2007) tested the binding efficiency in acetate buffer, simulated gastric fluid, and real gastric fluid and observed higher AfB1 adsorption in real GF than in simulated GF. Pepsin was included in the simulated gastric solution and possibly present in the real gastric fluid too, but the effect of the protein on aflatoxin adsorption was not discussed. These studies suggested that low pH was one of the main factors in

reducing the smectites's adsorption capacity for aflatoxin.

2.1.2.2 Proteins may hinder the adsorption of aflatoxins

Smectites can adsorb a wide range of proteins in the interlayer space by cation exchange reaction (Ensminger and Gieseking, 1941; Talibudeen, 1955; McLaren et al., 1958; Armstrong and Chesters, 1964; Harter and Stotzky, 1971). In the early studies by Ensminger and Gieseking (1941), the intercalation of proteins between the smectite layers was demonstrated by the expansion of the d001-value as the amount of adsorbed protein was increased. Greater adsorption was achieved at low pH values because of the protonation of the amino group in the proteins. The protonation increased the adsorption through cation exchange reaction. McLaren et al. (1958) and Armstrong and Chesters (1964) observed that the highest adsorption of pepsin was reached at acidic conditions (pH less than 3.0) around its isoelectric pH. The interaction of smectite with proteins is well known but the interference of proteins present in the gastrointestinal fluid on aflatoxin adsorption has not been fully addressed.

2.1.2.3 Concerns on nutrient uptake by smectites

Smectites are known for their capability of adsorbing numerous organic compounds. In the gastrointestinal fluids, many biological compounds may also interact with smectites. Adding smectite in feed may cause nutrient deficiency by retaining vitamins and inorganic nutrients. Deficiency of certain vitamins can affect the productivity and also increase the animal susceptibility to genotoxic effects of aflatoxins. One of the metabolic pathways for AfB1 is the formation of AfB1-8,9-epoxide (Bailey, 1994). This activated form of AfB1 can bind DNA, RNA and proteins and produce mutations. The formation of adduct between AfB1-epoxide and genetic molecules can be inhibited by vitamins A, C, and E (Alpsoy and Yalvac, 2011). In vitro experiments, using rat-liver cells, demonstrated that Vitamin A (retinol) and

its derivatives are the most effective mutagenic inhibitors (Bhattacharya et al., 1987). It is important to minimize the interactions between smectites and these essential nutrients so that the smectites do not interfere with the natural detoxification process for aflatoxin.

Certain vitamins, such as riboflavin (Mortland and Lawless, 1983) and thiamine (Schmidhalter et al., 1994; Joshi et al., 2009) can be adsorbed by smectites. On the contrary, Afriyie-Gyawu (2004) observed negligible adsorption of vitamin A by a bentonite (NovasilPlus). The solubility of an organic compound strongly affects the adsorption. Hydrophilic vitamins are more readily adsorbed by the smectite than fat-soluble vitamins. Quantification of vitamin A in liver of chickens exposed to aflatoxin diets with added clay binder did not show alteration of the vitamin levels in the presence of the clay (Chung et al., 1990). In an in vivo experiment by Pimpukdee et al. (2004), the incorporation of up to 0.5% smectite into aflatoxin contaminated feed did not show significant effect on the hepatic vitamin A concentration. It is important to know which proteins and vitamins will be adsorbed by the clays and if there is any competition from these nutrients with aflatoxin molecules for adsorption sites on the clay. Vekiru et al. (2007) observed that low adsorption of vitamin B5 (pantothenic acid) and H (biotin) in a buffer solution containing 4 ppm aflatoxin, while different amounts of vitamin B12 (cobalamin) were adsorbed depending on the binder. In their single concentration adsorption test, the high aflatoxin adsorption (<90%) was not affected by the simultaneous adsorption of vitamins.

The objectives of this study were to evaluate 1) the effect of simulated gastric fluid protein (pepsin) and pH on the aflatoxin adsorption by smectite, 2) the influence of the exchangeable cation of smectite on the aflatoxin adsorption in simulated gastric conditions, 3) the competition of vitamins with aflatoxin molecules for adsorption sites on the smectite, and 4) the aflatoxin adsorption in the presence of vitamin B1

in the simulated fluid.

2.2 Materials and methods

2.2.1 Clay treatments for dispersion and adsorption

A raw Ca-bentonite (4TX) sample, which has shown high efficiency in binding aflatoxin in vitro and in vivo (Barrientos Velazquez, 2011), was used for this study. The sample was provided by BYK additives company (formerly Southern Clay Products). The $<2\mu$m clay fraction of the bentonite sample was fractionated to concentrate the smectite following the procedures described by Deng etal., 2006. The fractionation process produced a Na-saturated clay that was used for the adsorption isotherm analysis.

The clay fraction was dominated by montmorillonite and had a cation exchange capacity of 103.6 cmol(+)/kg (Barrientos Velazquez, 2011). A portion of the Na-montmorillonite was exchanged with Ca^{2+} and Ba^{2+} by washing the clay with 0.5M $CaCl_2$ and 0.5M $BaCl_2$ solution three times, respectively, and the residual electrolytes were removed by washing with DI water three times. The different cation saturated smectites were used to address the effect of the exchange cations on aflatoxin adsorption.

To test the effect of clay dispersion on aflatoxin adsorption, a portion of the Ca-saturated clays was subjected to four additional treatments: 1) oven dried clay at 60°C, 2) freeze dried clay powder, 3) sonicated clay suspension, and 4) anionic polyacrylamide (PAM) stabilized clay suspension. The polymer was used to promote dispersion of the clay particles. This polymer is commonly used to reduce soil erosion and to stabilize clay particles. The polymer-clay suspension was prepared by dispersing the clay in a 160 mg/L anionic polyacrylamide (PAM836A) solution (Deng et al., 2006). The treated clay samples were used for the single point aflatoxin

adsorption.

2.2.2 Preparation of simulated gastric fluid (GF) solution

To mimic the digestive solution in the stomach, a simulated gastric fluid solution was prepared according to Lemke (2000) with minor modifications. Pepsin (from porcine gastric mucosa), citric acid, malic acid, acetic acid, and lactic acid were obtained from Sigma Aldrich. A stock solution of simulated GF was prepared by adding 312 mg pepsin, 125 mg citric acid, 125 mg malic acid, 125 μL acetic acid, and 105 μL lactic acid to DI water to make a 250 mL solution. The simulated GF solution was filtered and centrifuged to remove the undissolved pepsin.

2.2.3 Aflatoxin adsorption

Single aflatoxin concentration was used to test the effect of the clay dispersion on the aflatoxin adsorption. A 4.8 ppm aflatoxin solution was prepared by diluting a 1000 ppm AfB1/acetonitrile stock solution with the prepared simulated gastric fluid. A similar 4.8 ppm solution was prepared in DI water for comparison. One milligram of each clay was added to 20 mL of the respective solutions (DI water or simulated GF). Each point was replicated three times. The samples were shaken on a temperature controlled orbital shaker for two hours at 37°C, and then centrifuged at 4500 rpm for 57 min. The aflatoxin concentration in the supernatant was analyzed using Beckman Coulter DU800 UV-spectrophotometer at 365 nm.

As will be shown in the results section, the single concentration adsorption indicated that the sonicated Ca-saturated clay suspension was more efficient than the other three treatments in removing aflatoxin from the solution, and therefore this dispersed sample was used in adsorption experiments.

To further evaluate the influence of the simulated GF and exchange cations on the aflatoxin, adsorption isotherms were conducted following the procedures described

by Kannewischer et al. (2006). In brief, 8 ppm aflatoxin solutions were prepared in DI water and simulated GF by diluting a 1000 ppm AfB1 stock solution with the corresponding GF solution or water. For each isotherm point, a total volume of 5 mL of AfB1 solution with varied concentrations was prepared in a 15 mL centrifuge tube. Then 50 μL of the 2 mg/mL of the Ba-, Ca-, or Na-sonicated 4TX clay dispersion was added into the tube. The samples were shaken on a temperature controlled orbital shaker for two hours at 37°C, and then centrifuged at 4500 rpm for 57 min. The aflatoxin concentration in the supernatant was analyzed using UV-spectrophotometer.

2.2.4 Pepsin adsorption

As will be shown in the results section, pepsin is one of the major interfering compound in AfB1 adsorption. Pepsin-smectite interactions were evaluated by conducting adsorption isotherms, X-ray diffraction (XRD), and Fourier transform infrared (FTIR) spectroscopy analyses. For the adsorption isotherms, simulated GF solution with increments of 0, 0.25, 1, 2, 3, 4, and 5 mL was diluted with DI water to make a total volume of 5 mL in each tube. A standard curve was prepared using the same concentrations without adding smectite. Fifty micro-liters of smectite dispersion were added into each sample tube in duplicate. Pepsin adsorption isotherms were conducted with both Na- and Ca-saturated smectite samples.

2.2.5 Preparation of AfB1-pepsin-montmorillonite complex

To test if pepsin competed with AfB1 for interlayer adsorption in smectite, one milligram Ca-smectite was saturated with simulated GF, and another 1 mg of Ca-smectite was saturated with pepsin plus AfB1. Each sample was mixed three times with 40 mL of the corresponding solution and washed twice with DI water. The smectite complexes were air dried on zero background slides for X-ray diffraction

analysis (XRD). A D8 Advance Bruker diffractometer with CuK_α radiation source and Sol-X detector was used to record the diffraction patterns at room temperature, and after heating the complexes at 300°C in a furnace for 1 hr.

A portion of the prepared smectite complex was air dried on ZnS discs for FTIR analysis. The samples were placed in a dewar accessory purged with N_2 to reduce moisture. The spectra were recorded in transmission mode in a Spectrum 100 Perkin Elmer FTIR spectrometer with 32 scans and a resolution of 2 cm^{-1}.

2.2.6 Vitamin adsorption

Vitamin B_1 (thiamine chloride), vitamin D_3 (cholecalciferol), and vitamin E (tocopherol) were obtained from Sigma Aldrich. A similar adsorption procedure used for aflatoxin was performed for the adsorption of vitamins and smectite. Stock solutions of 10 ppm were prepared for vitamins B1 and D3, while a 30 ppm stock solution was prepared for vitamin E. The isotherms of these three vitamins were conducted using the unfractionated 4TX bentonite.

2.2.7 Competition of vitamin B1 with Afb1 for interlayer adsorption in smectite

To investigate the competition of vitamin B1 with aflatoxin for adsorption sites on the smectite, two solutions were prepared: one was an aqueous solution containing 8 ppm aflatoxin and 10 ppm vitamin B1, and the other one was the simulated gastric fluid solution containing 10 ppm vitamin B1 and 8 ppm aflatoxin. The adsorption isotherms of vitamin B1 and aflatoxin by the smectite in these two solutions were measured similarly as described in section 2.3.

2.3 Results

The single aflatoxin adsorption concentration experiments indicated that greater adsorption was achieved by increasing clay dispersion. Promoting the dispersion of

particles by sonication resulted in the highest adsorption of aflatoxin in water (0.30 mol/kg), followed by freeze dried clay (0.28 mol/kg) and polymer stabilized clay (PAM) (0.26 mol/kg) (Figure 2.1). The oven dry clay showed the lowest adsorption of 0.09 mol/kg, indicating that heating can affect the swelling property of the clays and restricted accessibility to the interlayer.

A similar trend was observed in the simulated GF. The better dispersed clays (sonicated and polymer stabilized clay) adsorbed more mycotoxin than the freeze dried and the oven dry clays. However, a significant reduction of 20-50% in all treatments was observed when the adsorption was carried out in simulated GF.

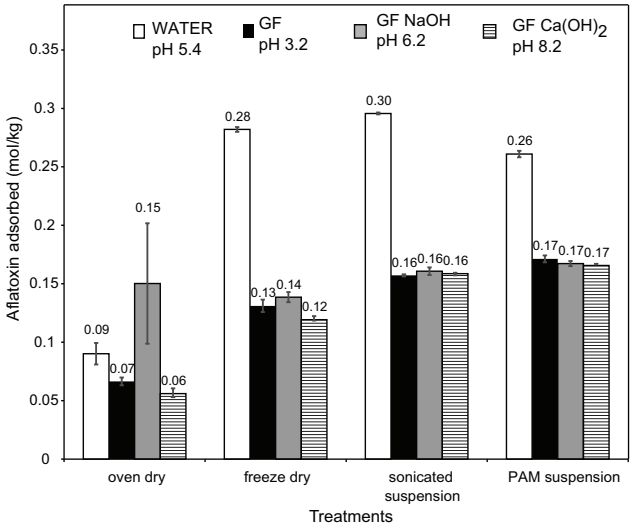

Figure 2.1: Aflatoxin adsorption of the clay dispersion treatments in DI water and simulated GF. The numbers at the top of the bars are the average aflatoxin adsorptions from the three replications.

2.3.1 Interference of pepsin on AfB1 adsorption

Smectite can adsorb large amounts of pepsin as shown by the adsorption isotherms (Figure 2.2). The presence of Na as exchangeable cation resulted in a higher pepsin

adsorption on the smectite. The XRD patterns of the complexes confirmed the presence of pepsin in the interlayer space of montmorillonite (Figure 2.3). At room temperature, the d001-value of smectite was expanded to 18.1 Å in the presence of the protein and to 17.5 Å in the presence of both pepsin and AfB1. Heating at 300°C collapsed the d001-value of smectite to 15.1 Å for pepsin and to 14.5 Å for the pepsin-AfB1 complex. The greater expansion of the pepsin-smectite sample might be due to more protein molecules present in the interlayer than in the AfB1-pepsin-smectite sample. Our earlier studies have suggested that aflatoxin can expand smectite to 15 Å at room T and the d001-value collapsed to about 13 Å at 300 °C (Deng et al., 2010). The higher d001-value of AfB1-pepsin-smectite complex than AfB1-smectite complex suggested the interlayer space of smectite was dominated by the pepsin.

The FTIR spectra confirmed that both pepsin and aflatoxin B1 were associated with the smectite (Figure 2.4). In the spectrum of the aflatoxin-pepsin-clay complex, the characteristic bands of both pepsin and aflatoxin were visible. The 1749 cm^{-1} band due to the C=O vibration of the aflatoxin molecules was observed, along with other minor AfB1 bands (1455 and 1382 cm^{-1}). The 1653 and at 1537 cm^{-1} vibrations, present in the pepsin spectra, were attributed to the amine I and amine II respectively (Sepelyak et al., 1984b). The 1724 cm^{-1} was attributed to the non deprotonated carboxyl groups of the aspartic components of the pepsin (Iliadis et al., 1994). In the pepsin-smectite complex, the 1724 cm^{-1} band intensity reduced significantly. The disappearance of this band was previously attributed to the ionization of the carboxyl groups (Sepelyak et al., 1984a). The much stronger pepsin IR bands than aflatoxin bands also suggested that the interlayer of smectite was dominated by pepsin.

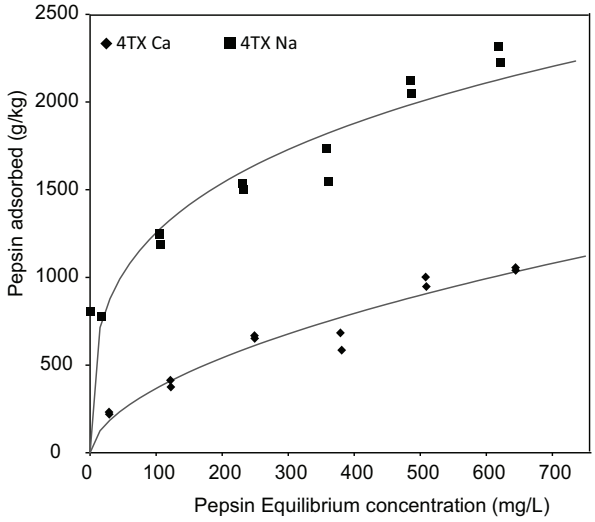

Figure 2.2: Adsorption of pepsin in simulated GF by Na- and Ca-smectite.

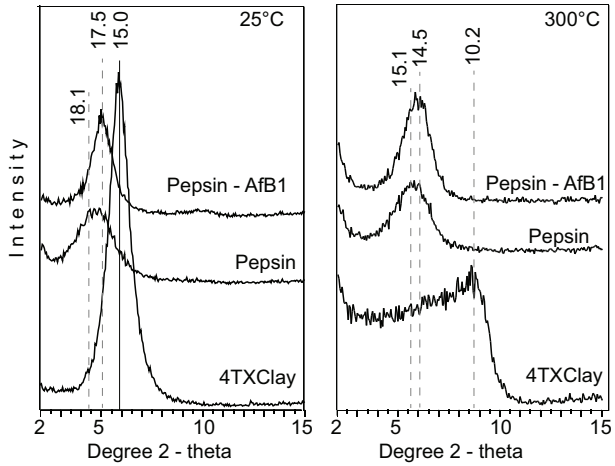

Figure 2.3: X-ray diffraction patterns of pepsin-smectite and pepsin-AfB1-smectite complexes at room temperature and heated at 300°C.

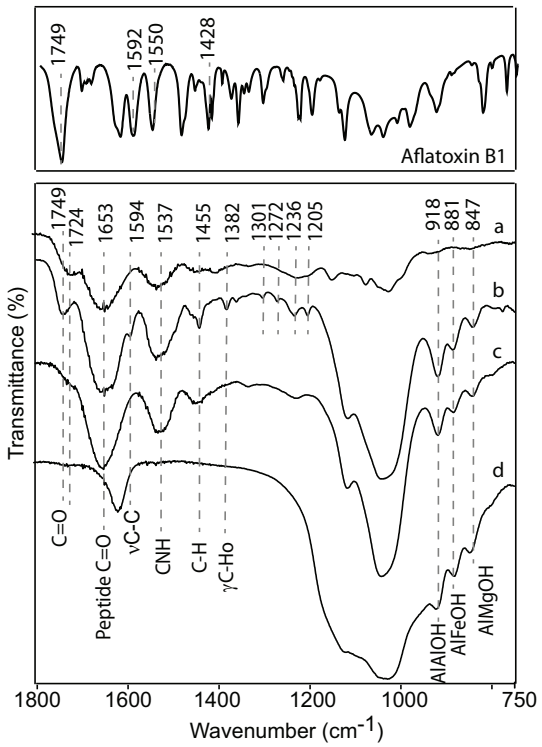

Figure 2.4: FTIR spectra of a) pepsin, b) AfB1 + pepsin + smectite, c) pepsin + smectite, and d) Ca-smectite.

2.3.2 Effect of simulated gastric fluid on AfB1 adsorption

The aflatoxin adsorption isotherms obtained in the two solutions, DI water and simulated GF, indicated that adsorption was decreased in the artificial gastric fluid (Figure 2.5). The isotherms in the simplified solution (DI water) had a L-shape, indicating a monolayer of aflatoxin molecules saturated the adsorption sites. On the contrary, in the simulated GF the affinity and adsorption maximum were lower and the Langmuir model did not fit the experimental curves. Instead the modified Langmuir QKML model was used to fit the experimental data (Deng et al., 2012) (Table 2.1). The low adsorption of 0.2 mol/kg might be partially due to the pH

difference. The pH of DI water was 5.4, and the pH of the simulated GI solution was 3.2. Acidic conditions may have resulted in the cation exchange of Ca by H^+, Al^{3+}, and protonation of the pepsin protein.

Table 2.1: Aflatoxin adsorption isotherm fit parameters in water and simulated GF on smectites with different cation saturation.

	Water			Simulated GF			
Exchange	*Exponential Langmuir*			*Modified Langmuir QKML*			
cation	Q_{max} (mol/kg)	K (μM^{-1})	η^2	Q_{max} (mol/kg)	K (μM^{-1})	b	η^2
Ba	0.58	1.11	0.96	0.33	0.040	-2.16	0.93
Ca	0.52	0.69	0.95	0.32	0.065	-0.89	0.97
Na	0.31	0.12	0.99	0.28	0.056	-2.11	0.99

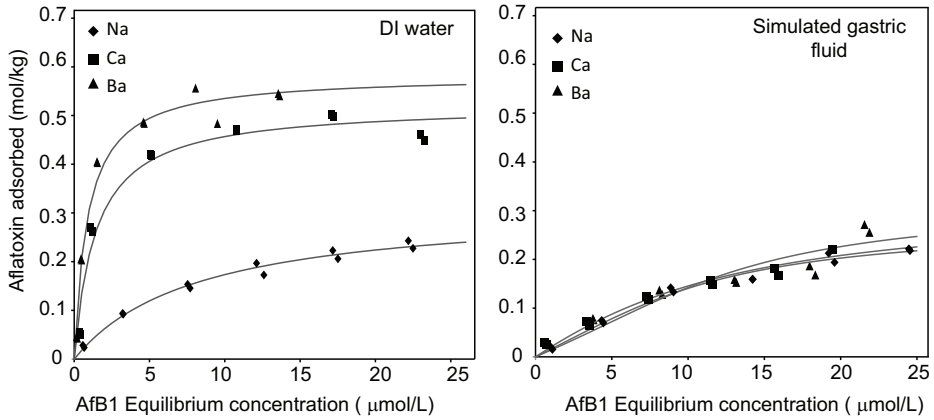

Figure 2.5: Aflatoxin adsorption isotherms of Na-, Ca-, and Ba-saturated smectites in (left) DI water and (right) simulated gastric fluid.

2.3.3 Effect of exchangeable cation on aflatoxin adsorption in simulated gastric fluid

In a simplified aqueous solution, the exchangeable cation on smectite demonstrated strong influence on the amount of aflatoxin adsorbed by the smectite (Figure 2.5, left). Smectite saturated with divalent cations had higher aflatoxin adsorption than the one with monovalent cation saturation. The highest adsorption was observed when the exchange cation on smectite was Ba (Deng et al., 2012). In simulated GF, however, no significant differences in aflatoxin adsorption were observed among the Na, Ca, and Ba saturation in this study (Figure 2.5). The lack of response in aflatoxin adsorption to exchange cation in the GF suggested strong masking effect of some compounds such as pepsin in the GF on the exchange cations.

2.3.4 Adsorption of vitamins and the effect of vitamin B on AfB1 adsorption by smectite

The smectite showed high affinity for the vitamin B1. The isotherm fitted the Langmuir model well, indicating a monolayer adsorption. On the contrary, the smec-

tite had little or no adsorption for vitamins D3 or E (Figure 2.6). Only the effect of vitamin B1 on aflatoxin adsorption was further investigated. The maximum aflatoxin adsorption of this Ca-smectite was 0.4 mol/kg (Figure 2.7). The inclusion of vitamin B1 in the solution showed a reduction in the adsorption capacity of AfB1, without affecting the binding affinity (the initial slope). The similar L-shape isotherm was not observed when the adsorption was conducted in the simulated GF. The affinity (the initial slope) was significantly reduced, but the maximum adsorption was 0.4 mol/kg, similar to the maximum adsorption of aflatoxin in water.

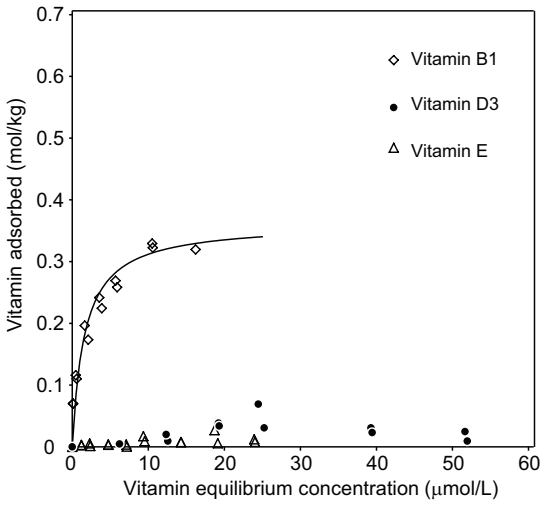

Figure 2.6: Ca-smectite adsorption of vitamins B1, D3, and E.

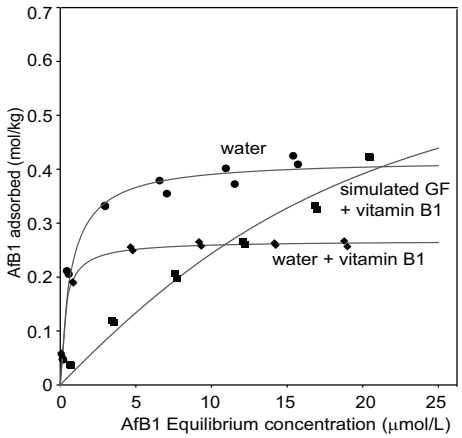

Solution	Aflatoxin adsorption			
	Q_{max}	K	b	η^2
	(mol/kg)	(μM^{-1})		
Water	0.41	1.41	-	0.96
Water + VitaminB1	0.27	3.15	-	0.99
GF + Vitamin B1	0.72	0.039	-0.512	0.98

Figure 2.7: Adsorption of aflatoxin on Ca-smectite in water, in water with vitamin B1 added, and in simulated GF in the presence of vitamin B1.

2.4 Discussion

The XRD data of the pepsin-smectite complexes (heated at 300°C) were in agreement with previous observations that the protein can be adsorbed in the interlayer space of smectite. The FTIR spectra confirmed the presence of both pepsin and aflatoxin molecules in the smectite. The pH of the simulated gastric fluid used in the present experiment was 3.2, thus favoring the adsorption of protonated pepsin rather than aflatoxin molecules. A possible explanation to the lower aflatoxin adsorption in the presence of pepsin is the configuration of the protein structure in the interlayer. Pepsin occurs as a globular protein with a diameter of 44 Å in water, if this configuration is retained once adsorbed a greater d-value should had been observed (Armstrong and Chesters, 1964; Theng, 1974). It was suggested that the lack of the large expansion on the basal reflection was due to pepsin changing its conformation from globular to the extended B-type (Theng, 1974).

The XRD data demonstrated the intercalation of pepsin into the smectite where the protein can replace the exchangeable cations. As the pepsin existed in a more extended conformation, a much larger surface area was required to accommodate the pepsin molecule. The extensive required surface area from pepsin indicated that the basal surfaces of the smectite (polar and non-polar) were mostly occupied by pepsin molecules. In addition, the FTIR spectrum of the pepsin-smectite complex indicated the presence of ionized carboxyl groups that could occupy or be oriented toward the non-polar sites of the smectite basal surface, and therefore, intercalation of pepsin into the interlayer of smectite had blocked the adsorption sites for aflatoxin molecules.

Another consideration for the adsorption quantification is the amount of pepsin added to the simulated gastric solution. The concentration of pepsin used in the experiment can differ from the real gastric fluids. The simulated gastric fluid in the present study was based on the one described by Lemke et al. (2001), but the amount of smectite used was reduced from 125 mg to 1 mg. In Lemke et al. (2001) experimental set up, about 100% aflatoxin binding was achieved in both water and simulated GF. On the contrary, our experiment demonstrated a significant adsorption reduction in the simulated GF. The difference can be attributed to the amount of smectite used in the two adsorption experiments.

The aflatoxin adsorption isotherms showed a significant reduction of aflatoxin adsorption in simulated gastric fluid. The adsorption capacity of the smectite for aflatoxin was 0.5 mol/kg in water, but was only 0.2 mol/kg in the acidic gastric solution. It was possible that the difference in binding capacity was resulted from the pH difference between the DI water and the simulated gastric fluid. When the pH of the gastric solution was raised (pH 8), however, the adsorption capacity was not improved. This observation indicated that although the pH might have some

effect, other factors were restricting the aflatoxin adsorption.

2.4.1 Effect of the exchangeable cation

The exchange cations in the interlayer space of the smectites can affect the adsorption of organic compounds. Harter and Stotzky (1971) showed that H- and Na-saturated smectite retained more proteins (pepsin included) than other cations tested (Ca, Al, and Th). Monovalent cations are easily replaced by proteins than higher valence cations that are more tightly attracted to the smectites surface. The adsorption mechanism of aflatoxin molecules involves a direct ion-dipole interaction with the exchangeable cation and a H-bonding with the hydration shell of the interlayer ion. In this mechanism, higher mycotoxin adsorption was observed with divalent cations (Deng et al., 2010; Deng and Szczerba, 2011). The present results indicated that the aflatoxin adsorption was not affected by the exchangeable cation in the presence of pepsin, as the same adsorption values were observed with the Na-, Ca-, and Ba-saturated smectites. It was likely that the exchangeable cations were replaced by pepsin due to the high affinity of smectite for the protein and the large entropy gains from the protein adsorption. The strong pepsin band on the IR spectra (Figure 2.4) suggested high loading of pepsin on the smectite. Aflatoxin molecules will occupy the non-polar sites, but the large size of the pepsin molecules could extend to these sites and inhibited the adsorption of aflatoxin.

2.4.2 Vitamin adsorption

In the present study, low to negligible adsorption of vitamin D and E demonstrated the weak interaction between lipophilic organic compounds and clay particles. These observations indicated that in vivo deficiency of vitamins D and E is not likely to occur due to clay retention. Similarly to the adsorption of vitamin D and E, the lipophilic vitamin A had shown low in vitro binding by smectite (Afriyie-Gyawu,

2004). Negligible bentonite interference of vitamin A utilization has been observed (Chung et al., 1990; Pimpukdee et al., 2004).

In contrast, the smectite sample showed high affinity for vitamin B1 in aqueous solution. The high adsorption of vitamin B1 by smectite in water suggested that adding smectite in the animal feed may cause vitamin deficiency. Further research is needed to quantify the adsorption of vitamin B1 in real gastric conditions by the smectite, and to address if the vitamin retention could result in vitamin deficiency. In animal experiments where bentonite was added to the feed, the animals reached body weight and feed production index similar to the control group, with no signs of vitamin deficiencies (Abdel-Wahhab et al., 1999; Rosa et al., 2001; Pimpukdee et al., 2004; Bailey et al., 2006). The animal feeding experiments suggested the vitamin B1 adsorption on smectite in real gastric fluid may be weaker than that in water.

A reduction in the aflatoxin adsorption maxima was observed when vitamin B1 was present in the aflatoxin solution, indicating a possible competition for interlayer space. An important observation was the high aflatoxin adsorption values reached in the presence of vitamin B1 in the simulated GF solution in comparison to the artificial gastric fluid alone. Both adsorption conditions reduced the smectite's affinity for aflatoxin, as described by the low K values, but when pepsin and vitamin B1 were present, a higher amount of aflatoxin was adsorbed. This could indicate that the presence of vitamin B1 reduced the amount of pepsin adsorption. As both vitamin B1 and pepsin could intercalate the smectite at low pH, we hypothesized that vitamin B1 competed with pepsin to occupy the negative charge sites on the clay structure. The occupation of vitamin B1 on the exchange sites could leave more non-polar sites available for aflatoxin molecules. Considering that there are proteins and vitamins present in the complex gastrointestinal fluid, the present results implied that the smectites can still efficiently sequester aflatoxin molecules and reduce the toxicity

under in vivo conditions.

2.5 Conclusions

Several factors in the complex gastric fluids affect aflatoxin adsorption by smectite. The low pH in gastric fluid reduced the adsorption of aflatoxin molecules but the adsorption capacity for aflatoxin in GF can still be significant. The low pH favors the adsorption of proteins (pepsin) on the smectite, the adsorbed pepsin occupied large areas in the smectite surface and reduced the available adsorption sites for aflatoxin molecules. The adsorption of aflatoxin was not affected by the exchangeable cation in the presence of pepsin, likely due to masking effect of the strong pepsin adsorption at low pH.

Vitamins present in the gastric fluids could also compete for aflatoxin adsorption sites. The lipophilic vitamins were not adsorbed by the smectite. The presence of vitamin B1 could reduce the amount of pepsin allocated in the interlayer space and allowed for more adsorption sites available for aflatoxin molecules, yet the affinity of the smectite for the aflatoxin in the presence of vitamin B1 and pepsin was still low when compared with aflatoxin adsorption in water.

3. INFLUENCE OF CHARGE ORIGIN AND LAYER CHARGE OF SMECTITES ON AFLATOXIN ADSORPTION

3.1 Introduction

Incorporating bentonites into aflatoxin-contaminated animal feed is an effective and low cost measure to reduce the bioavailability of these toxic and potent carcinogenic compounds. Bentonites could adsorb up to 20% (w/w) of aflatoxin, but this high in vitro adsorption capacity was not always observed in animal trials.

Great variation in the aflatoxin adsorption capacity was observed among bentonites. Although a screening procedure to select effective aflatoxin binders has been proposed (Dixon et al., 2008), a correlation between a single clay property and aflatoxin adsorption has not been observed (Magnoli et al., 2008b; Mulder et al., 2008; Tenorio Arvide et al., 2008). Tenorio Arvide et al. (2008) observed that the structural composition of the octahedral layer in smectites affected their aflatoxin adsorption capacity: the smectites with certain amount of structural Fe and Mg octahedral substitutions had higher aflatoxin adsorption capacities than the smectites with less octahedral substitutions for Al. Mulder et al. (2008) investigated the effect of physical properties of bentonites such as particle size and morphology on aflatoxin adsorption. A linear correlation (R^2=0.73) between clay content and maximum aflatoxin adsorption (Qmax) was observed, but outliers were observed when bentonites had poor dispersion and high aflatoxin adsorption capacity. The morphological analysis indicated that the better adsorbents occurred as thin particles, while the moderate to low adsorbents were observed as thicker particles. Their results indicated that the aflatoxin adsorption was affected by several smectite properties. The investigation of smectite properties that affect the adsorption of the mycotoxins

can also offer the scientific basis for the modification of the clays to increase the clays adsorption and selectivity for aflatoxin.

Smectite, the dominant clay mineral in bentonites, has an expandable layer structure. Adsorption of aflatoxin molecules has been shown to occur mainly in the interlayer of smectite (Kannewischer et al., 2006). Based on the strong effect of the exchangeable cation on aflatoxin adsorption, it was proposed that the adsorption mechanism was an ion-dipole interaction between the carbonyl oxygen of the mycotoxin and the exchangeable cations under low humidity, and H-bonding between the carbonyl group and the hydrated ions (Deng et al., 2010). It has been demonstrated that the hydration energy of the exchange cations significantly influenced the amount of aflatoxin adsorbed (Deng et al., 2012). Smectite saturated with divalent cations, such as Ba^{2+}, with low hydration energies showed higher affinity and adsorption capacities for aflatoxins.

High-charge density smectites had shown low adsorption and poor affinity for aflatoxin (Jaynes and Zartman, 2011; Deng et al., 2012). Jaynes and Zartman (2011) found that the aflatoxin adsorption efficiency of the smectites was inversely related to the layer charge density. Furthermore, the aflatoxin adsorption of the high charge density clay was improved by decreasing the layer charge with the incorporation of Li^{+} into the vacant octahedral site. Deng et al. (2012) also reported that smectites with high CEC (CEC=130 cmol/kg) were not as effective as the smectites with lower CEC values (CEC 78-94 cmol/kg) in adsorbing aflatoxin. It was proposed that the lower charge density of smectites had more non-polar sites on the mineral's surface for aflatoxin molecules.

Montmorillonite is one of the most common smectite that has been used in many batch equilibrium experiments and animal trials. The other members of the smectite group minerals such as beidellite, hectorite, nontronite, and saponite have similar

2:1 expandable interlayer structure but different layer charge origins and octahedral cation compositions. The negative layer charge in both montmorillonite and hectorite originates from the substitutions in the octahedral sheet, while in saponite, beidellite and nontronite the charge is located in the tetrahedral sheets. In montmorillonite, Al^{3+} dominates the octahedral position and the charge deficiency is generated from the isomorphic substitutions of Mg^{2+} for Al^{3+}. On the other hand, Mg^{2+} prevails in hectorite with Li^{+} being the replacement ion. Beidellite, nontronite and saponite have Al, Fe, and Mg as the dominant octahedral structural ions, respectively.

Limited studies have reported the use of beidellite, saponite, hectorite, and nontronite as aflatoxin binders. Beidellite and saponite, however had been used as adsorbents of no-ionic organic compounds such as atrazine and showed high adsorption efficiency (Aggarwal et al., 2006).

The effect of octahedral structural cations and the layer charge origin in smectite on aflatoxin adsorption has not been systematically addressed. The objective of this study was to determine the effects of the charge origin, octahedral cation composition and layer charge density of the smectites on the smectites' selectivity and adsorption capacity for aflatoxin.

3.2 Materials and methods

3.2.1 Mineral and chemical characterization of smectites

Six smectite samples with different octahedral cation compositions and layer charge origins were selected. Beidellite and hectorite samples were obtained from the Clay Minerals Society repository (SBCa-1 and SHCa-1, respectively). Nontronite was a sample taken from near Spokane, Washington. The montmorillonite sample (4TX) was collected from Gonzales, TX. Two saponite samples one from Toledo, Spain, and the other one from Western Australia were used. The samples were

fractionated to collect the <2 μm clay fraction (Deng et al., 2009).

Approximately 60 mg of each clay sample were saturated with Mg^{2+} and K^{+} to facilitate the identification of phyllosilicates. The saturated clays suspensions were air dried on glass discs. The X-ray diffraction (XRD) patterns of Mg-saturated clays were recorded at room humidity and after glycerol solvation. The K-saturated samples were recorded at room temperature, and after 330 °C and 550 °C heating. XRD patterns were recorded from 3 to 32 degrees two-theta using a Bruker D8 ADVANCE diffractometer with Cu Kα radiation, 30 rpm spin rate, and 0.017 step size. A 1-D position sensitive detector LynxEye was used during XRD analyses.

The octahedral cation composition of each clay fraction was determined by mixing 10 mg of dry clay with 300 mg of KBr using a Wig-L-Bug mixer. The FTIR spectra were recorded using diffuse reflectance infrared (DRIFT) accessory in a Perkin Elmer Spectrum 100 FTIR spectrometer with an average of 32 scans at a resolution of 2 cm^{-1}.

Cation exchange capacity (CEC) was determined by saturating 100 mg of clay with Ca^{2+} then replacing the adsorbed Ca with Mg^{2+}. Atomic adsorption was used to quantify the Ca^{2+} concentration.

3.2.2 Layer charge reduction of high charge density smectite

To test the effect of the layer charge density on the aflatoxin adsorption, one high charge montmorillonite (5OK with 0.49 charge/half unit cell) and the nontronite were subjected to a lithium saturation/heating treatment, to reduce the layer charge of smectites by incorporating Li^{+} into their vacant octahedral sites after heating the sample at high temperatures, this is known as the Hofmann and Klemen effect (Lim and Jackson, 1986; Jaynes and Bigham, 1987). The clay fractions of both samples were mixed with LiCl/NaCl solutions that have different Li/Na molar ratios. Fifty

milligrams of clay were washed with the corresponding Li:Na solution three times and with DI water twice. The samples were placed in aluminum dishes, dried at 100 °C, and then heated at 250 °C for 12 hrs. A 1:1 water:ethanol solution was used to redisperse the samples. One control sample was prepared by using the 15% Li:Na solution without heating. The nontronite and montmorillonite 5OK samples that were treated with Li^+ to reduce the layer charge density were redispersed and saturated with 0.5 M $BaCl_2$. After saturation with Ba^{2+} solution the clays were washed twice with 1:1 methanol water. Twelve milligrams of the Ba-saturated smectites were added to 50 mL centrifuge tubes, and digested using 2 mL of aqua regia and 3 mL of hydrofluoric acid (HF). Standard Li^+ solutions were prepared using the same digestion solution. The samples and standards were placed on an orbital shaker at 200 mot/min overnight. Saturated boric acid was added to each tube up to the 25 mL mark to promote the formation of soluble fluoroborates of cations. The concentration of lithium in solution was quantified using flame emission on a Perkin Elmer AAnalyst 400 atomic adsorption spectrometer. The CEC values of the Li-treated smectites were obtained by subtracting the lithium content (cmol(+)/kg) from the original CEC value of untreated smectites.

3.2.3 Aflatoxin adsorption isotherms

Each smectite sample was saturated with Na, Ca, or Ba to test the effect of the exchange cation size and valence on the adsorption of aflatoxin. The samples were saturated three times with 1 M Na or 0.5 M Ca or Ba chloride solutions and then washed twice with DI water. Clay dispersions were prepared to have a concentration of 2 mg/mL. Fifty μL of the clay dispersion was used for each isotherm point. An 8 ppm aflatoxin solution was diluted with distilled water to obtain the desired aflatoxin concentrations (Kannewischer et al., 2006). After overnight shaking

at room T, the samples were centrifuged at 4500 rpm for 57 min and the aflatoxin concentration in the supernatant was quantified using a Beckman Coulter DU 800 UV-spectrophotometer. Aflatoxin adsorption isotherms were also performed for the reduced-charge Ba-montmorillonite and Ba-nontronite following the procedure described above.

3.3 Results

3.3.1 Mineralogical composition of smectites

After Mg^{2+} saturation and glycerol solvation, all clays showed an intense expanded interlayer spacing of 18 Å, which indicated the dominance of smectite in all samples (Figure 3.1). No additional minerals where identified on the XRD patterns of montmorillonite (4TX) or nontronite samples but the FTIR spectrum of nontronite showed a weak 3699 cm^{-1} band of kaolinite (Figure 3.3). The 7.1 Å kaolinite peak was present in beidellite and Spain saponite. This peak was present in K-saturated hectorite sample only, and the presence of kaolinite was confirmed by TEM (Figure 3.2). The 10 Å and 3.33 Å peaks observed in Spain saponite were due to presence of mica. Beidellite, hectorite and Australia saponite also contained mica which was only observed with TEM (Figure 3.2). Additionally, Australia saponite showed a peak at 4.04 Å, which was characteristic of opal-CT.

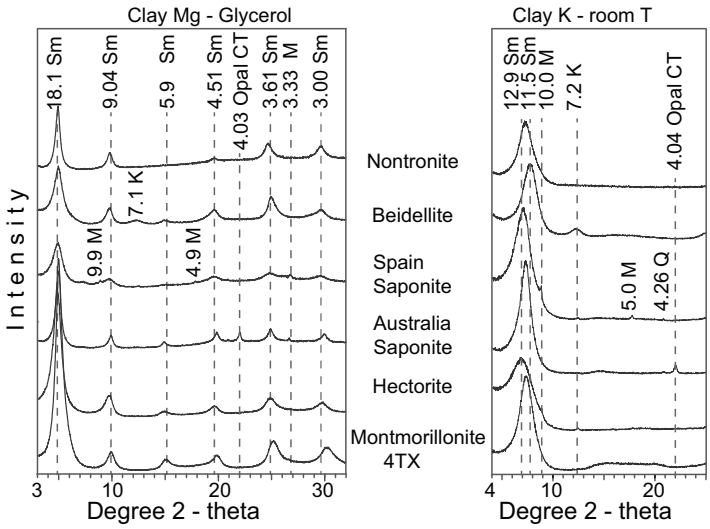

Figure 3.1: XRD patterns of clay fractions Mg-glycerol solvation (left) and K-saturated clays (right). (Sm: smectite, M: mica, K: kaolinite)

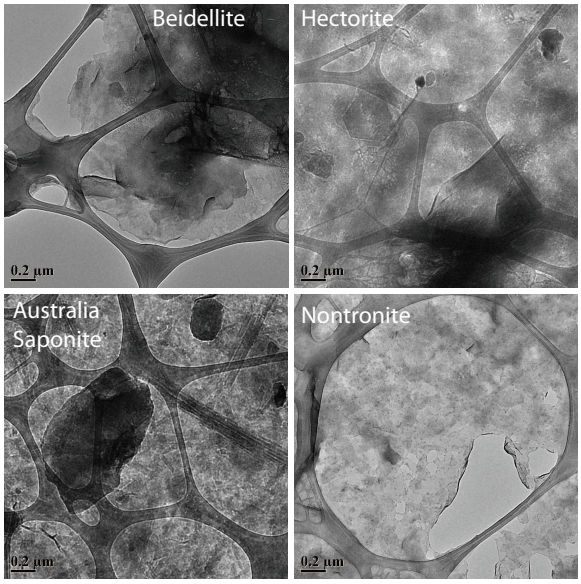

Figure 3.2: TEM images of the clay fraction of beidellite, hectorite, nontronite, and Australia saponite samples.

Distinct OH stretching vibration differences in 4000 to 3000 cm $^{-1}$ region (Figure 3.3) were observed among the smectites. Beidellite and montmorillonite showed a distinctive band at 3623 cm^{-1} that is due to the dominance of Al^{3+}-OH in the octahedral sheet. The dominance of the octahedral Mg^{2+} in the hectorite and the Spain saponite resulted in the band at 3678 cm^{-1}. This band was not present in Australia saponite, instead a band at 3623 cm $^{-1}$ was present indicating a montmorillonite-like composition. Nontronite showed the distinctive 3564 cm^{-1} band due to octahedral Fe^{3+}-OH (Madejová, 2003). The band at 3697 cm^{-1} confirmed the presence of kaolinite in beidellite and nontronite.

For beidellite, montmorillonite and Australia saponite the AlAl-OH bending vibrations occurred at 916 cm^{-1}, $Al^{3+}Fe^{3+}$-OH bending at $\sim$ 885 cm^{-1}, and Al^{3+} Mg^{2+}-OH bending at $\sim$ 845 cm^{-1} (Gates, 2005). The major bands for hectorite and Spain saponite were observed at 691 cm^{-1} attributed to the Mg-OH. The distinctive bending vibrations at 798 and 622 cm $^{-1}$ in Australia saponite were attributed to cristobalite (van der Marel and Beutelspacher, 1976).

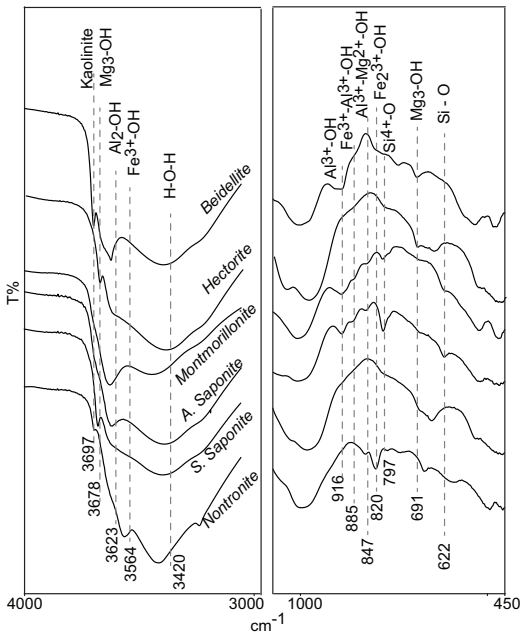

Figure 3.3: FTIR spectra of clay fractions

3.3.2 Effect of interlayer cation on aflatoxin adsorption

The exchangeable cation strongly influenced the aflatoxin adsorption on all smectites. A similar trend was observed on all the samples: the lowest adsorption of aflatoxin molecules was observed in the Na-saturated clays (<0.2 mol/kg), while most samples showed a higher adsorption when the clays were saturated with Ca and Ba (Figure 3.5)(Table 2.1). The FTIR spectra of the AfB1-smectite complexes showed similar aflatoxin band positions for all samples (Figure 3.4). The lack of major shifts on the IR bands indicated that the same aflatoxin adsorption mechanism occurred in all smectite samples.

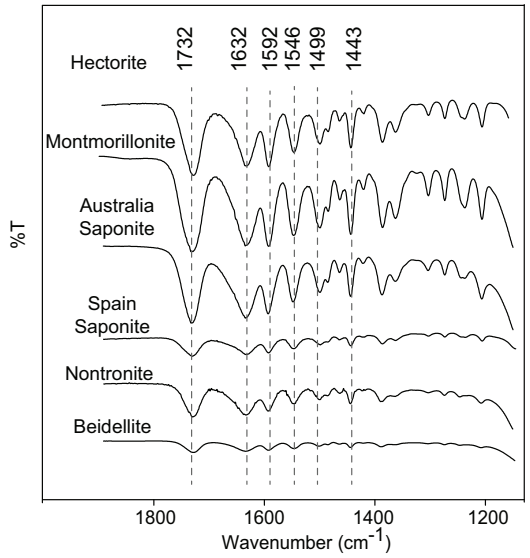

Figure 3.4: FTIR spectra of AfB1-smectite complexes showing the 1800 to 1200 cm^{-1} region where the major AfB1 bands occur.

3.3.3 Effect of layer charge origin on aflatoxin sequestration by smectite

Both octahedral-charged smectites, montmorillonite and hectorite, showed the greatest effect of exchange cation type (Figure 3.5). Ba-saturated montmorillonite showed the maximum adsorption of 0.5 mol/kg, and hectorite showed the highest adsorption of 0.8 mol/kg. Beidellite and the two saponites had similar isotherm shapes and adsorption maxima. Aflatoxin adsorption isotherms in nontronite did not fit the Langmuir model due to the low affinity that produced S-type shape isotherm (Table 2.1). In this case, the modified Langmuir equation (QKLM) described in Grant et al. (1998) and Deng et al. (2012) was used to calculate the adsorption maxima (Qmax) and the affinity parameter (K). Although the aflatoxin adsorption affinity of nontronite remained poor, the maximum adsorption improved with the divalent cation saturation.

Montmorillonite 4TX and nontronite had similar CEC values, 103.6 and 107.9 cmol/kg respectively (Table 3.2). Montmorillonite showed high adsorption capacity and affinity for aflatoxin, while nontronite was a poor aflatoxin adsorbent. The difference in adsorption can be related to the layer charge origin. In montmorillonite, the negative charge arises from the octahedral substitutions while in nontronite from the tetrahedral sheets. A similar trend was observed when hectorite was compared with beidellite and saponites: the samples had similar CEC values (Table 3.2) but the highest aflatoxin adsorption was observed in the octahedral charge origin smectite (hectorite).

Table 3.1: Smectite AfB1 adsorption isotherm fit parameters with different cation saturation.

Sample	Exchange cation	*Langmuir*			
		Q_{max} (mol/kg)	K (μM^{-1})	η^2	
Montmorillonite	Ba	0.58	1.11	0.96	
	Ca	0.52	0.69	0.95	
	Na	0.31	0.12	0.99	
Hectorite	Ba	0.87	0.48	0.96	
	Ca	0.52	1.27	0.89	
	Na	0.25	0.11	0.82	
Australia Saponite	Ba	0.55	0.22	0.99	
	Ca	0.42	0.33	0.98	
Spain Saponite	Ba	0.33	0.31	0.98	
	Ca	0.42	0.33	0.98	
		Exponential Langmuir			
		Q_{max}	K	N	η^2
Beidellite	Ba	0.45	0.16	1.47	0.98
	Ca	0.25	0.106	1.15	0.99
	Na	0.13	0.008	2.15	0.99
Australia Saponite	Na	0.17	0.18	1.101	0.90
Spain Saponite	Na	0.31	0.15	1.229	0.96
		Modified QKLM			
		Q_{max}	K	b	η^2
Nontronite	Ba	0.44	0.034	-3.77	0.96
	Ca	0.37	0.057	-2.29	0.98
	Na	0.19	0.024	-6.15	0.99

Table 3.2: Characterization of smectite samples.

Sample	CEC (cmol(+)/kg)	Octahedral composition	Charge origin
Beidellite	73.47	Al^{3+}	Tetrahedral
Hectorite	86.87	Mg^{2+}, Li^{+}	Octahedral
Montmorillonite 4TX	103.6	Al^{3+},Mg^{2+}	Octahedral
Montmorillonite 5OK	137		
Nontronite	107.9	Fe^{3+}	Tetrahedral
Saponite Australia	105.74	Mg^{2+}	Tetrahedral
Saponite Spain	77.50		

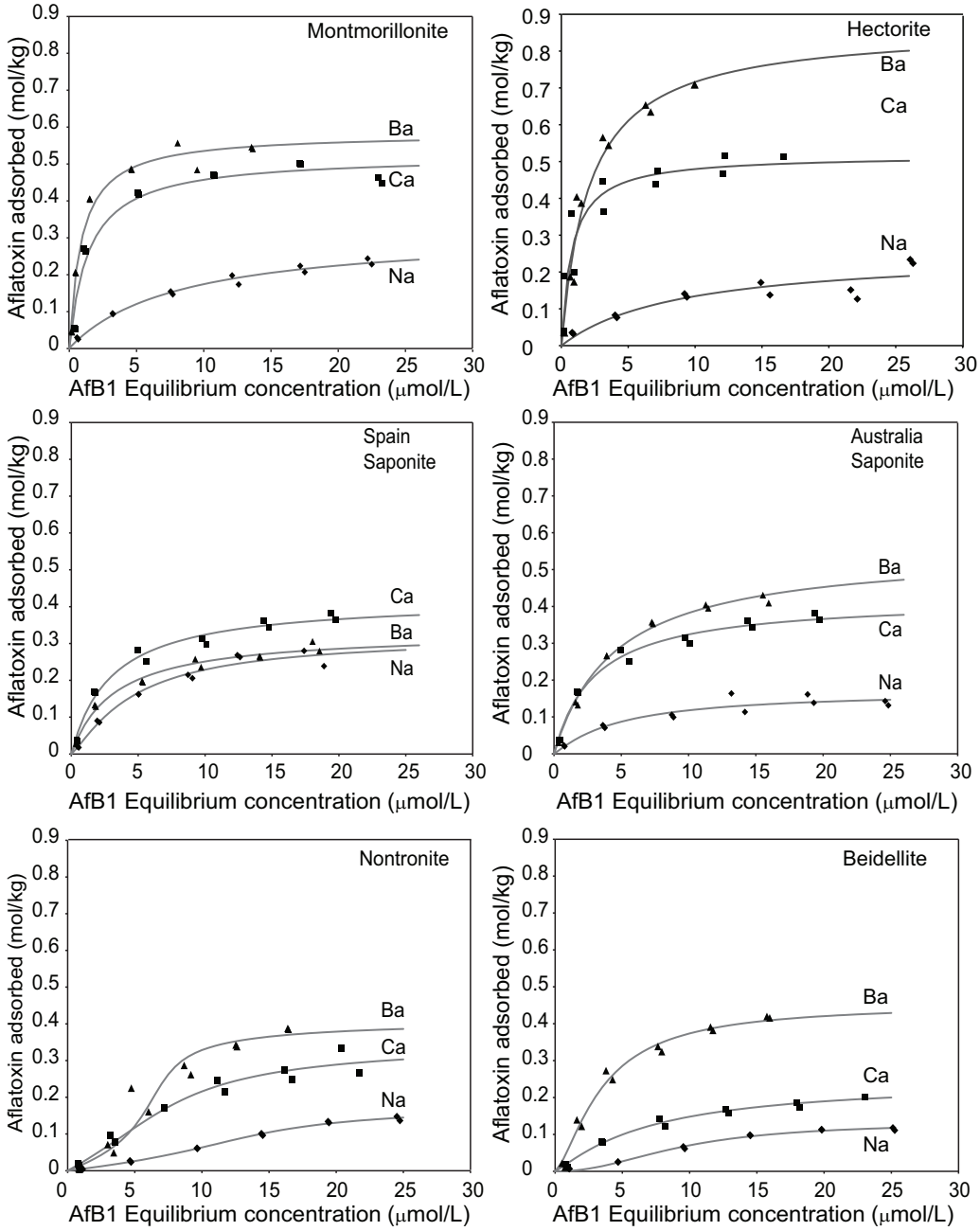

Figure 3.5: Aflatoxin adsorption isotherms (room T) of smectites saturated with different cations.

3.3.4 Effect of layer charge density on aflatoxin adsorption

Montmorillonite 5OK, with high CEC (137 cmol(+)/kg), had a maximum adsorption of 0.3 mol/kg and low affinity for aflatoxin (Figure 3.6). As the CEC of this smectite was reduced, due to the different amount of Li incorporated in the octahedral sheet, the adsorption capacity increased first. The highest aflatoxin adsorption was observed when the CEC was reduced to 86 cmol(+)/kg. Further reduction of the layer charge to 26 cmol(+)/kg caused the adsorption to decrease to 0.4 mol/kg. Similar trend was observed on nontronite, as the CEC was reduced, the adsorption capacity increased initially until it reached a maximum CEC of 81 cmol(+)/kg. Although there was an increase in the amount of aflatoxin adsorbed, the affinity of nontronite for aflatoxin was not improved in comparison to montmorillonite 5OK (Figure 3.7).

The effect of layer charge reduction of montmorillonite 5OK on aflatoxin adsorption indicated that the optimal CEC for the highest adsorption was $\sim$ 86 cmol/kg. Hectorite, a trioctahedral smectite with an octahedral charge origin, had an optimal CEC of 87 cmol(+)/kg and showed the highest adsorption and affinity. Thus, montmorillonite and hectorite were able to adsorb similar amounts of aflatoxin at similar CEC values.

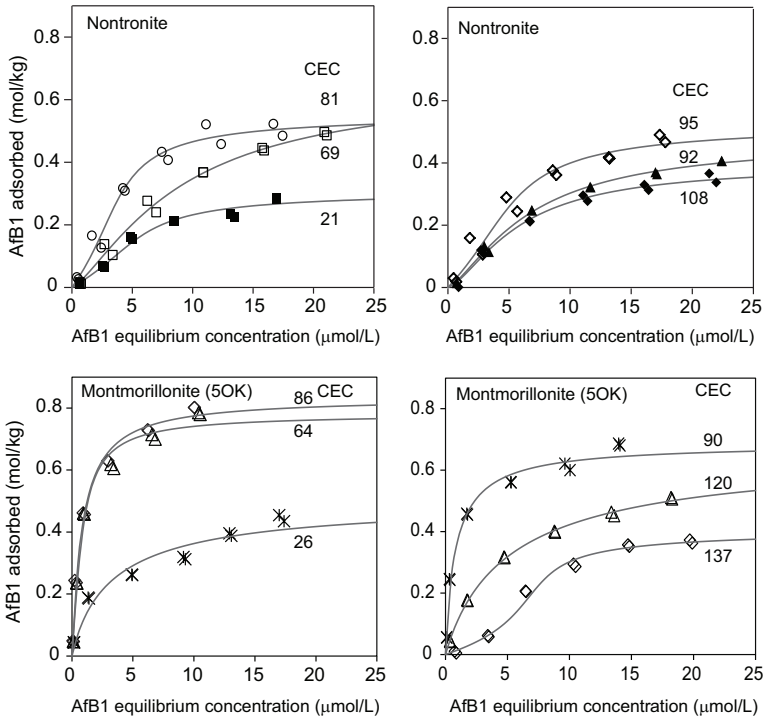

Figure 3.6: Aflatoxin adsorption isotherms (room T) of charge-reduced montmorillonite 5OK and nontronite. CEC (cmol/kg) data showed at the end of the plot. The isotherm data for montmorillonite (5OK) was re-plotted from Lian (2013).

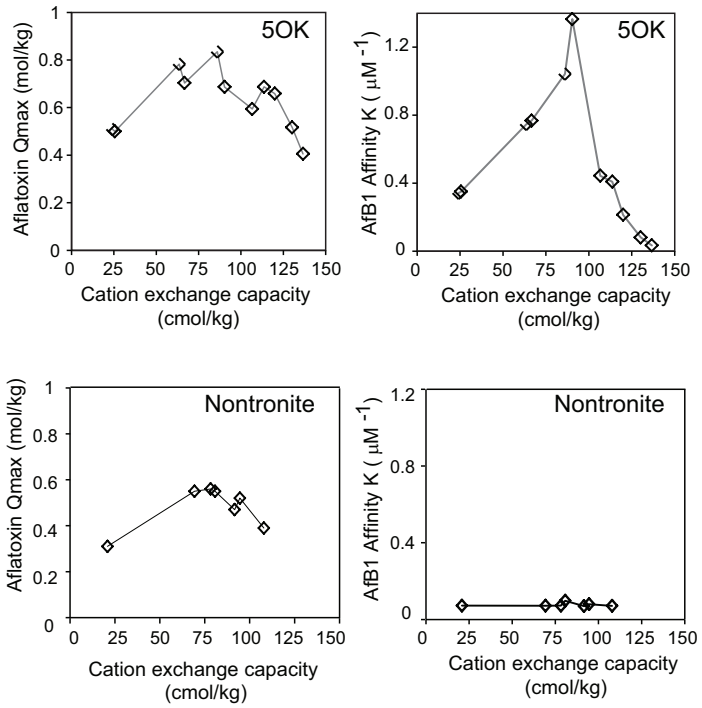

Figure 3.7: Q(max) and affinity (K) plots at different CEC values of the Li-treated montmorillonite 5OK and nontronite.

3.3.5 FTIR comparison of Li-treated montmorillonite and nontronite

The major structural changes on the high-charge dioctahedral smectite (5OK) were observed at high Li-concentrations, 85% saturation (Figure 3.8). As the structural Li^+ increased, the intensity of the OH-stretching band at 3619 cm^{-1} reduced and a shoulder appeared at 3665 cm^{-1}. In the OH-bending region, the band due to the AlAlOH vibration at 914 cm^{-1} shifted to a higher wavenumber and the intensity of this band decreased. A shift to lower wavenumber was observed for the 622 cm^{-1} band. The band shifts were more evident as the Li^+ content was increased, indicating incorporation of Li in the octahedral sheet. On the contrary, no changes in the IR band position or intensities were observed for the nontronite samples for up to 50%

of Li saturation. It is possible that the incorporated structural Li concentration was not enough to produce significant shifts in the band positions of nontronite, but the Li quantification after nontronite digestion and the increase in aflatoxin adsorption indicated migration of Li to the smectite layers. Madejová et al. (2000) studied the perturbation of the infra-red bands of smectites by the incorporation of Li in their structures. A ferruginous smectite with a tetrahedral charge origin showed minor shifts on the Si-O bands, which suggested that Li^+ ion migrates to the hexagonal cavity formed by the tetrahedral sheets (Komadel, 2003).

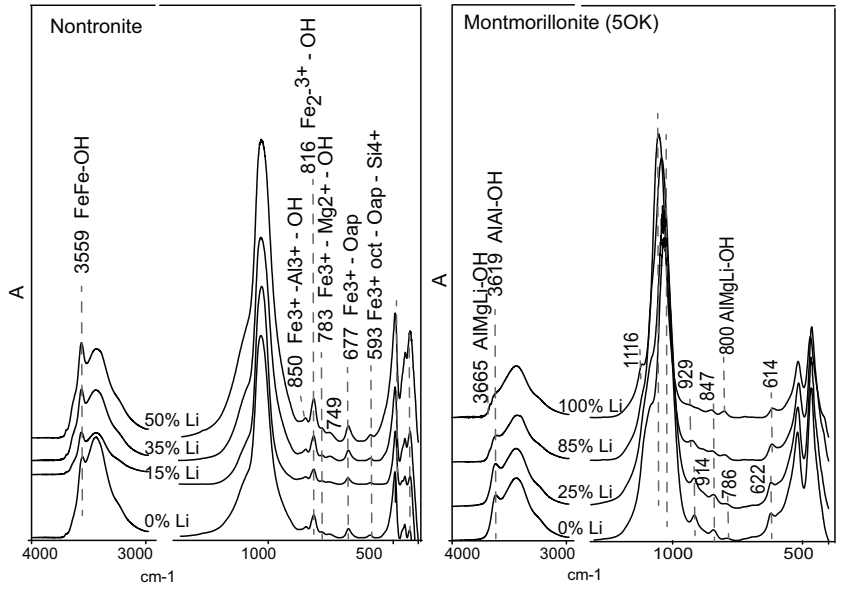

Figure 3.8: FTIR spectra of Li-treated montmorillonite 5OK and nontronite at 0% humidity.

3.4 Discussion

3.4.1 Effects of exchangeable cation on aflatoxin adsorption

The effect of the exchangeable cation has been observed in the adsorption of non-ionic compounds by smectites (Johnston et al., 2004; Aggarwal et al., 2006; Liu et al., 2012; Deng et al., 2012). The effects of the cations, however, differed from compound to compound. The adsorption of atrazine by beidellite and saponite was enhanced with Cs^+ and K^+ saturation but low adsorption was observed on Ca^{2+} and Na^+ saturated clays (Aggarwal et al., 2006). The lower hydration energy of Cs^+ and K^+ allowed the cation to get closer to the surface charge and reduce the interlayer space. Closer layers enhanced the adsorption of atrazine due to the planar molecule oriented parallel to the clay's surface and bound tightly to the hydrophobic surfaces (Aggarwal et al., 2006).

The present study demonstrated that the interlayer cation exerted the same effects on the adsorption of aflatoxin for all the smectite samples. The higher adsorption observed in the Ba-saturated clays, was in agreement with previous reported experiments (Deng et al., 2012). The lower hydration energy of Ba resulted in less amount of water held in the interlayer space, which allowed more space for aflatoxin molecules.

3.4.2 Effect of layer charge density on aflatoxin adsorption

The affinity of smectites for neutral organic compounds was also determined by the structural charge of the smectite. In the early studies by Laird et al. (1992), the adsorption of atrazine by different smectites showed an inverse correlation between the clay affinity and the CEC. Jaynes and Zartman (2011) observed a similar effect of the clays charge density on the adsorption of aflatoxin in corn meal solution, in which proteins and other organic compounds were present. At low afla-

toxin concentrations, the mycotoxin retention was higher for the low-charge smectite (CEC=76.4 cmol(+)/kg) in comparison to the high-charge smectite (CEC=125 cmol(+)/kg (Jaynes and Bigham, 1987). The results by Deng et al. (2012) also demonstrated that high layer charge density can significantly reduce the affinity and maximum adsorption of aflatoxin molecules. When a high charge smectite (5OK)(0.49 charge/half unit cell) was used, the maximum aflatoxin adsorption of the Ba-saturated clay was 0.4 mol/kg. The aflatoxin adsorption isotherm of this high charge smectite did not fit the Langmuir model. In contrast, a low charge smectite (0.34 charge/half unit cell) adsorbed aflatoxin up to 0.61 mol/kg.

Jaynes and Zartman (2011) observed an increase in the aflatoxin adsorption in corn meal when the layer charge density of a high charge smectite was reduced by Li-treatment. Similarly, reducing the layer charge of montmorillonite 5OK and nontronite, increased the adsorption of aflatoxin in both samples. As the CEC was reduced, a maximum toxin adsorption was reached at an optimal CEC around 86 cmol/kg. The main difference was that Li-nontronite only adsorbed up to 0.5 mol/kg, while Li-montmorillonite (5OK) reached a maximum adsorption of 0.8 mol/kg at the similar CEC value. In addition, the low adsorption affinity in nontronite at the original CEC was increased as the layer charge was reduced. The results indicated that it is possible to modify high charge density clays to improve their adsorption for aflatoxin.

3.4.3 Effect of layer charge origin on aflatoxin adsorption

Most of the studies observed an increase on the adsorption of non-polar organic compounds like atrazine and dioxins with tetrahedral charged clays (Aggarwal et al., 2006). A comparison of the atrazine adsorption on two smectites (beidellite and montmorillonite) with similar CEC but different layer charge origin demonstrated

the higher binding affinity of the tetrahedral charged clay (beidellite) (Aggarwal et al., 2006).

The results from the Li-treated montmorillonite and nontronite indicated the influence of the layer charge origin. Comparing the maximum adsorption of both Li-treated clays at a CEC about 80 cmol/kg, montmorillonite reached a higher adsorption than nontronite. This observation indicated that octahedral charged clays, montmorillonite, are better aflatoxin binders than smectites with the charge arises from the tetrahedral sheets. Another evidence of the charge location effect was observed by comparing aflatoxin adsorption on hectorite and beidellite. The CEC of beidellite was similar to hectorite but the adsorption of aflatoxin was significantly lower in the tetrahedral charged beidellite. A possible explanation could be the structural configuration of aflatoxin. Atrazine and dioxins are planar compounds that benefit from a closer or reduced interlayer spacing. The aflatoxin molecule is not completely planar, and it has a tilted end furan ring. The reduced layer charge of Ba-nontronite increased the adsorption but the more localized charge and the lower hydration energy of the Ba cations can reduce the swelling of the interlayer, which could restrict the accessibility for aflatoxin molecules. The results of the present study indicated that smectites with high tetrahedral charge can be improved to adsorb more aflatoxin, but they were not as effective as the octahedral charged smectite.

3.4.4 Effect of octahedral cation composition on aflatoxin adsorption

The aflatoxin adsorption experiments by Jaynes and Zartman (2011) showed a slight difference in the adsorption capacity between hectorite and montmorillonite, both octahedral charge smectites with similar CEC (89 and 76 cmol/kg, respectively). The trioctahedral smectite (hectorite) absorbed more aflatoxin in compari-

son to the dioctahedral smectite (montmorillonite), but this effect was not addressed. The higher adsorption of the hectorite in this study in comparison to montmorillonite (4TX) was mainly attributed to the lower CEC of the hectorite.

The influence of the octahedral cation composition was also addressed by comparing the aflatoxin adsorption of similar charge origin and layer charge clays. In beidellite and saponite, the charge arise from the tetrahedral sheets and both have similar CEC (70 cmol/kg). The main difference is the dominant octahedral cation, Al in beidellite and Mg in saponite. The adsorption isotherms were very similar indicating a negligible effect of the octahedral cation composition.

3.5 Conclusions

The results corroborated previous observations that the exchangeable cation strongly affects the aflatoxin adsorption and demonstrated that the effect was similar on all smectites. The exchangeable cation influenced the size and polarity matching between the adsorbing domains and aflatoxin molecules in the interlayer.

The adsorption capacity of the smectites was influenced by the layer charge density, as the negative sites on the smectite surface increased the non-polar sites available for aflatoxin molecules decreased. The results also demonstrated that the low adsorption of high charged clays can be improved by reducing the CEC.

The charge origin had a slight effect on the aflatoxin adsorption. The greater affinity and adsorption capacity of octahedral charged smectites was attributed to more diffused layer charge that reduced the repulsion of aflatoxin molecules and allowed more interlayer expansion in comparison to the more localized layer charge on tetrahedral charged smectites. Furthermore, the CEC reduction treatment demonstrated that octahedral charged smectites were the best adsorbents for aflatoxin.

The octahedral structural composition of the smectites had negligible effect on the

aflatoxin adsorption. Similar adsorption capacities were observed when comparing di- and tri-octahedral smectites with either octahedral charge origin (montmorillonite and hectorite) or tetrahedral charge origin (beidellite, nontronite, and saponite).

4. MINERALOGICAL CHARACTERIZATION OF TEXAS BENTONITES IN THE MANNING FORMATION OF JACKSON GROUP

4.1 Introduction

Bentonites are clay rocks formed from the alteration of volcanic glass and that have predominant smectite composition (Christidis and Huff, 2009). This definition is also used to describe clay rocks that contain smectites other than montmorillonite such as beidellite, saponite, and nontronite. The type of smectite, the chemical composition and the presence of additional minerals depended upon the environment in which diagenesis occurred (Grim and Guven, 1978). Diagenetic alteration of volcanic ash and hydrothermal alteration are the most common formation processes of bentonites.

Due to the importance of mineralogy in selecting clay processing procedures, their commercial applications, and as an indicator of the diagenetic processes, it is important to understand the origin, age, deposition environment, transport history, and mineral transformations that occurred in the bentonite deposits.

In the Texas bentonites, calcium is the dominant interlayer cation with minor contents of magnesium, potassium, and sodium (Grim and Guven, 1978). Bentonite deposits in Texas occur in the Eocene Yegua and Jackson groups that extend across the southeast part of the state (Figure 4.1). The Jackson group is generally divided into three formations: Cadell (lowest unit), Wellborn, and Manning (uppermost unit), and this group underlies the Catahoula formation. Roberson (1964) collected 50 samples representing different stratigraphic positions across a wide geographical distribution. All the samples showed montmorillonite as the dominant clay mineral and the presence of additional minerals was different in the strata. The samples

from the Cadell and the lower part of the Manning formations contained quartz and cristobalite in small amounts, while the samples at higher strata (upper Manning and Catahoula) container greater amounts of quartz, feldspars and calcite. Differences in the crystallinity of montmorillonite were also observed. Well crystallized montmorillonite occurred in the Cadell and the lower Manning formation indicating in situ alteration of volcanic ash. On the contrary, poorly crystallized clays from the upper Manning and Catahoula formations suggested a re-deposit material. Roberson (1964) suggested that the bentonites from the lower part of the Jackson group formed in a lacustrine environment.

The bentonitic samples studied by Chen (1968) in the Gonzales County occur in the Manning formation, and were characterized by terrestrial sediments with predominant white bentonites. The presence of very fine glass shards in the bentonite indicated that the bentonite source was a very fine vitric dust. Chen (1968) proposed that the bentonite deposits in Gonzales county formed by a process that started with the deposition of the very fine glass material in both restricted water bodies and open sea. The ash deposited on sea water remained suspended allowing for more reaction time with alkalic water. In this process, the Mg from sea water promoted the formation of montmorillonite. The high opal content in the central deposits was due to accumulation of silica during diagenesis of the volcanic ash in a restricted depositional environment.

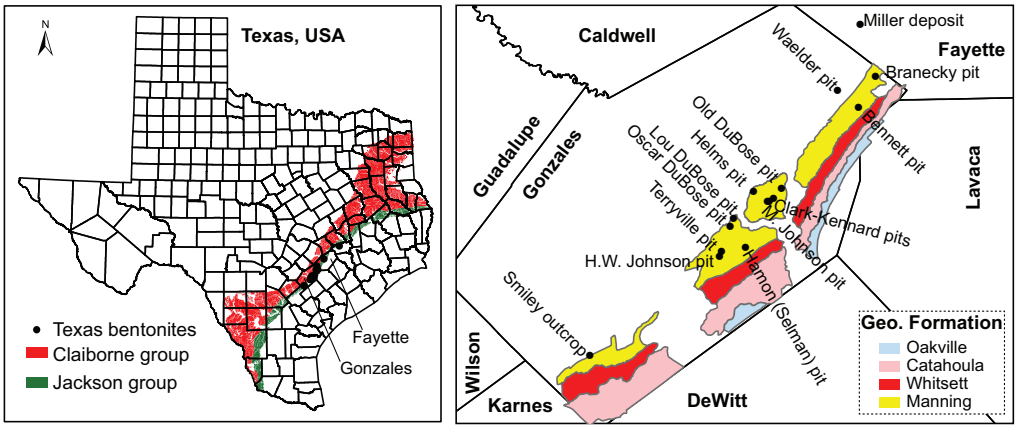

Figure 4.1: Location of the Yegua and Jackson groups in Texas (left), and (right) the location of the bentonite deposits in Gonzales county with delineation of the geologic formations of the Jackson group according to Chen (1968).

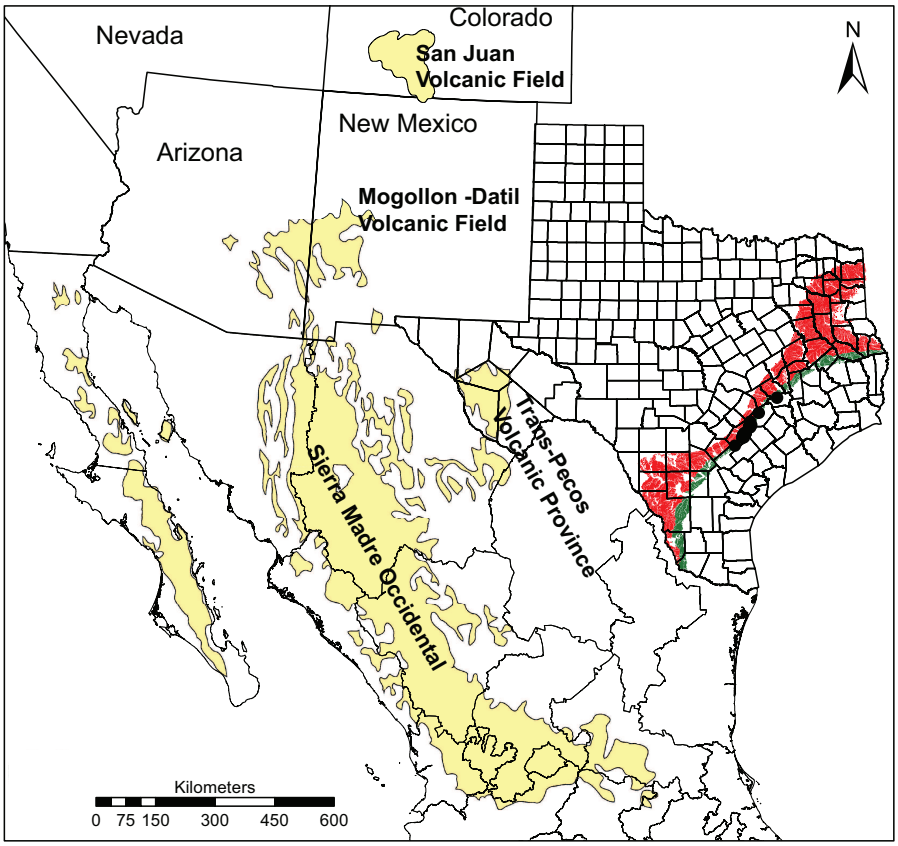

Figure 4.2: Location of the Texas bentonite deposits sampled (black circles), and the possible sources of volcanic ash. The map representing the tertiary volcanic rock (volcanic fields) is based on Swanson et al. (2006).

4.1.1 Volcanic ash source

One of the main questions about the bentonite deposit in Texas is the source of the rhyolitic volcanic ash. The major volcanic activity from middle to late Eocene (46-27.5 Ma (Heintz et al., 2014)) was reported from the volcanic fields from the western part of USA and Northwest of Mexico (Figure 4.2).

Michaelides (2011) compared the rare earth elements (REE) and trace elements available for the North America Volcanic and Intrusive Rock Database (NAVDAT) samples from southern Mexico. Although, the Gonzales bentonites matched the composition of NAVDAT CON-75 sample from Oaxaca state in Mexico, this volcano is younger (30.6-32.2 Ma) than the Ar-Ar dating reported for the Texas deposits. More recently the studies by Heintz et al. (2014) demonstrated that the Sierra Madre Occidental of Mexico was the source of the rhyolitic volcanic ash.

Debates on the origin and the geochemical processes affecting the deposits remain unsettled. The objectives of this study were: 1) to delineate the geological and geochemical processes affecting east-central Texas bentonites, based on reported and new mineralogical data, and 2) To analyze the mineralogical properties of natural Texas bentonites for the selection of aflatoxin binders.

4.2 Materials and methods

Bentonite and partially altered volcanic ash samples were collected from six locations: 1) a white ash layer from the Somerville Lake spillway in Washington County, 2) brown and yellow clays at the Miller pit, 3) white and blue clays at the Helms, Clark-Kennard, Magdalene Johnson, and DuBose pits, 4) white gray clay at the HW Johnson pit, 5) a partially altered white volcanic ash at Smiley outcrop, and 6) a white clayey volcanic ash at Sickenious pit in Karnes County. Based on the delineation of the geologic formation of the Jackson group described in Chen (1968)

the bentonite deposits in Gonzales county belong to the Manning formation. The smiley outcrop is located in the boundaries between the Manning and the Whitsett, and the Miller deposit belongs to the Clairborne group (Figure 4.3). Five volcanic ash samples were collected to compare the chemical composition of the ash: 1) Somerville spillway upper ash, 2) Somerville spillway lower ash, 3)Kennard ash, 4) Smiley outcrop ash, and 5) Sickenious ash.

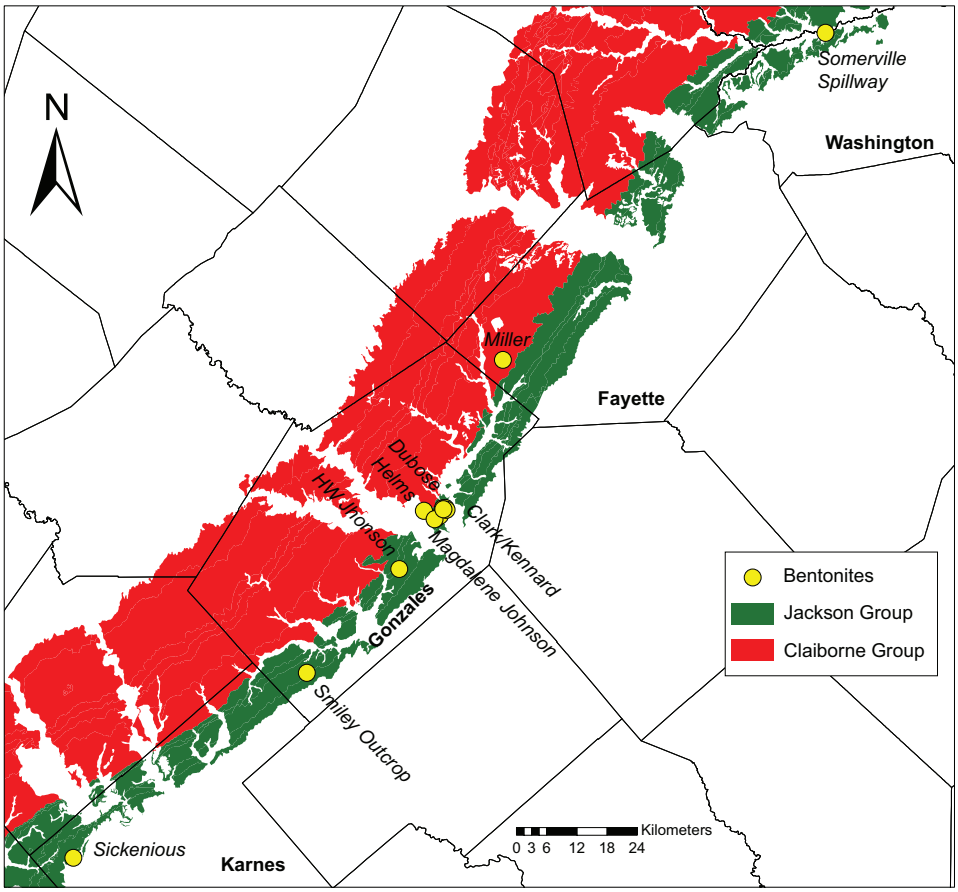

Figure 4.3: Location of the bentonite and ash samples collected in Washington, Fayette, Gonzales, and Karnes Counties. The Miller deposit occurred on the Clairborne group (middle Eocene) and the other deposits or sites occurred on the Jackson group (upper Eocene).

4.2.1 Description of the bentonite deposits and samples

4.2.1.1 Somerville spillway

Different strata were observed in the Somerville profile but the mid section was chosen as two ash layers can be distinguished. A white ash layer occurred above the lignite which was underlaid by another ash layer denominated as lower ash. The white ash and the lower ash samples were included in the analysis to compare the composition with the ash from the bentonite deposits in Gonzales County. Detailed stratigraphic data and the chemical composition has been previously addresses by Yancey and Guillemette (1998) for the Somerville spillway (Figure 4.4).

4.2.1.2 Miller deposit

Located in Fayette County, the Miller deposit is characterized by brown bentonites. The miller deposit occurred on the Yegua formation (Figure 4.3), which was the oldest deposit among the bentonite samples collected. Three layers where distinguished in this pit: 1) a top mudstone, 2) a brown bentonite, and 3) a yellow bentonite (Figure 4.5).

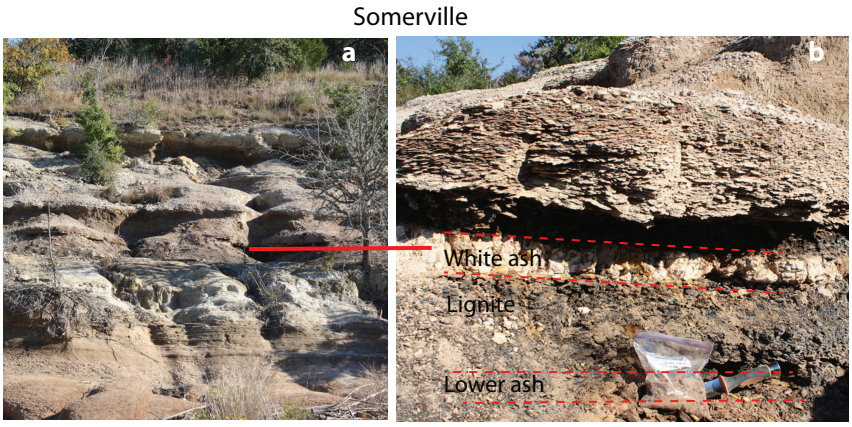

Figure 4.4: Somerville spillway sample profile: a) full stratigraphic profile, and b) upper white ash layer above the lignite and the lower ash layer underneath.

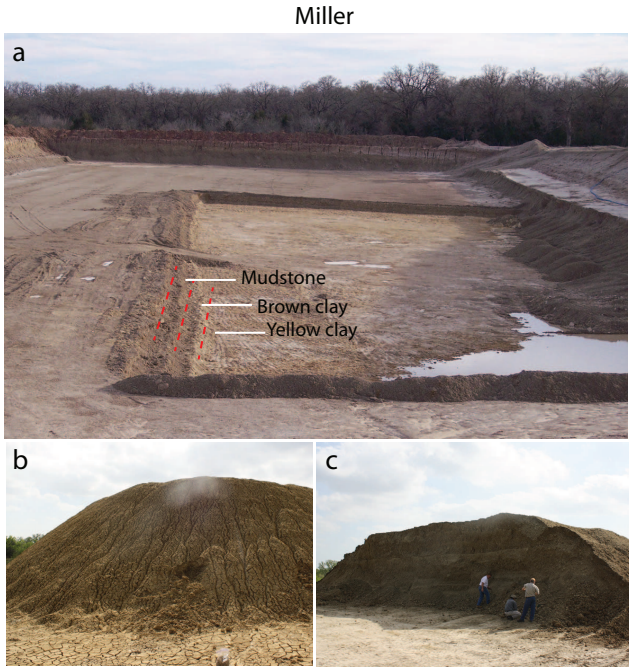

Figure 4.5: Miller deposit sample profile: a) the Miller pit showing the three layers (mudstone, brown clay, yellow clay), b) the pile of brown bentonite were sample was collected, and c) the pile of yellow bentonite were sample was collected.

4.2.1.3 Central deposits: Clark-Kennard, Magdalene Johnson, DuBose

The central deposits are the same continuous bentonite layer occurring at different properties. The bentonite bed on the northeast side was the DuBose pit characterized by a blue bentonite (Figure 4.6). The deposit has been divided into sections for bentonite extraction. In DuBose No. 2 pit, there was a layer of ash-like material above the bentonite layer and the bentonite bed was confined by a sandstone layer underneath. A sample was collected from the bottom of the bentonite bed at DuBose No.2 pit. The DuBose No. 3 pit is a continuation of the blue bentonitic bed from the DuBose No.2, with a distinct thin (10 cm) band of white bentonite above the blue bentonite. The blue clay extents to the Kennard deposit. In these two deposits, an ash layer was observed above the blue bentonite and both layers were sampled. The Clark pit was adjacent to the Kennard pit but in this deposit the bentonite had a distinct white color. In the Clark deposit, two layer of bentonites were observed as a hard-clay and a soft-clay. The Magdalene Johnson deposit occurs on the west side to the Clark deposit and occurred as pinkish clay.

Figure 4.6: Images and sample description of the central bentonite deposits in Gonzales, TX: a&b) Old DuBose deposit with characteristic blue bentonite and visible pyrite oxidation, c) also blue bentonite in the Kennard deposit, d) Clark deposit contained a layer of hard clay above a soft clay layer, and e) Magdalene Johnson deposit containing similar white-pink bentonite as in Clark deposit but gypsum precipitated at the top of the bed.

4.2.1.4 Helms

In the Helms deposit, a partially altered volcanic ash layer is sandwiched between a thin (10 to 30 cm) upper white bentonite layer and a thick (1.5 m) lower white bentonite layer. Samples were collected from the upper white bentonite, the ash layer subdivided into upper and lower ash, and the bentonite layer underneath the ash. In the Helms deposit, large masses of manganese oxides occur in the lower bentonite as well as red, orange, and black coatings along the surfaces of bentonite blocks. Samples of the Mn-oxides pockets and the iron oxides coatings were collected (Figure 4.7).

4.2.1.5 HW Johnson

The HW Johnson deposit was characterized by a layer of blue bentonite between two layers of white bentonite. The thickness of the blue bentonite layer varied across the deposit. The blue bentonite layer became thinner toward the Northeast side of the pit. Black manganese oxide coatings were observed at the top of the upper white bentonite layer. A sample of each bentonite layer was collected (Figure 4.8).

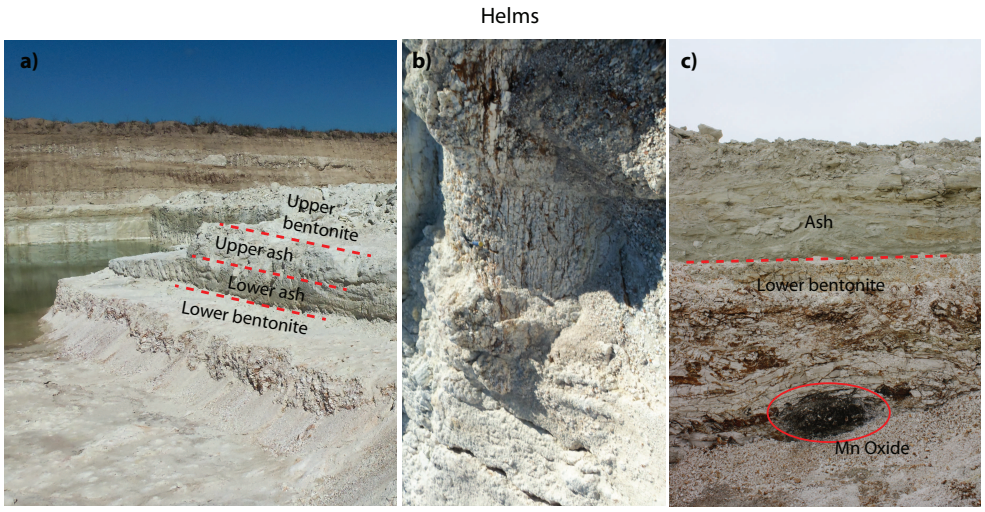

Figure 4.7: Helms deposit: a) illustration of the bentonite and ash layers, b) Fe-oxides and Mn-oxides precipitations along the cracks in the bentonite layer, and c) Mn-oxide pockets concentrated in the lower bentonite layer.

Figure 4.8: HW Johnson deposit: a) shows the three bentonite layers and the extent of the blue bentonite layer, b) closer image of the boundary between the top white bentonite and the blue bentonite layer, c) Fe-oxides and Mn-oxides coatings present in the upper white bentonite layer.

4.2.1.6 Smiley outcrop

The outcrop was located in the southwestern part of the Gonzales county. A white ash was identified above a white bentonite layer (Figure 4.9).

4.2.1.7 Sickenious

The Sickenious sample was located in Kernes County and consisted of a white ash. This sample was previously reported by Heintz et al. (2014).

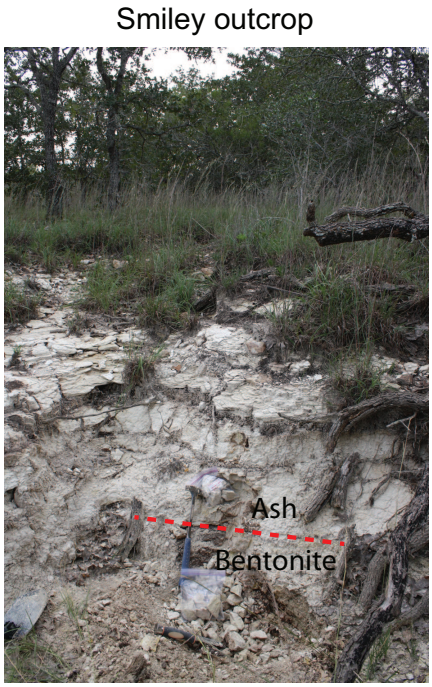

Figure 4.9: Smiley outcrop sample profile showing the white ash and white bentonite layers.

4.2.2 Mineralogical characterization

The samples were air-dried and ground to pass the 60 mesh sieve. Each sample was fractionated to obtain the sand, silt, and clay fractions following the procedures described in Deng et al. (2006).

The sand and silt fractions were oven-dry, ground and mounted for powder X-ray diffraction (XRD) analysis. The XDR patterns were recorded from 2 to 70 degree 2-theta using a D8 Bruker ADVANCE diffractometer, CuKα radiation, 30 rpm spin rate, and a 0.05 step size. A Sol-X detector was used during the XRD analysis. The clay fraction was saturated with K and Mg. The diffraction patterns were recorded from 2 to 32 degree 2-theta for the K-saturated clays at room T, and after heating at 300°C and 550°C, and for Mg-saturated clays at room T and after glycerol solvation.

A few drops of the silt fractions were kept in suspension and one or two drops were added on a PELCO image tabs (Ted Pella INC) for Scanning electron microscope analysis (SEM). The samples were coated with platinum/palladium and SEM images were obtained using a FEI QUANTA 600F. Chemical composition was checked with energy dispersive X-ray spectra (EDS).

A diluted clays dispersion was used for the transmission electron microscope (TEM) sample analysis. One drop of the clay dispersion was placed on a lacey carbon type-A copper grid (Ted Pella INC) and dried under a heating lamp.

The structural composition of the clay fractions was also analyzed with Fourier Transform Infrared (FTIR) spectroscopy. A portion of the clay suspension was placed on ZnS windows and air-dried. FTIR spectra were recorded using a transmission mode on a Perkin Elmer Spectrum 100 FTIR spectrometer with an average of 32 scans at a resolution of 2 cm^{-1}.

4.3 Results

4.3.1 Mineralogical characterization of bentonite deposits

4.3.1.1 Miller deposit

The mineralogical characterization of the mudstone, brown clay, and yellow clay showed smectite as the main mineral but major differences were observed in the silt fraction (Figure 4.10). The top layer (mudstone) showed a broad and intense peak due to opal at 4.08 Å. The two clay layers showed a very sharp peak at similar d-value due to feldspars, indicating low opal content. The quartz and feldspars were concentrated in the lower layer, the yellow clay, which also contained minor amounts of clinoptilolite (9.01 and 7.92 Å) and mica (9.92 Å).

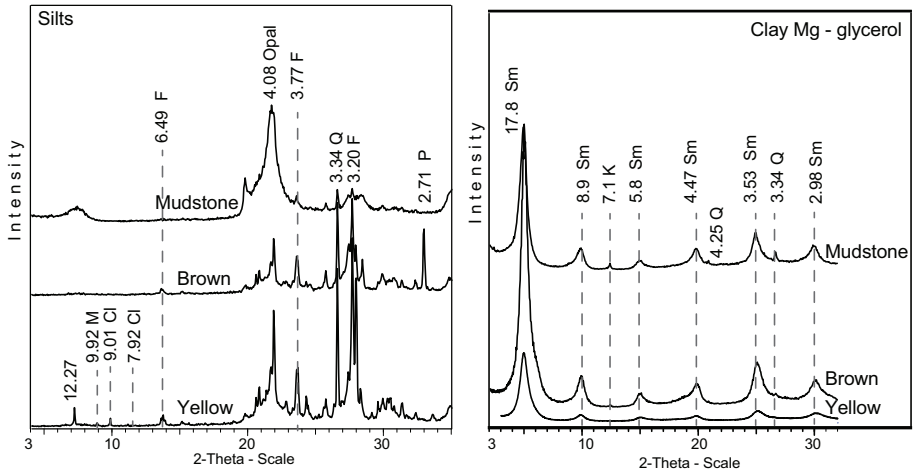

Figure 4.10: XRD patterns of the Miller deposit samples: left) silt fraction and right) the Mg-glycerol clay treatment. Cl: clinoptilolite, M: mica, Q: quartz, F: feldspars, P:pyrite. The d-value units are Å.

4.3.1.2 Central deposits: DuBose, Kennard, Clark, and Magdalene Johnson

The DuBose pit is characterized by blue and white bentonites. The profile in the Dubose No.3 site was distinguished by an upper thin layer of white bentonite, underlain by sand, and a thicker blue bentonite bed. Located about 0.35 miles from the previous pit, in the Dubose No.2 site there was presence of blue bentonite layer underlaid by sandstone.

The mineralogical composition of the three samples collected at Dubose No.3 site indicated that smectite was the major mineral in all samples, as indicated by the 14.7 Å peak (Figure 4.12). Quartz and feldspars were present but more concentrated in the upper bentonite layer, indicated a more reworked material. Additionally the sharp 4.04 Å peak in the upper white bentonite was associated with feldspars, but the broad reflection in the lower bentonite layer was characteristic of opal. The color difference was attributed to pyrite (2.71 Å peak) in the blue bentonite layers.

A similar mineral abundance trend was observed on the DuBose No. 2 pit, the layer above the bentonite contained more quartz and feldspars than the bentonite (Figure 4.12), and the opal was only present in the lower bentonite layer. The bentonite sample was used for Ar-Ar dating analysis. The radiometric dating indicated that this bed was 35.196 ± 0.010 Ma years old (Heintz et al. (2014)). The Kennard deposit, which is a continuation of the DuBose pit, had a similiar mineral composition dominated by the presence of feldspars (Figure 4.11).

The central deposits, Clark and Magdalene Johnson, characterized by white-pink bentonite also showed high feldspars composition. Greater amount of opal-CT was observed in the Clark deposit than in the Magdalene Johnson (Figure 4.11). The difference between the Clark hard-clay and soft-clay was attributed to the presence of opal-CT in the hard-clay (Figure 4.13).

The Clark and Magdalene Johnson deposits occurred at lower depth than the DuBose and Kennard deposits. Pyrite was the mineral identified in all blue bentonite samples. The cemented sandstone layer underneath the blue bentonite might have caused poor drainage and therefore anaerobic conditions that favored the precipitation of pyrite.

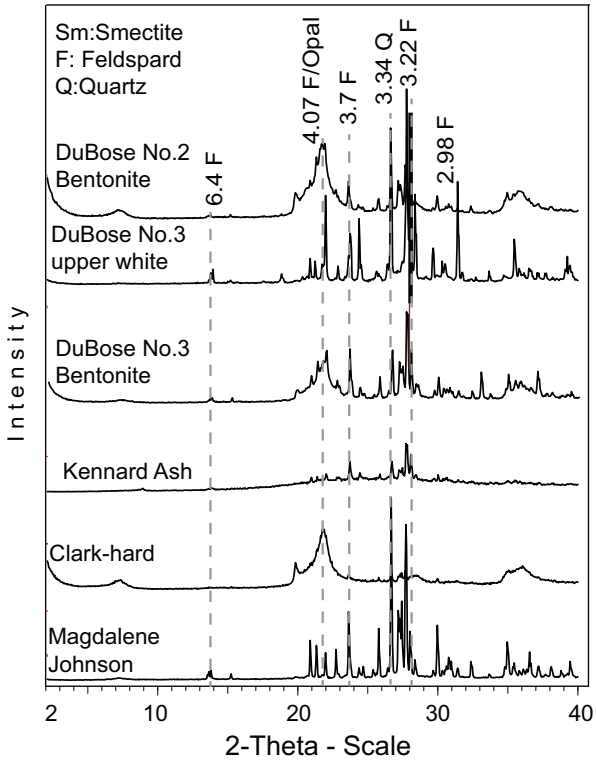

Figure 4.11: XRD patterns of the silt fractions of the central bentonite deposits. M: mica, Q: quartz, F: feldspars. The d-value units are Å.

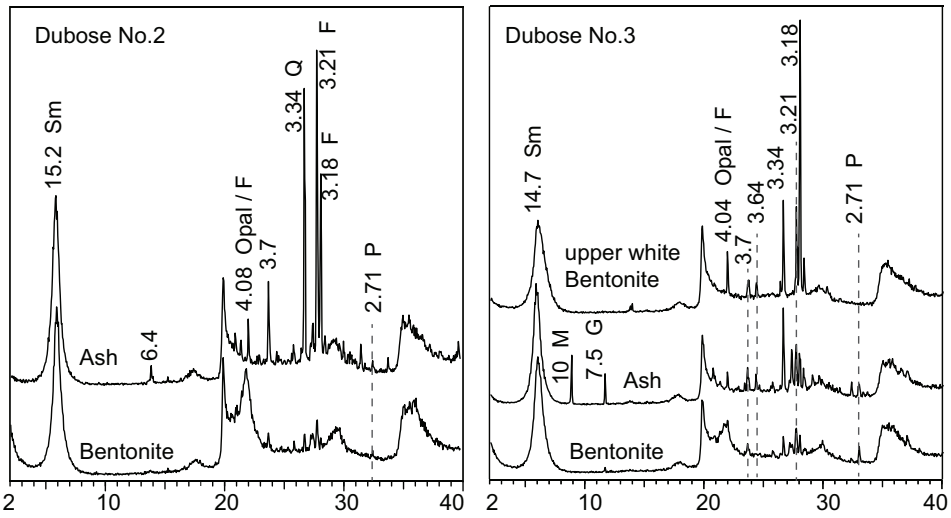

Figure 4.12: Mineralogical composition of the BuBose No.2 and No.3 unfractionated samples. G:gypsum, M: mica, Q: quartz, F: feldspars, P:pyrite, Sm: smectite. The d-value units are Å.

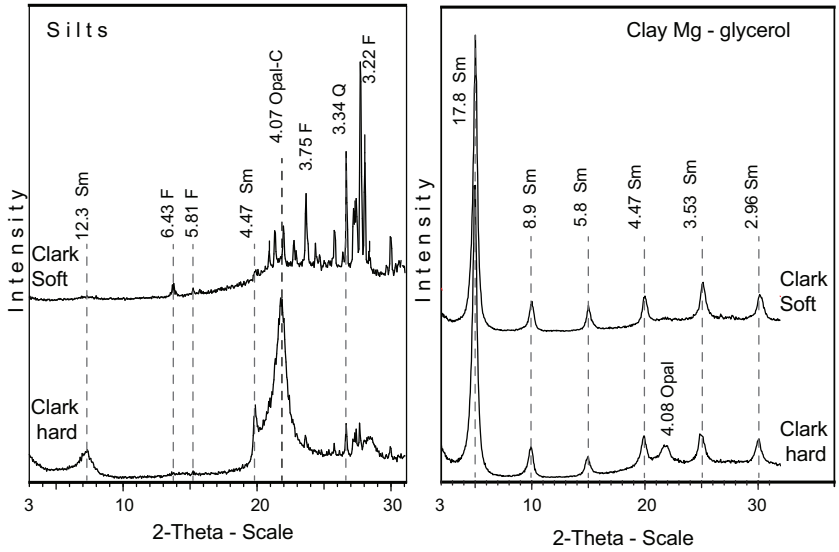

Figure 4.13: Mineralogical characterization of the soft-clay and hard-clay samples of the Clark deposit. Q: quartz, F: feldspars, and Sm: smectite. The d-value units are Å.

Helms pit

The upper and lower bentonite layers were similar in their mineralogy composition: smectite was the major mineral and both samples contained opal-C (Figure 4.14). The major difference between the bentonites was the presence of quartz only in the upper layer. Suggesting that the lower bentonite formed in place while the upper bentonite was a reworked material.

In the helms deposit, two Mn-oxides samples were collected: 1) from the accumulation piles separated during the mining process, and 2) from a pocket occurring at the lower bentonite layer. The mineralogical characterization indicated different Mn-oxides minerals present in both samples. Rancieite and birnessite were identified in the Mn-oxide sample from the piles (Figure 4.15). The 7.4 Å peak due to rancieite disappeared upon heating at 300°C. Diverse morphology was observed in the clay particles by TEM (Figure 4.16). The elongated lath shaped particles were identified as birnessite and the small globular aggregates were attributed to rancieite particles. The distinction was based on measurement form the fringes that gave d-value corresponding to each Mn-mineral, furthermore, the chemical composition indicated calcium content in the globular particles, a particular characteristic of rancieite with non-exchangeable Ca. The second Mn-oxide sample had todorokite and birnessite (Figure 4.17). In the TEM images, characteristic particle twining was observed for the Mn-oxide particles (Figure 4.18).

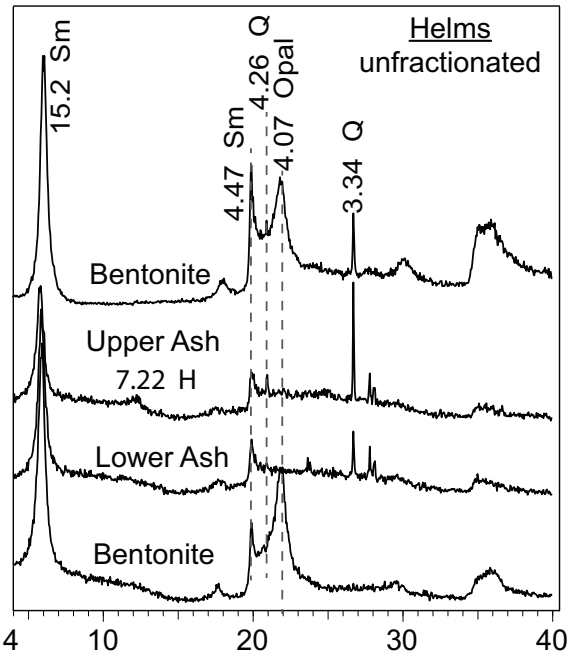

Figure 4.14: Mineralogical composition of the unfractionated samples of the Helms profile. Q: quartz and Sm: smectite. The d-value units are Å.

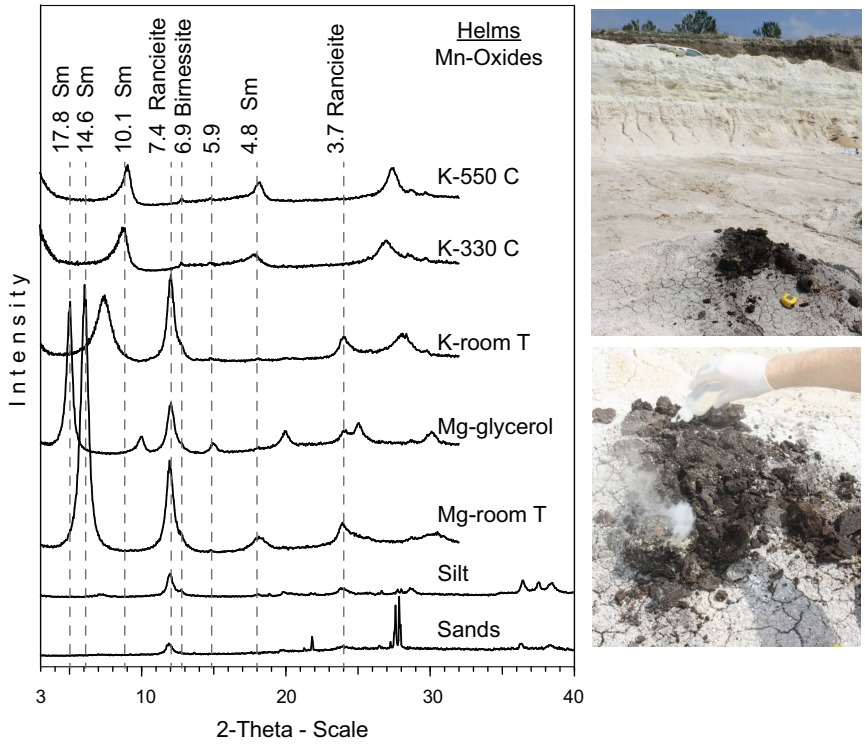

Figure 4.15: X-ray diffraction pattern of the sand and silt fractions and the clay treatments of the Mn-oxides pockets sample.

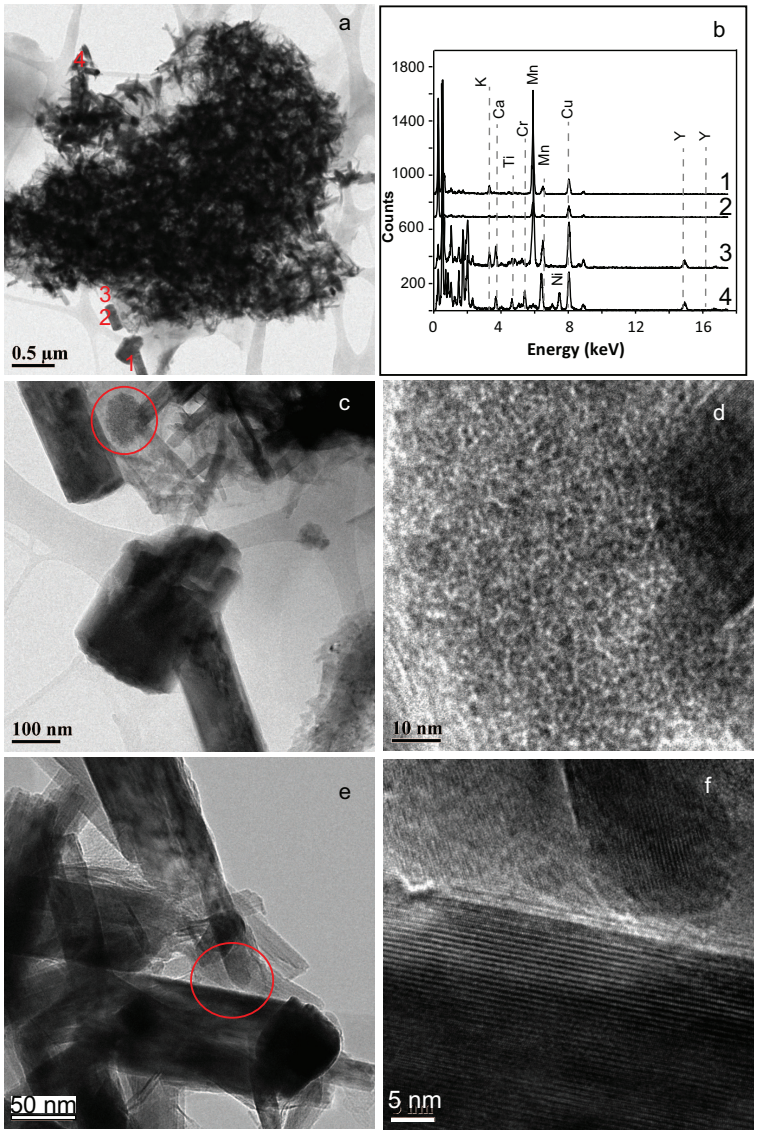

Figure 4.16: TEM images of the clay fraction of the Mn-oxides pockets sample: a) cluster of Mn-oxide particles, b) EDS spectrum of each particle numbered in figure a), c)lath-shape particles identified as birnessite, d)higher magnification of the cluster of particles in image c), e&f) closer magnification and lattice fringes observed in the lath particles.

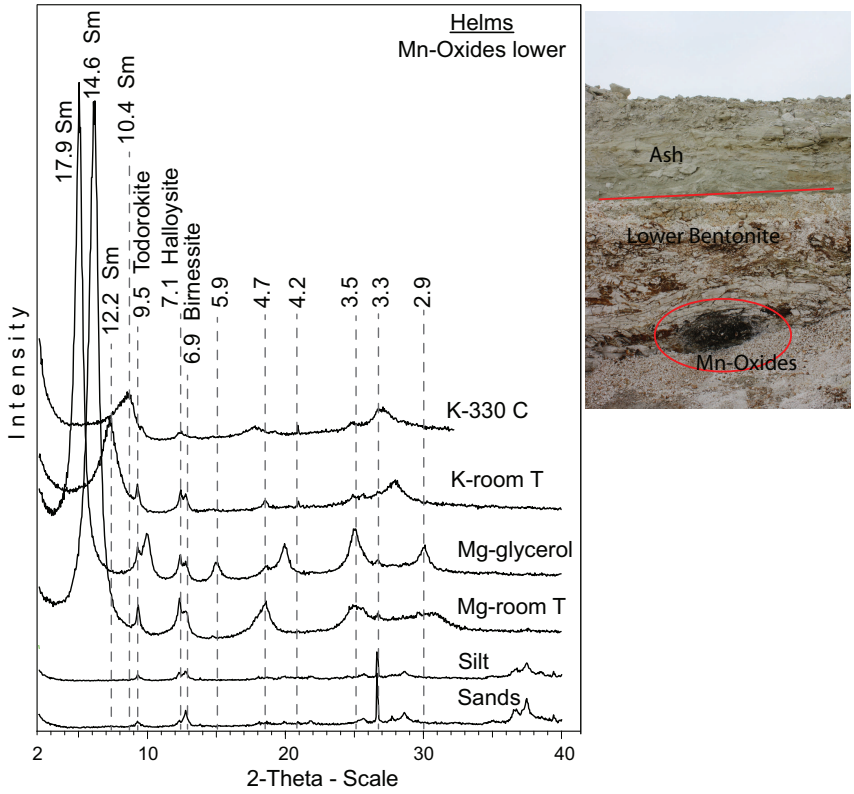

Figure 4.17: XRD patterns of silt, sand and clay-treatments for the Mn-oxide sample collected from the pocket at the bentonite layer.

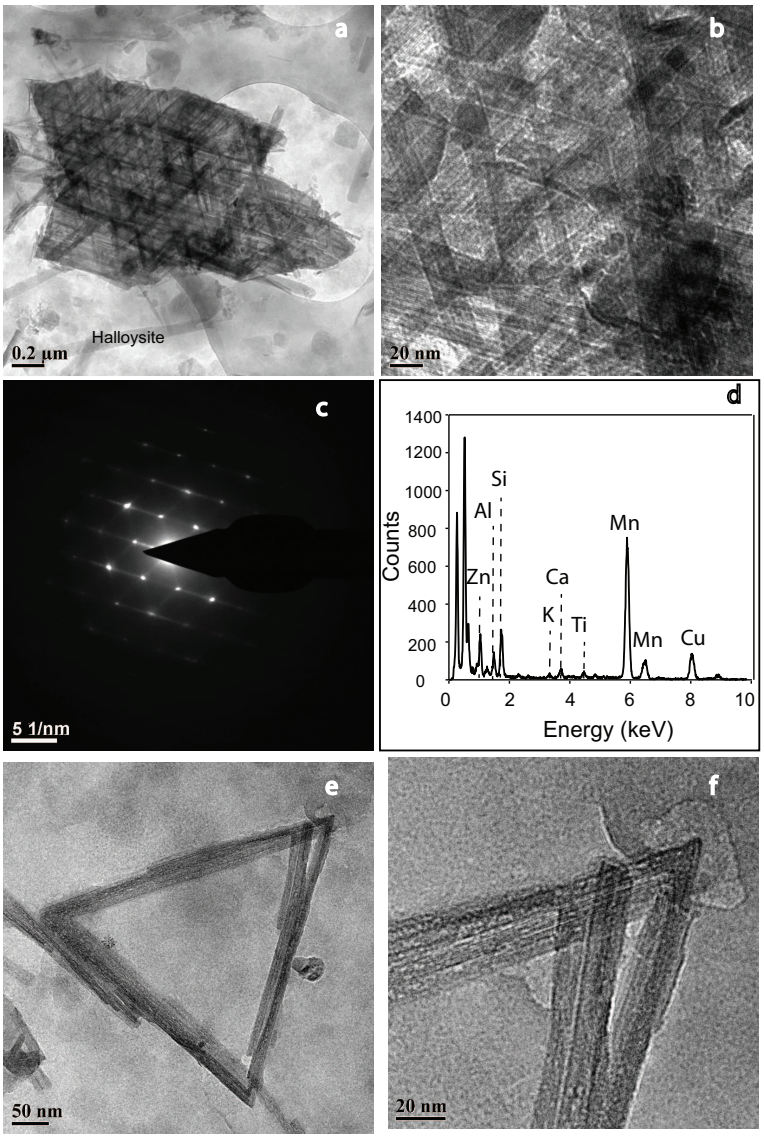

Figure 4.18: TEM images of the Mn-oxides pocket sample collected at the bentonite layer: a) Mn-oxide particle, b) higher magnification of particle a), c) selected area electron diffraction of particle a), d) EDS spectrum showing the chemical composition of particle a), and e&f) todorokite particles.

HW Johnson pit

In this deposit a blue bentonite was sandwiched between two layers of white bentonite and abundant manganese oxides coatings were observed on the top of the upper white bentonite. The samples contained more than 90% clay dominated by smectite with opal concentrated in upper white bentonite. The silt fractions showed that quartz and feldspars concentration increased with depth and additional minerals as clinoptilolite and mica were only present in the lower bentonite layer (Figure 4.19). Pyrite was only present in the middle blue layer. The SEM images showed abundant feldspard and opal particles with similar chemical composition (Figure 4.20).

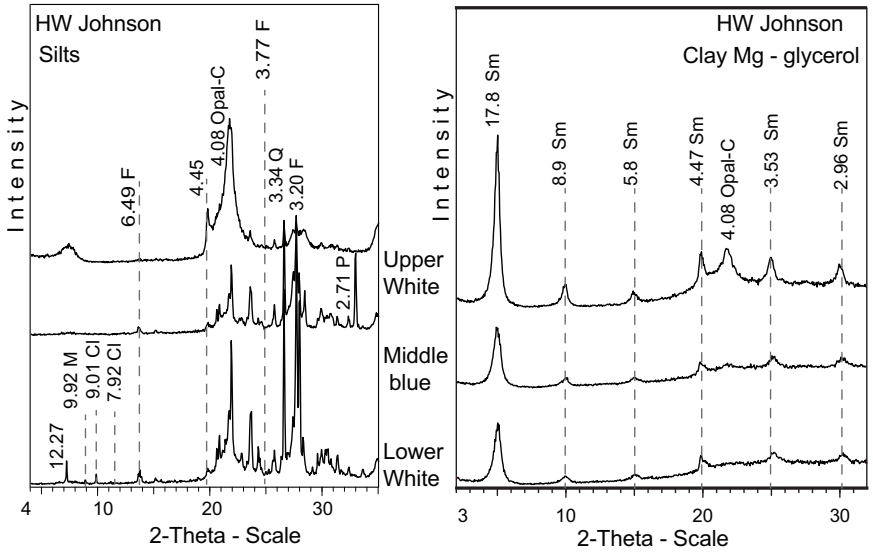

Figure 4.19: X-ray diffraction of the silt and clay fractions of HW Johnson samples. Cl:clinoptilolite, M: mica, Q: quartz, F: feldspars, P:pyrite, and Sm: smectite. The d-value units are Å.

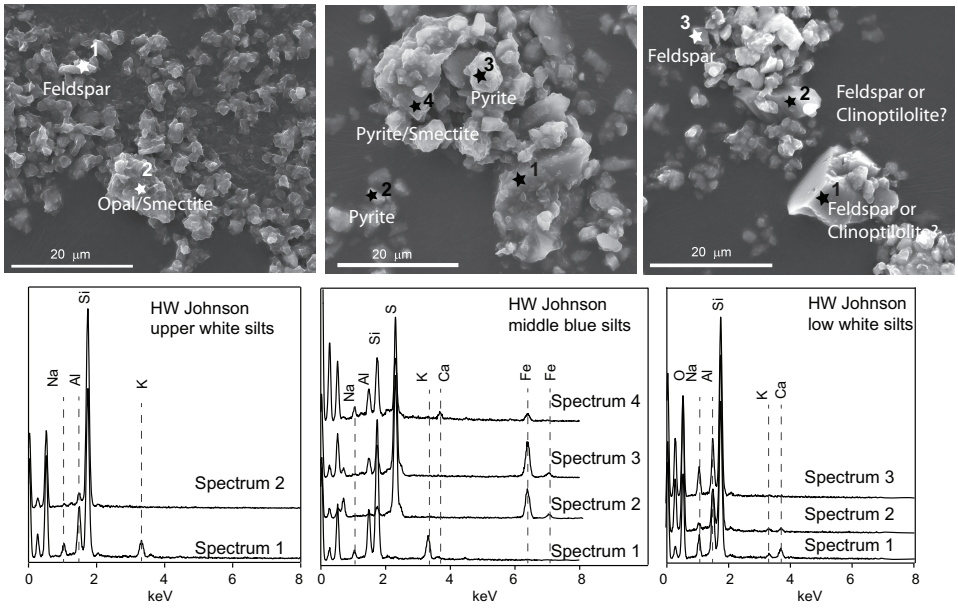

Figure 4.20: SEM images of the silt particles in the HW Johnson samples with the respective EDS spectrum below.

4.3.2 Sickenious

Feldspars were the dominant mineral in the sand and silt fractions with less content of quartz. Smectite was the only mineral identified in the clay fraction (Figure 4.21).

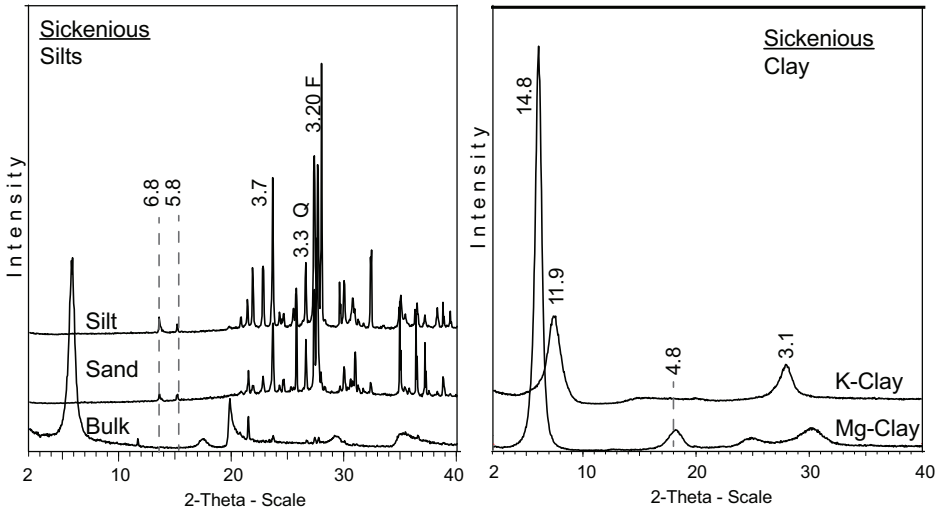

Figure 4.21: XRD patterns of the silt and Mg- and K-clay of the Sickenious sample. Q: quartz, F: feldspars, and Sm: smectite. The d-value units are Å.

4.3.3 Comparison of the volcanic ash samples

The XRD patterns of the silt fractions of ash samples collected from the Gonzales County showed quartz and feldspars as the major minerals (Figure 4.22). The presence of quartz in the Helms and Smiley ash samples indicated a reworked material. The presence of a broad "hump" in the XRD patterns indicated the presence of amorphous material such as ash.

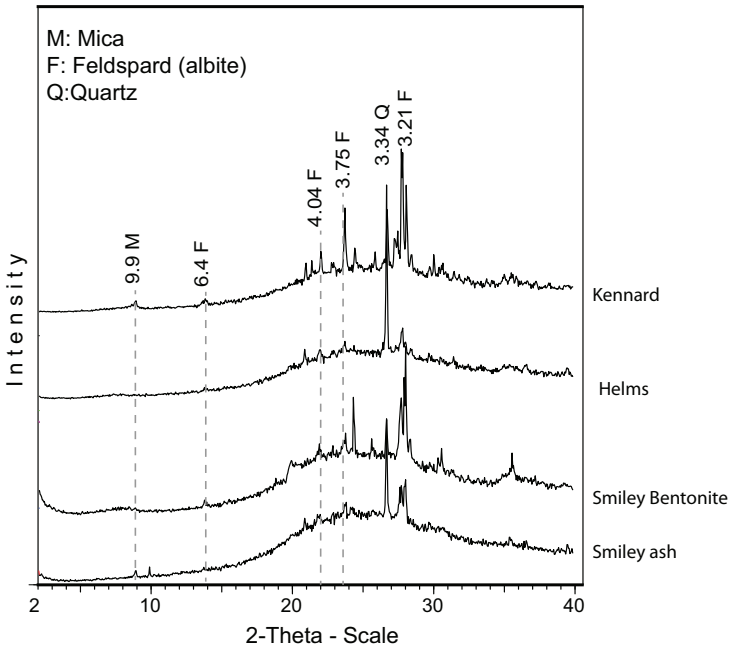

Figure 4.22: XRD patterns of the silt fractions of the ash samples. M: mica, Q: quartz, and F: feldspars. The d-value units are Å.

Significant differences were observed in the mineralogical composition of the Somerville ash samples. The upper ash sample contained smectite as dominant mineral as shown by the 15.8 Å peak. Greater accumulation of gypsum and kaolinite was observed on the XRD pattern of the lower ash sample by the presence of the sharp 7.5 Å peak and 7.1 Å peak, respectively. (Figure 4.23).

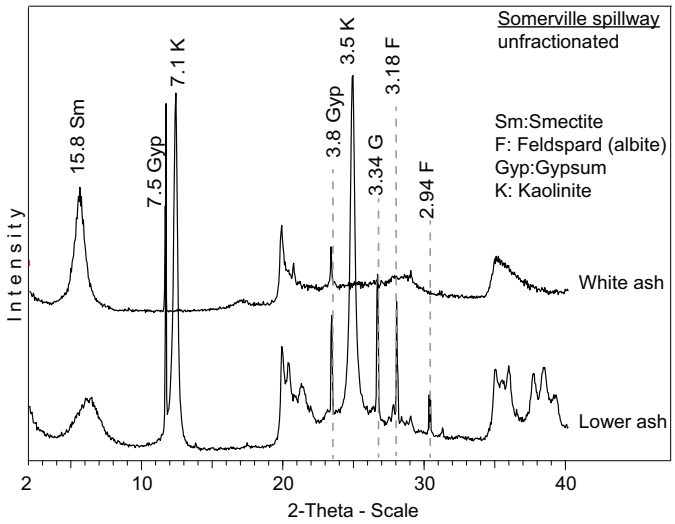

Figure 4.23: XRD patterns of the Somerville samples. G:gypsum, K: kaolinite, F: feldspars, and Sm: smectite. The d-value units are Å.

Smectite particle with the characteristic curling morphology were observed in the silt fraction of the upper ash. Additional feldspar particles were identified based on the chemical composition (Figure 4.25). The silt fraction of the lower ash layer showed abundant vermiform kaolinite particles as indicated by the diffraction patterns (Figure 4.25).

For the central deposits the only ash sample collected was in the Kennard pit. Feldspars were the main particles observed in the silt fraction by SEM. Different morphology were observed from planar to elongated particles with visible channel-like spaces but the chemical composition was similar (Figure 4.26). The channel-like morphology was an indication of air bubbles released during cooling of magma. In the silt fraction, a typical diatom particle was observed indicating the formation of the bentonites in a marine environment. Apatite particles were also observed in the silt fraction (Figure 4.26).

The ash layer of the Helms deposit contained feldspars in addition to quartz and smectite, but opal was absent in this sample. Furthermore, halloysite was identified in the upper ash sample as indicated by the 7.22 Å peak and the SEM images.

Abundant amorphous volcanic ash was still present in the Smiley outcrop samples as indicated by the broad XRD patterns (Figure 4.24). Feldspars were also identified in both ash and bentonite layers, and quartz was more noticeable in the upper ash layer. Montmorillonite was the dominant clay mineral with minor presence of halloysite, as also observed in the SEM images (Figure 4.25). On the surface of the volcanic glass particles, holes of diverse diameters were observed. The chemical composition of an ash particle where large holes were absent showed some K (Figure 4.25), but the content of K was less in the large pores, indicating weathering.

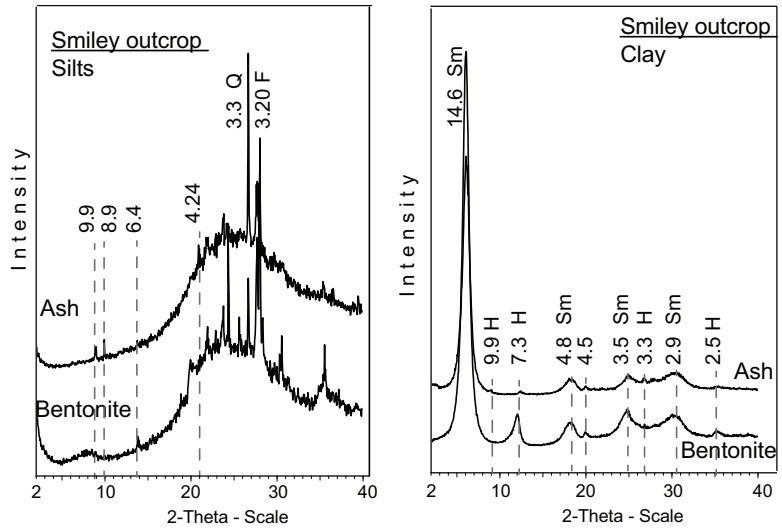

Figure 4.24: XRD patterns of the silt and Mg-clay of the ash and bentonite layers on the Smiley outcrop. Q: quartz and F: feldspars. The d-value units are Å.

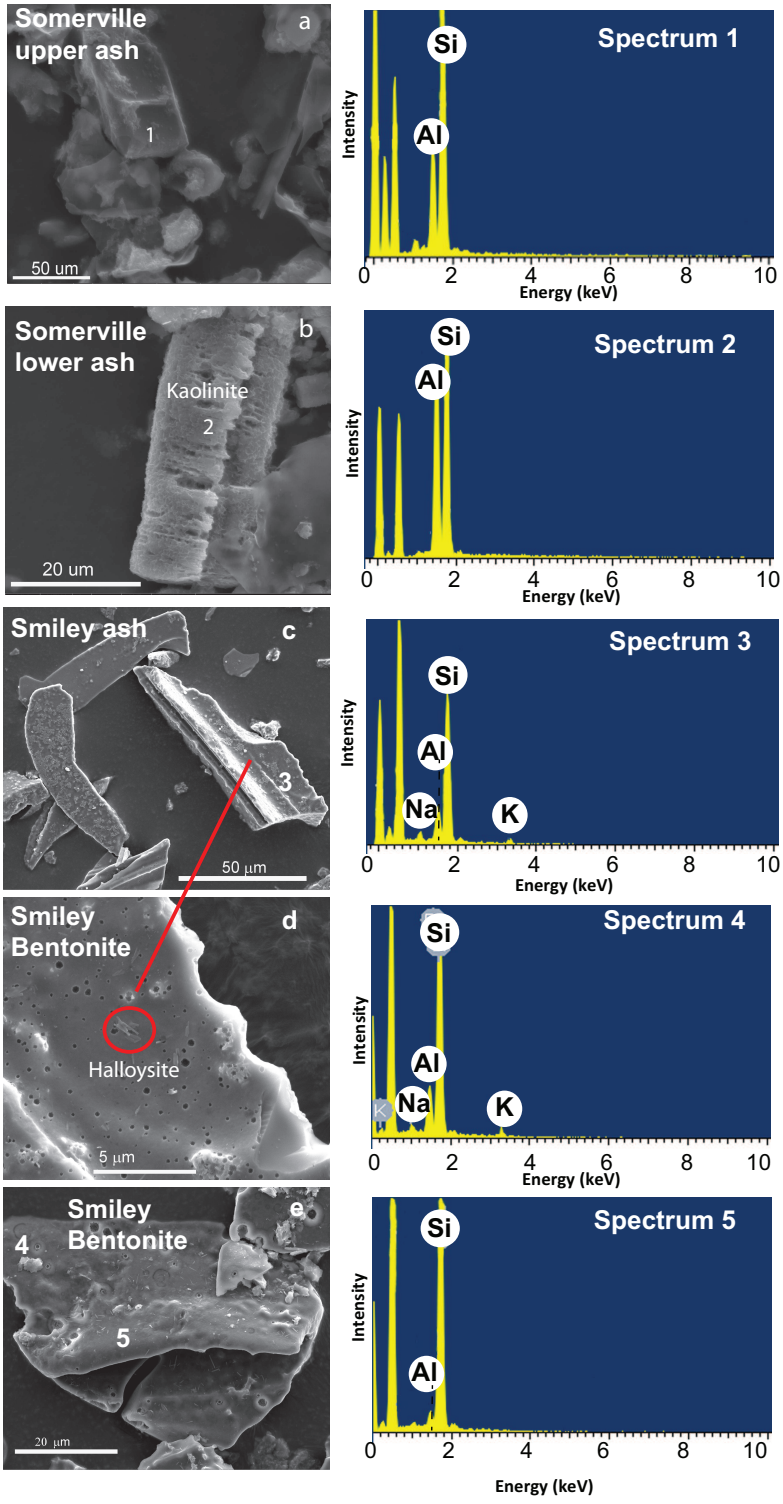

Figure 4.25: SEM images of silt particles of Somerville spillway (a) upper ash and (b) lower ash with their respective EDS spectra.

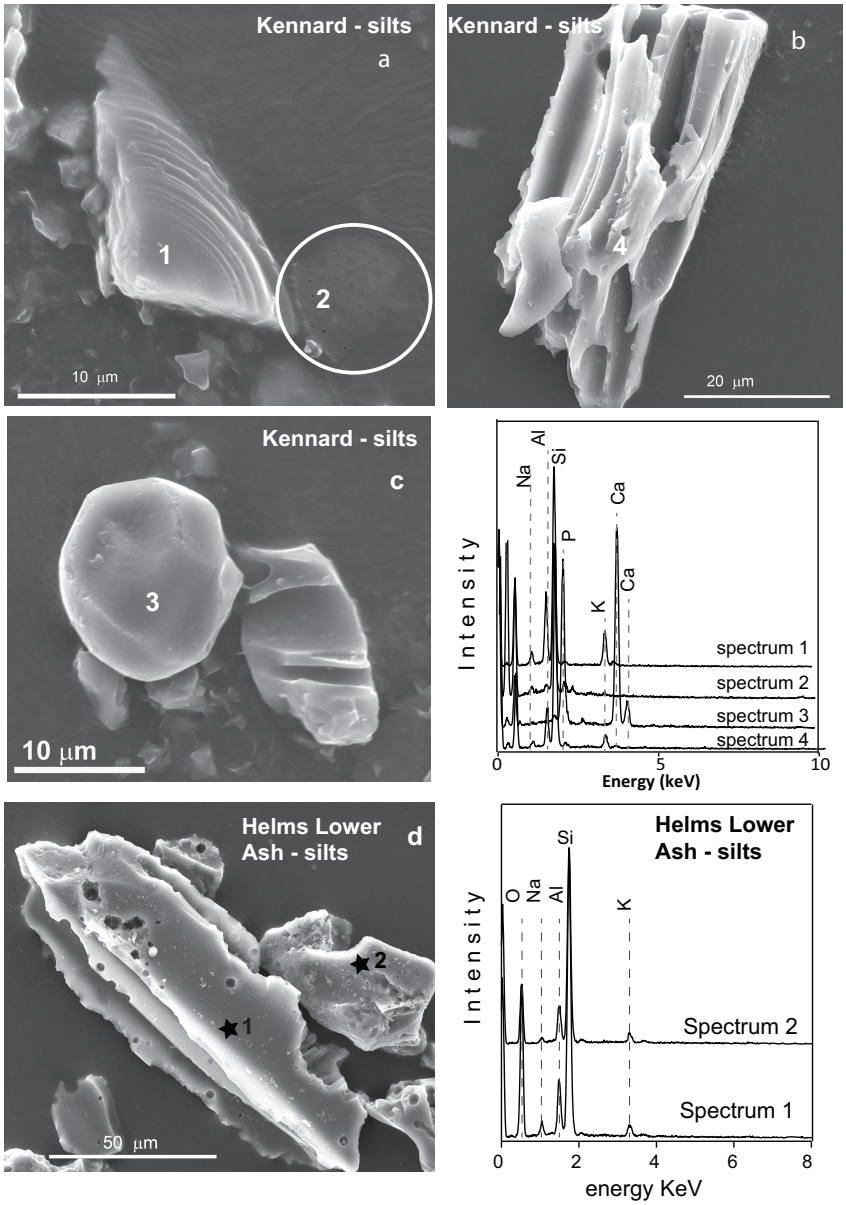

Figure 4.26: Scanning electron images of the silt particles: a&b&c) Kennard ash sample with the respective EDS spectra, and d) Helms lower ash layer with the respective EDS spectra at the left.

4.3.4 Octahedral composition

The FTIR analysis of the clay fractions showed differences in the structural cation composition (Figure 4.27). The FTIR spectra of the clays from the central deposits (Helms, Clark-Kennard, Magdalene Johnson, and DuBose) showed the distinct AlAlOH band at 918 cm^{-1} which indicated that Al^{3+} was the dominant octahedral cation, and the band at 845 cm^{-1} was attributed to Mg^{2+} substitutions. Similar AlAlOH and AlMgOH bands were observed in the FTIR spectra of the Somerville ash, Miller, HW Johnson, Smiley outcrop and the Sickenious clays, but these samples also showed a band at 885 cm^{-1} due to Fe for Al substitutions. The dominance of Al in the octahedral sheet with substitution from Mg and Fe indicated that montmorillonite was the smectite present in these bentonite samples.

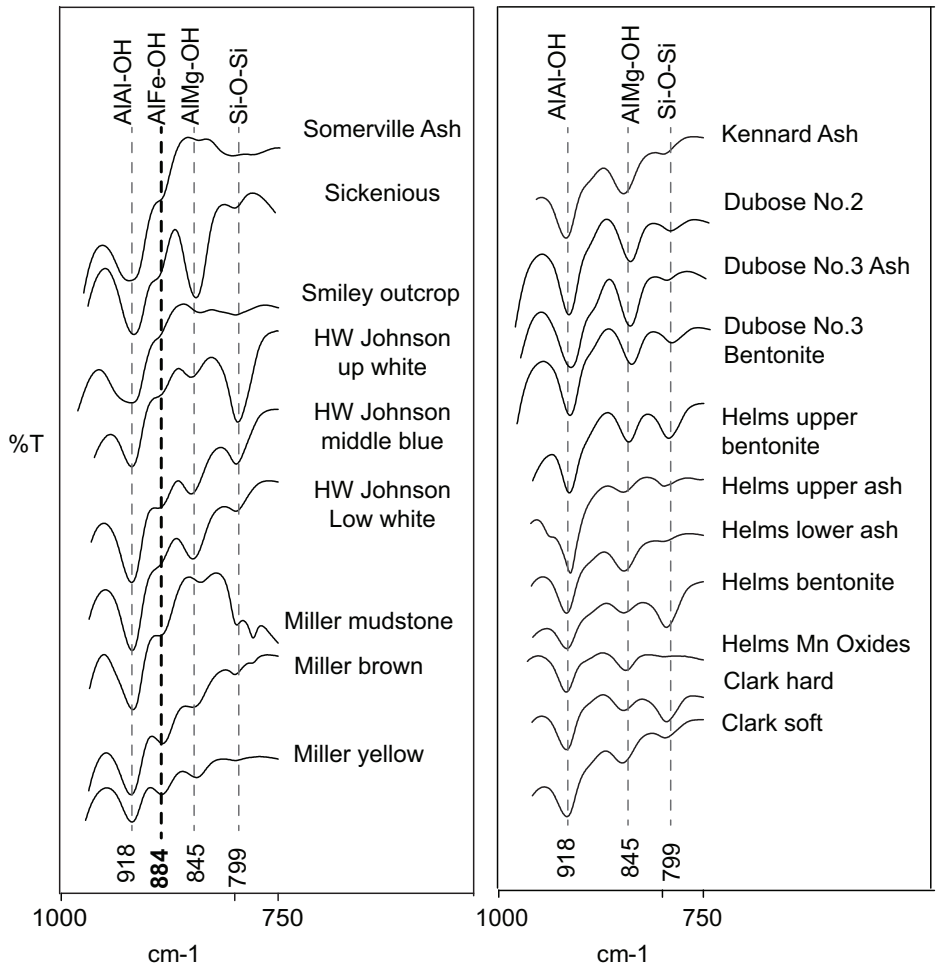

Figure 4.27: FTIR spectra of clay fractions of bentonites showing only the OH-bending region (1000 - 750 cm^{-1}). Left: the montmorillonite samples with Fe^{3+} in the octahedral sheet, and right: the smectite samples without Fe^{3+} in the octahedral sheet.

4.4 Discussion

The major mineralogical differences among the bentonites were in the sand and silt composition. Michaelides (2011) suggested that for the Miller deposit the mudstone above the clay layers was a probable source of Fe during the bentonite formation. The mudstone and brown clay in the Miller deposit were similar in their min-

eralogy. Compared with bentonites from other deposits, the bentonites in the Miller pit contain more quartz, feldspar, mica, and kaolinite due to mixing with outside sediment. The yellow clay sample has the highest clay content. The brown/yellow color of the bentonites in this deposit was due to the presence of iron oxides. The homogeneous distribution of bentonite with the iron oxides may indicate a reworked material. In contrast, iron oxides precipitation on Helms and HWJ deposits occur as layers or well localized nodules indicating precipitation after bentonite formation.

The color difference between white and blue clays was due to the presence of pyrite in the blue samples. The presence of opal-cristobalite was the main difference in the clay fraction of the central deposits, which indicates a poor drainage system when the bentonite formed. In the Helms deposit, opal-cristobalite was concentrated in the bentonite layer but was absent in the upper ash. Halloysite occurs in the upper volcanic ash but not in the lower ash layer, suggesting an environment with insufficient Mg to form smectites. Similar trend was observed in the Clark deposit where the difference between soft and hard clays correlates to the amount of opal.

The accumulation of massive pockets of Mn-oxides in the lower bentonite layer of the Helms deposit suggested crystallization after bentonite formation. The manganese oxide pockets precipitated and crystallized caused a bending of the bentonite bed (as shown in Figure 4.17). Birnessite and rancieite both have a layer structure but Ca is not exchangeable in ranceite. Todorokite is a tectomanganate and can form from the alteration of birnessite.

In the HW Johnson pit the upper white clay layer was dominantly smectite and opal-cristobalite with minor amounts of quartz and feldspar. The middle blue layer composition is similar to the upper white bentonite but pyrite was also present. Opal-cristobalite occurs in the lower white clay layer, but clinoptilolite was present in the silt fraction. These mineralogy differences in the same bentonite pit suggest

local hydrology-controlled variation in diagenesis.

The volcanic ashes are rhyolitic and had similar chemical composition. Similar chemical composition of the ash samples from Helms, Kennard, and Smiley outcrop indicates a similar volcanic ash source but possible different ash fall events. The lack of Fe in the glass shards observed in the silt fraction of the Smiley outcrop suggested that depositional environment or the local hydrology were the sources of Fe available during the formation of the smectite.

Roberson (1964) indicated the dioctahedral composition of the smectites in the Texas bentonites based on the mineralogical characterization of 50 bentonitic samples that showed the characteristic d060-value from 1.49 to 1.50 Å. The present FTIR analysis further demonstrated the Al dominance with substitution for Mg and Fe characteristic of montmorillonites. The major difference observed among the montmorillonites was the presence of structural Fe. The lack of Fe in the ash samples collected, based on the EDS analysis, indicate that the depositional environment was the source.

4.4.1 Selection of bentonites with high aflatoxin adsorption

The mineralogical composition in bentonites is dominated by smectite. Montmorillonite is the smectite clay mineral that can adsorb aflatoxin (Kannewischer et al., 2006). The efficiency of an aflatoxin binder strongly depends on the amount of smectite present in the bentonite. The Texas bentonite samples had a mineralogical composition dominated by smectite. The major mineralogical differences between the bentonite samples of the Gonzales County, Miller deposit and the Sickenious site were the non-adsorbing minerals such as quartz, feldspars, opal-CT, pyrite, and kaolinite. The Somerville ash samples contained abundant kaolinite and gypsum. The presence of these non-absorbing minerals diluted the smectite content.

Barrientos Velazquez (2011) reported the aflatoxin efficiency of two bentonites from the Gonzales County deposits. The poultry experiment showed higher body weight in the aflatoxin-feed amended with a yellow clay (Miller deposit) than with a blue clay (Kennard deposit). The difference was partially attributed to the mineralogical composition. Both samples contained smectite, but the yellow clay had 87% clay content and the blue clay had 65% clay. Depending on the smectite content the ratio of bentonite:feed should be adjusted to account for the dilution effect. The presence of minerals such as pyrite can be associated with heavy metals and may raise concerns of its effect on animal health.

The octahedral structural composition indicated some isomorphic substitutions of Al by Mg, indicating a high layer charge density in some montmorillonite samples that may reduce the aflatoxin adsorption effectiveness. The presence of octahedral Fe in some montmorillonite samples has negligible effect on their aflatoxin adsorption. The majority of the Texas bentonites samples collected are potentially good aflatoxin adsorbents due to the dioctahedral charge origin smectites present and the moderate content of Mg in the octahedral sheet.

4.5 Conclusions

The volcanic ashes are rhyolitic and had similar chemical composition of the ash in central deposits (Helms , Kennard, Smiley Outcrop). The mineralogy differences in the deposits and the strata of the same deposit suggested that local hydrology control genesis and had determinative roles in the mineralogical and chemical compositions of the deposits and the structural cation compositions of the smectites in the deposits.

Ash to bentonite transformation rate, occurrence of redox sensitive minerals either as dispersed phases in the matrix or as coatings were affected by the local hydrology, which in turn, might have been determined by the landscape and the

permeability of both overlaying and underneath materials.

High smectite content and moderate layer charge density can be used as screening properties for bentonites as aflatoxin binders.

5. CONCLUSIONS

Over the past 20 years many strategies to prevent, decontaminate, or detoxify aflatoxin contaminated food commodities have been developed. The occurrence of aflatoxin seems unavoidable despite the numerous research on the prevention of mycotoxin contamination in crops. The use of aflatoxin contaminated feed above the regulatory levels for human consumption (< 20 ppb) have shown to affect the productivity of animals exposed. Incorporation of aflatoxin binding products into the feed have shown to effectively protect the animals from aflatoxicosis without altering the nutritional feed's value or affecting animal health. Most research has been focused on the use of bentonites as aflatoxin adsorbents. The clay mineral montmorillonite is the reactive mineral that can adsorb large amounts of aflatoxin in its interlayer structure.

Numerous studies have addressed the in vivo and in vitro aflatoxin adsorption capacity of montmorillonite. High variability has been observed among bentonite samples. The variation on the aflatoxin adsorption by bentonites can be attributed to the physical and chemical properties of the binders and to the complexity of the solution where adsorption occurs.

Aflatoxin adsorption can be reduced in acidic conditions, but the adsorption capacity for aflatoxin in simulated gastric fluid can still be significant. The lower aflatoxin adsorption in simulated gastric fluid was due to competition from biological compounds (pepsin) with aflatoxin for adsorption sites. Smectite showed high affinity and adsorption for vitamin B1 in the simplified solution. The adsorption of vitamin B1 by smectite in animal experiments has not been reported in literature and future animal trials should address any vitamin deficiency produced by the adsorption of the

binders. Future studies are also requested to minimize the interference of biological compounds with aflatoxin molecules for adsorption sites.

The exchangeable cation strongly influenced the adsorption capacity of smectite in a simplified solution but this effect was not observed in the simulated gastrointestinal fluid due to the replacement of the cations by pepsin.

Montmorillonite is the most common used smectite clay mineral in all reported batch adsorption isotherms and animal experiments. Hectorite was also effective as an aflatoxin binder. Charge origin appeared to have less influence in the adsorption capacity but optimal CEC values might depend on the charge origin. The charge density had the greatest effect on aflatoxin adsorption, and high charged clays could be improved by reducing the CEC.

Detailed mineralogical and chemical characterization of aflatoxin binders is usually not reported for the binders used in animal trials. Animal experiments should be conducted to corroborate the effect of layer charge on aflatoxin adsorption in complex gastrointestinal fluids.

REFERENCES

Abdel-Wahhab, M. A., Nada, S. A., and Amra, H. A. (1999). Effect of aluminosilicates and bentonite on aflatoxin-induced developmental toxicity in rat. *J. Appl. Toxicol.*, 19(3):199–204.

Afriyie-Gyawu, E. (2004). *Safety and efficacy of NovaSil clay as a dietary supplement to prevent aflatoxicosis*. PhD thesis, Texas A&M University.

Aggarwal, V., Li, H., and Teppen, B. J. (2006). Triazine adsorption by saponite and beidellite clay minerals. *Environ. Toxicol. Chem*, 25(2):392–399.

Alpsoy, L. and Yalvac, M. (2011). Key roles of vitamins A, C, and E in aflatoxin B1-induced oxidative stress. *Vitam. Horm.*, 86:287 – 305.

Armstrong, D. E. and Chesters, G. (1964). Properties of protein-bentonite complexes as influenced by equilibrium conditions. *Soil Sci.*, 98(1):39–52.

Bailey, C. A., Latimer, G. W., Barr, A. C., Wigle, W. L., Haq, A. U., Balthrop, J. E., and Kubena, L. F. (2006). Efficacy of montmorillonite clay (NovaSil PLUS) for protecting full-term broilers from aflatoxicosis. *J. Appl. Poultry Res.*, 15(2):198–206.

Bailey, G. S. (1994). Role of Aflatoxin-DNA Adducts in the Cancer Process. In Eaton, D. L. and Goopman, J. D., editors, *The Toxicology of Aflatoxins Human Health, Veterinary, and Agricultural Significance*. Academic Press, Inc., San Diego.

Bailey, R., Kubena, L., Harvey, R., Buckley, S., and Rottinghaus, G. (1998). Efficacy of various inorganic sorbents to reduce the toxicity of aflatoxin and T-2 toxin in broiler chickens. *Poultry Sci.*, 77(11):1623–1630.

Barrientos Velazquez, A. L. (2011). Texas bentonites as amendments of aflatoxin-contaminated poultry feed. Master's thesis, Texas A&M University, College Sta-

tion.

Bbosa, G. S., Kitya, D., Odda, J., and Ogwal-Okeng, J. (2013). Aflatoxins metabolism, effects on epigenetic mechanisms and their role in carcinogenesis. *Health*, 5(10):21.

Bhattacharya, R. K., Francis, A. R., and Shetty, T. K. (1987). Modifying role of dietary factors on the mutagenicity of aflatoxin B1: In vitro effect of vitamins. *Mutat. Res.*, 188(2):121–128.

Bojemueller, E., Nennemann, A., and Lagaly, G. (2001). Enhanced pesticide adsorption by thermally modified bentonites. *Applied Clay Science*, 18(56):277–284.

Chen, P.-Y. (1968). *Geology and mineralogy of the white bentonite beds of Gonzales County, Texas*. PhD thesis, University of Texas.

Christidis, G. E. and Huff, W. D. (2009). Geological aspects and genesis of bentonites. *Elements*, 5(2):93–98.

Chung, T. K., Erdman, J. W., J., and Baker, D. H. (1990). Hydrated sodium calcium aluminosilicate: effects on zinc, manganese, vitamin A and riboflavin utilization. *Poultry Sci.*, 69(8):1364–1370.

Dakovic, A., Kragovic, M., Rottinghaus, G. E., Ledoux, D. R., Butkeraitis, P., Vojislavljevic, D. Z., Zaric, S. D., and Stamenic, L. (2012). Preparation and characterization of zinc-exchanged montmorillonite and its effectiveness as aflatoxin B1 adsorbent. *Materials Chemistry and Physics*, 137(1):213–220.

Dakovic, A., Matijasevic, S., Rottinghaus, G. E., Ledoux, D. R., Butkeraitis, P., and Sekulic, Z. (2008). Aflatoxin B1 adsorption by natural and copper modified montmorillonite. *Colloids Surf., B*, 66(1):20–25.

Deng, Y., Barrientos Velazquez, A. L., Billes, F., and Dixon, J. B. (2010). Bonding mechanisms between aflatoxin B1 and smectite. *Appl. Clay Sci.*, 50(1):92–98.

Deng, Y., Dixon, J. B., and White, G. N. (2006). Adsorption of polyacrylamide on

smectite, illite, and kaolinite. *Soil Sci. Soc. Am. J.*, 70(1):297–304.

Deng, Y., Liu, L., Barrientos Velazquez, A. L., and Dixon, J. B. (2012). The determinative role of the exchange cation and layer-charge density of smectite on aflatoxin adsorption. *Clays Clay Miner.*, 60(4):374–386.

Deng, Y. and Szczerba, M. (2011). Computational evaluation of bonding between aflatoxin B1 and smectite. *Appl. Clay Sci.*, 54(1):26–33.

Deng, Y., White, G. N., and Dixon, J. B. (2009). *Soil mineralogy laboratory manual*.

Dixon, J. B., Kannewischer, I., Tenorio Arvide, M. G., and Barrientos Velazquez, A. L. (2008). Aflatoxin sequestration in animal feeds by quality-labeled smectite clays: an introductory plan. *Appl. Clay Sci.*, 40:201–208.

Eaton, D. L., Ramsdell, H. S., and Neal, G. E. (1994). Biotransformation of aflatoxins. In Eaton, D. L. and Groopman, J. D., editors, *The Toxicology of Aflatoxins: Human Health, Veterinary, and Agricultural Significance*. ACADEMIC PRESS, INC, San Diego.

EFSA (2010). Scientific opinion on the safety and efficacy of bentonite as a technological feed additive for all species. *EFSA J.*, 10(7):2787.

EFSA (2011). Scientific opinion on the safety and efficacy of bentonite (dioctahedral montmorillonite) as feed additive for all species. *EFSA J.*, 9(2):2007.

Eisenhour, D. D. and Brown, R. K. (2009). Bentonite and its impact on modern life. *Elements*, 5(2):83–88.

Ensminger, L. E. and Gieseking, J. E. (1941). The adsorption of proteins by montmorillonitic clays and its effect on base-exchange capacity. *Soil Sci.*, 51:125–132.

Fowler, J., Li, W., and Bailey, C. (2015). Effects of a calcium bentonite clay in diets containing aflatoxin when measuring liver residues of aflatoxin B(1) in starter broiler chicks. *Toxins*, 7(9):3455–64. Using Smart Source Parsing 2015 Aug 26; doi: 10.3390/toxins7093455.

Gates, W. (2005). *Infrared spectroscopy and the chemistry of dioctahedral smectites*, pages 125–168. The Clay Minerals Society, Aurora, CO.

Grant, P. G., Lemke, S. L., Dwyer, M. R., and Phillips, T. D. (1998). Modified Langmuir equation for S-shaped and multisite isotherm. *Langmuir*, 14(15):4292–4299.

Grant, P. G. and Phillips, T. D. (1998). Isothermal adsorption of aflatoxin B1 on HSCAS clay. *Journal of Agricultural and Food Chemistry*, 46(2):599–605.

Grim, E. R. and Guven, N. (1978). *Bentonites: Geology, mineralogy, properties and uses*, volume Volume 24 of *Developments in Sedimentology*. Elsevier.

Harter, R. D. and Stotzky, G. (1971). Formation of clay-protein complexes. *Soil Sci. Soc. Am. J.*, 35(3):383–389.

Heathcote, J. and Hibbert, J. (1978). *Aflatoxins: chemical and biological aspects.*, volume 1 of *Developments in food science*. Elsevier, Amsterdam.

Heintz, M. L., Yancey, T. E., Miller, B. V., and Heizler, M. T. (2014). Tephrochronology and geochemistry of eocene and oligocene volcanic ashes of east and central Texas. *Geological Society of America Bulletin*.

Hendricks, J. D. (1994). Carcinogenicity of aflatoxins in nonmammalian organism. In Eaton, D. L. and Groopman, J. D., editors, *The Toxicology of Aflatoxins: Human Health, Veterinary, and Agricultural Significance*. ACADEMIC PRESS, INC, San Diego.

Hussein, H. S. and Brasel, J. M. (2001). Toxicity, metabolism, and impact of mycotoxins on humans and animals. *Toxicology*, 167(2):101–134.

Huwig, A., Freimund, S., Kppeli, O., and Dutler, H. (2001). Mycotoxin detoxication of animal feed by different adsorbents. *Toxicol. Lett.*, 122(2):179–188.

IARC (2002). Iarc monographs on the evaluation of carcinogenic risk to humans. Technical report, World Health Organization.

Iheshiulor, O., Esonu, B., O.K., C., A.A., O., Okoli, I., and Ogbuewu, I. (2011). Effects of mycotoxins in animal nutrition: A review. *Asian J. Anim. Sci.*, 5:19–33.

Iliadis, G., Zundel, G., and Brzezinski, B. (1994). Aspartic proteinases Fourier transform IR studies of the aspartic carboxylic groups in the active site of pepsin. *FEBS Lett.*, 352(3):315–317.

Ishida, H., Campbell, S., and Blackwell, J. (2000). General approach to nanocomposite preparation. *Chem. Mater*, 12(5):1260–1267.

Jaynes, W. F. and Bigham, J. M. (1987). Charge reduction, octahedral charge, and lithium retention in heated, li-saturated smectites. *Clays Clay Miner.*, 35(6):440–448.

Jaynes, W. F. and Zartman, R. E. (2011). Influence of soluble feed proteins and clay additive charge density on aflatoxin binding in ingested feeds. In G., G.-G. R., editor, *Aflatoxins - Biochemistry and Molecular Biology*. InTech.

Johnston, C. T., Boyd, S. A., Teppen, B. J., and Guangyao, S. (2004). Sorption of nitroaromatic compounds on clay surfaces. In Auerbach, S. M., Carrado, K. A., and Dutta, P. K., editors, *Handbook of Layared Materials*. Marcel Dekker, Inc., New York.

Joshi, G. V., Patel, H. A., Kevadiya, B. D., and Bajaj, H. C. (2009). Montmorillonite intercalated with vitamin B1 as drug carrier. *Appl. Clay Sci.*, 45(4):248–253.

Kannewischer, I., Arvide, M. G. T., White, G. N., and Dixon, J. B. (2006). Smectite clays as adsorbents of aflatoxin B1: initial steps. *Clay Sci.*, 12(Supplement 2):199–204.

Komadel, P. (2003). Chemically modified smectites. *Clay Minerals*, 38(1):127–138.

Laird, D. A., Barriuso, E., Dowdy, R. H., and Koskinen, W. C. (1992). Adsorption of atrazine on smectites. *Soil Sci. Soc. Am. J.*, 56(1):62–67.

Lemke, S. L. (2000). *Investigation of clay-based strategies for the protection of ani-*

mals from the toxic effects of selected mycotoxins. PhD thesis.

Lemke, S. L., Ottinger, S. E., Mayura, K., Ake, C. L., Pimpukdee, K., Wang, N., and Phillips, T. D. (2001). Development of a multi-tiered approach to the in vitro prescreening of clay-based enterosorbents. *Anim. Feed Sci.Tech*, 93(1-2):17–29.

Li, J., Suo, D., and Su, X. (2010). Binding capacity for aflatoxin B1 by different adsorbents. *Agric. Sci. China*, 9(3):449–456.

Lian, L. (2013). Determinative role of exchange cation and charge density of smectite on their adsorption capacity and affinity for aflatoxin B1. Master's thesis, Texas A&M University, College Station.

Lim, C. H. and Jackson, M. L. (1986). Expandable phyllosilicate reactions with lithium on heating. *Clays Clay Miner.*, 34(3):346–352.

Lindemann, M. D., Blodgett, D. J., Kornegay, E. T., and Schurig, G. G. (1993). Potential ameliorators of aflatoxicosis in weanling growing swine. *J. Anim. Sci.*, 71(1):171–178.

Liu, C., Li, H., Johnston, C. T., Boyd, S. A., and Teppen, B. J. (2012). Relating clay structural factors to dioxin adsorption by smectites: Molecular dynamics simulations. *Soil Sci. Soc. Am. J.*, 76(1):110–120.

Madejová, J. (2003). FTIR techniques in clay mineral studies. *Vib. Spectrosc.*, 31(1):1–10.

Madejová, J., Bujdák, J., Petit, S., and Komadel, P. (2000). Effects of chemical composition and temperature of heating on the infrared spectra of Li-saturated dioctahedral smectites. (I) Mid-infrared region. *Clay Minerals*, 35(5):739–751.

Magnoli, A. P., Alonso, V. A., Cavaglieri, L. R., Dalcero, A. M., and Chiacchiera, S. M. (2011a). Effect of monogastric and ruminant gastrointestinal conditions on in vitro aflatoxin B1 adsorption ability by a montmorillonite. *Food Addit. Contam. A*, 30(4):743–9.

Magnoli, A. P., Cavaglieri, L. R., Magnoli, C. E., Monge, J. C., Miazzo, R. D., Peralta, M. F., Salvano, M. A., Da Rocha Rosa, C. A., Dalcero, A. M., and Chiacchiera, S. M. (2008a). Bentonite performance on broiler chickens fed with diets containing natural levels of aflatoxin B1. *Rev. Bras. Med. Vet*, 30(1):55–60.

Magnoli, A. P., Monge, M. P., Miazzo, R. D., Cavaglieri, L. R., Magnoli, C. E., Merkis, C. I., Cristofolini, A. L., Dalcero, A. M., and Chiacchiera, S. M. (2011b). Effect of low levels of aflatoxin B1 on performance, biochemical parameters, and aflatoxin B1 in broiler liver tissues in the presence of monensin and sodium bentonite. *Poultry Science*, 90(1):48–58.

Magnoli, A. P., Tallone, L., Rosa, C. A. R., Dalcero, A. M., Chiacchiera, S. M., and Torres Sanchez, R. M. (2008b). Commercial bentonites as detoxifier of broiler feed contaminated with aflatoxin. *Appl. Clay Sci.*, 40(1-4):63–71.

Maurice, D. V., Bodine, A. B., and Rehrer, N. J. (1983). Metabolic effects of low aflatoxin B1 levels on broiler chicks. *Appl. Environ. Microbiology*, 43(3):980–984.

McLaren, A. D., Peterson, G. H., and Barshad, I. (1958). The adsorption and reactions of enzymes and proteins on clay minerals: IV. Kaolinite and montmorillonite. *Soil Sci. Soc. Am. J.*, 22(3):239–244.

Michaelides, M. N. (2011). *Depositional and diagenetic processes in the formation of the Eocene Jackson Group bentonites, Gonzales County, Texas*. PhD thesis.

Mortland, M. and Lawless, J. (1983). Smectite interactions with riboflavin. *Clays Clay Miner.*, 31:435–439.

Mulder, I., Barrientos Velazquez, A. L., Tenorio Arvide, M. G., White, G. N., and Dixon, J. B. (2008). Smectite clay sequestration of aflatoxin B1: mineral dispersivity and morphology. *Clays Clay Miner.*, 56:559–571.

Nones, J., Nones, J., Riella, H. G., Poli, A., Trentin, A. G., and Kuhnen, N. C. (2015). Thermal treatment of bentonite reduces aflatoxin b1 adsorption and affects stem

cell death. *Mater. Sci. Eng., C*, 55:530–537.

Pappas, A. C., Tsiplakou, E., Georgiadou, M., Anagnostopoulos, C., Markoglou, A. N., Liapis, K., and Zervas, G. (2014). Bentonite binders in the presence of mycotoxins: Results of in vitro preliminary tests and an in vivo broiler trial. *Appl. Clay Sci.*, 99:48–53.

Pasha, T. N., Farooq, M. U., Khattak, F. M., Jabbar, M. A., and Khan, A. D. (2007). Effectiveness of sodium bentonite and two commercial products as aflatoxin absorbents in diets for broiler chickens. *Anim. Feed Sci. Tech.*, 132(1-2):103–110.

Phillips, T. D., Afriyie-Gyawu, E., Williams, J., Huebner, H., Ankrah, N. A., Ofori-Adjei, D., Jolly, P., Johnson, N., Taylor, J., Marroquin-Cardona, A., Xu, L., Tang, L., and Wang, J. S. (2008). Reducing human exposure to aflatoxin through the use of clay: a review. *Food Additives and Contaminants, Part A: Chemistry, Analysis, Control, Exposure and Risk Assessment*, 25(2):134–145.

Phillips, T. D., Kubena, L. F., Harvey, R. B., Taylor, D. R., and Heidelbaugh, N. D. (1988). Hydrated sodium calcium aluminosilicate: a high affinity sorbent for aflatoxin. *Poultry Sci.*, 67:243–247.

Phillips, T. D., Sarr, A. B., and Grant, P. G. (1995). Selective chemisorption and detoxification of aflatoxins by phyllosilicate clay. *Nat. Toxins*, 3:204–213.

Pimpukdee, K., Kubena, L. F., Bailey, C. A., Huebner, H. J., Afriyie-Gyawu, E., and Phillips, T. D. (2004). Aflatoxin-induced toxicity and depletion of hepatic vitamin A in young broiler chicks: protection of chicks in the presence of low levels of NovaSil PLUS in the diet. *Poultry Sci.*, 83(5):737–744.

Reid-Soukup, D. A. and Ulery, A. L. (2002). Chapter 15 smectites. In Dixon, J. B. and Schulze, D. G., editors, *Soil mineralogy with environmental applications*, Soil Science Society of America book series; no. 7, pages 467– 495. Soil Science Society of America, Madison, WI.

Roberson, H. E. (1964). Petrology of Tertiary bentonites of Texas. *Journal of Sedimentary Research*, 34(2):401–411.

Rosa, C., Miazzo, R., Magnoli, C., Salvano, M., Chiacchiera, S., Ferrero, S., Saenz, M., Carvalho, E., and Dalcero, A. (2001). Evaluation of the efficacy of bentonite from the south of Argentina to ameliorate the toxic effects of aflatoxin in broilers. *Poultry Sci.*, 80(2):139–144.

Schmidhalter, U., Evéquoz, M., Studer, C., Oertli, J. J., and Kahr, G. (1994). Adsorption of Thiamin (Vitamin B1) on soils and clays. *Soil Sci. Soc. Am. J.*, 58(6):1829–1837.

Seifert, L. E., Davis, J. P., Dorner, J. W., Jaynes, W. F., Zartman, R. E., and Sanders, T. H. (2010). Value-added processing of peanut meal: Aflatoxin sequestration during protein extraction. *J. Agric. Food Chem.*, 58(9):5625–5632. doi: 10.1021/jf9045304.

Sepelyak, R. J., Feldkamp, J. R., Moody, T. E., White, J. L., and Hem, S. L. (1984a). Adsorption of pepsin by aluminum hydroxide I: Adsorption mechanism. *J. Pharm. Sci.*, 73(11):1514–1517.

Sepelyak, R. J., Feldkamp, J. R., Regnier, F. E., White, J. L., and Hem, S. L. (1984b). Adsorption of pepsin by aluminum hydroxide II: Pepsin inactivation. *J. Pharm. Sci.*, 73(11):1517–1522.

Shi, Y. H., Xu, Z. R., Feng, J. L., and Wang, C. Z. (2006). Efficacy of modified montmorillonite nanocomposite to reduce the toxicity of aflatoxin in broiler chicks. *Anim. Feed Sci. Tech.*, 129(1-2):138–148.

Shi, Y. H., Xu, Z. R., Feng, J. L., Xia, M. S., and Hu, C. H. (2005). Effects of modified montmorillonite nanocomposite on growing/finishing pigs during aflatoxicosis. *Asian Australas. J. Anim. Sci*, 18(9):1305–1309.

Spotti, M., Fracchiolla, M. L., Arioli, F., Caloni, F., and Pompa, G. (2005). Aflatoxin

B_1 binding to sorbents in bovine ruminal fluid. *Vet. Res. Commun.*, 29(6):507–515.

Swanson, E. R., Kempter, K. A., McDowell, F. W., and McIntosh, W. C. (2006). Major ignimbrites and volcanic centers of the Copper Canyon area: A view into the core of Mexico's Sierra Madre Occidental. *Geosphere*, 2(3):125–141.

Talibudeen, O. (1955). Complex formation between montmorillonoid clays and amino-acids and proteins. *Trans. Faraday Soc.*, 51:582–590.

Tenorio Arvide, M. G., Mulder, I., Barrientos Velazquez, A. L., and Dixon, J. B. (2008). Smectite sorption of aflatoxin b1 and molecular changes suggested by FTIR. *Clays Clay Miner.*, 56:572–579.

Theng, B. K. G. (1974). *The Chemistry of Clay-Organic Reactions*. John Wiley and Sons, New York.

Thieu, N. and Pettersson, H. (2008). Evaluation of the capacity of zeolite and bentonite to adsorb aflatoxin in simulated gastrointestinal fluids. *Mycotoxin Res.*, 24(3):124–129.

Tomasevic-Canovic, M., Dakovic, A., Markovic, V., and Stojsic, D. (2001). The effect of exchangeable cations in clinoptilolite and montmorillonite on the adsorption of aflatoxin B1. *J. Serb. Chem. Soc.*, 66(8):555–561.

van der Marel, H. and Beutelspacher, H. (1976). *Atlas of infrared spectroscopy of clay minerals and their admixtures.* Elsevier, Amsterdam.

Vekiru, E., Fruhauf, S., Rodrigues, I., Ottner, F., Krska, R., Schatzmayr, G., Ledoux, D., Rottinghaus, G., and Bermudez, A. (2015). In vitro binding assessment and in vivo efficacy of several adsorbents against aflatoxin B1. *World Mycotoxin J., in press*, 0(aop):1–12.

Vekiru, E., Fruhauf, S., Sahin, M., Ottner, F., Schatzmayr, G., and Krska, R. (2007). Investigation of various adsorbents for their ability to bind aflatoxin B1. *Mycotoxin Res.*, 23(1):27–33.

Wan, X. L., Yang, Z. B., Yang, W. R., Jiang, S. Z., Zhang, G. G., Johnston, S. L., and Chi, F. (2013). Toxicity of increasing aflatoxin B1 concentrations from contaminated corn with or without clay adsorbent supplementation in ducklings. *Poultry Sci.*, 92(5):1244–1253.

Wilson, M. J. (2013). *Sheet Silicates: Clay Minerals*, volume 3C of *Rock-Forming minerals*. The Geological Society, London.

Yancey, T. E. and Guillemette, R. (1998). Major volcanic ash units in the late Eocene of East Texas. *Gulf Coast Association of Geological Societies Transactions*, 48:511–516.

APPENDIX A

MINERALOGICAL AND CHEMICAL CHARACTERIZATION SMECTITES

A.1 Fractionation

The pH of the samples was obtained from the unfractionated material using a water:sample ratio of 5:1. Hectorite and Spain saponite showed high pH due to the presence of calcite in the samples as indicated on the XRD patterns. Hectorite showed strong reaction to HCl and Spain saponite showed a moderate reaction. The sand, silt, and clay fractions were obtained from about 0.5 g of each smectite sample. Sand particles were not collected from beidellite and hectorite. All the samples showed more than 70% clay content (Table 3.2).

Table A.1: Characterization of smectite samples.

Sample	pH	fraction (%)		
		sand	silt	clay
Beidellite	5.53	-	23.5	76.44
Hectorite	9.13	-	4.21	95.48
Nontronite	5.57	17.75	8.88	73.35
Australia saponite	7.45	1.19	14.51	85.41
Spain saponite	9.82	12.65	15.27	72.06

A.2 SEM images of clay particles

Scanning electron images were recorded for the clay fraction after dialysis. In the beidellite sample, multiple fringes were observed (Figure A.3a). The d-values obtained from the fringes were 0.348 nm and 0.22 nm which correspond to kaolinite. The SEAD also suggested the presence of kaolinite as the diffraction showed crystalline phases. The beidellite clay particles showed the characteristic thin platy morphology typical of smectite (Figure A.3b), along with the diffuse ring patterns on the SAED.

As indicated on the XRD patterns, mica was present in hectorite. Figure A.4a shows a mica particle surrounded by thin hectorite particles. The SEAD pattern showed two diffraction rings due to the presence of these two minerals. The difference on the Al content between particle a and b was due to the presence of mica in particle a. Particle b was dominated by Mg, and the morphology showed typical platy particle with folding at the edges.

Numerous globular particles were observed in nontronite. At high magnification, fringes were visible and the values may correspond to iron oxides (Figure A.5).

Diverse particles were observed in Australia saponite(Figure A.6). The tubular morphology is characteristic of halloysite. In particle 3, the chemical composition indicates presence of K indicating a mica particle.

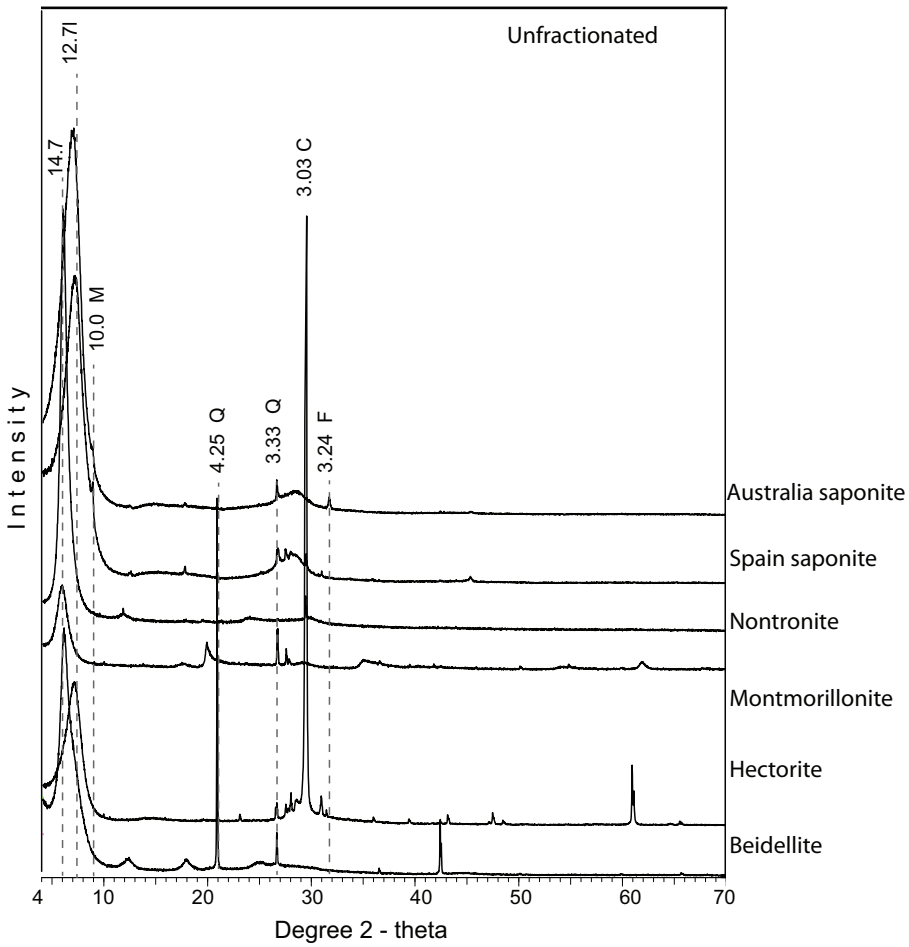

Figure A.1: X-ray diffraction patterns of the unfractionated smectite samples. M:mica, Q: quartz, F: feldspars, C: calcite.

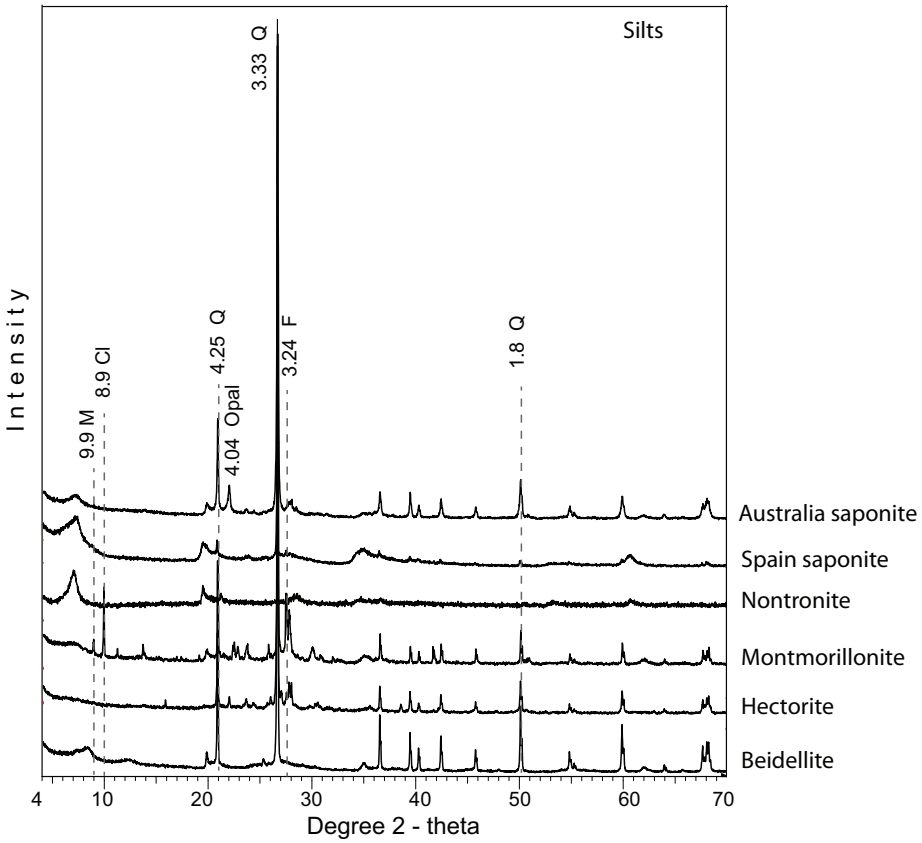

Figure A.2: X-ray diffraction patterns of the silt fractions of the smectite samples. M:mica, Q: quartz, Cl: clinoptilolite, F: feldspars.

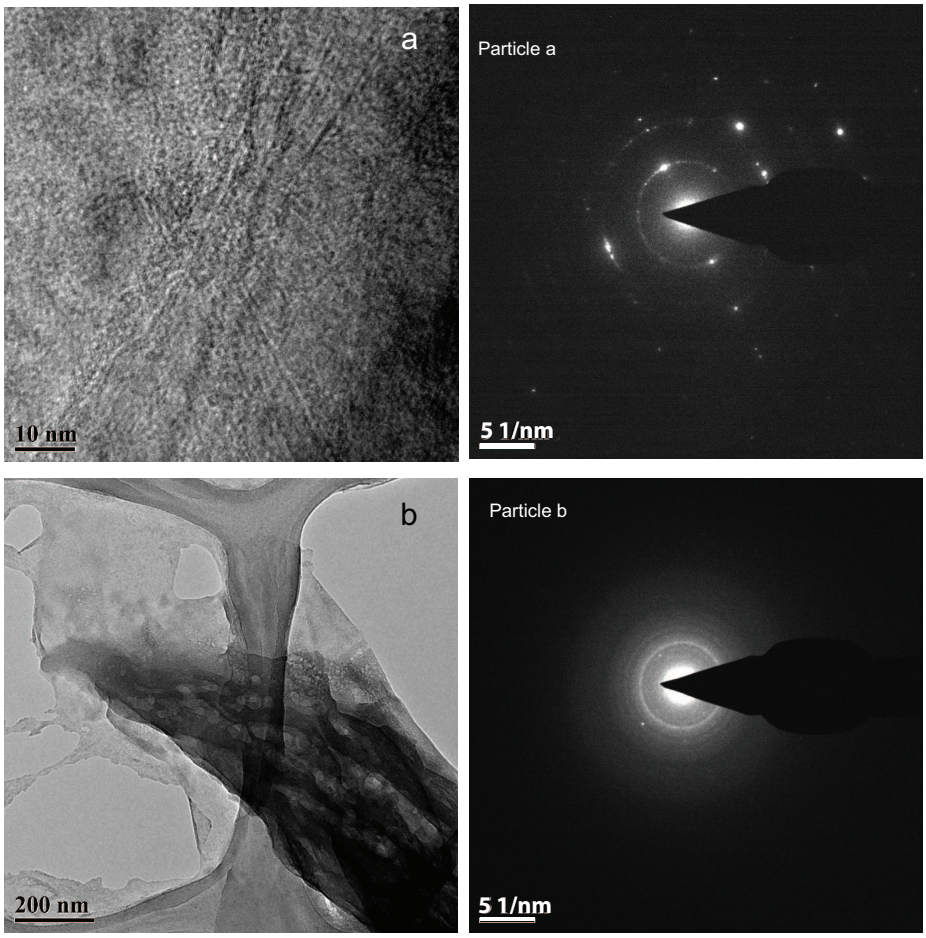

Figure A.3: TEM images of clay particles in beidellite sample with their respective SAED patterns on the left.

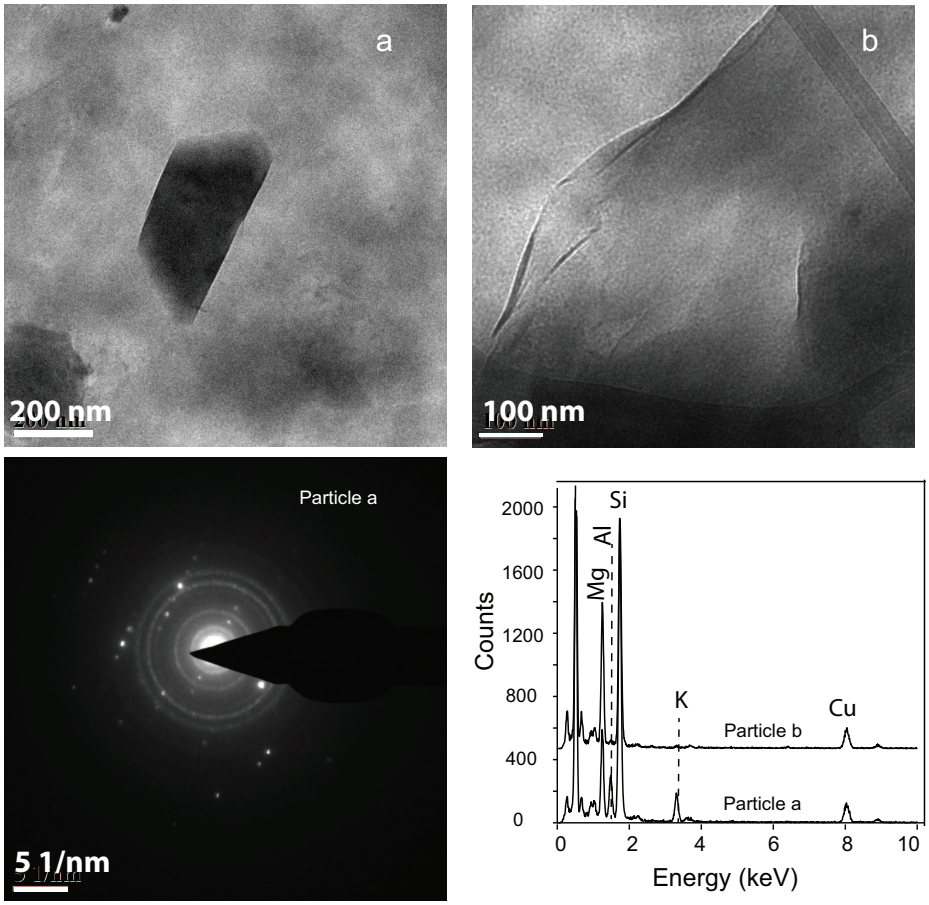

Figure A.4: TEM images of clay particles in hectorite sample with the respective EDS patterns. The SAED patterns corresponds to particle (a).

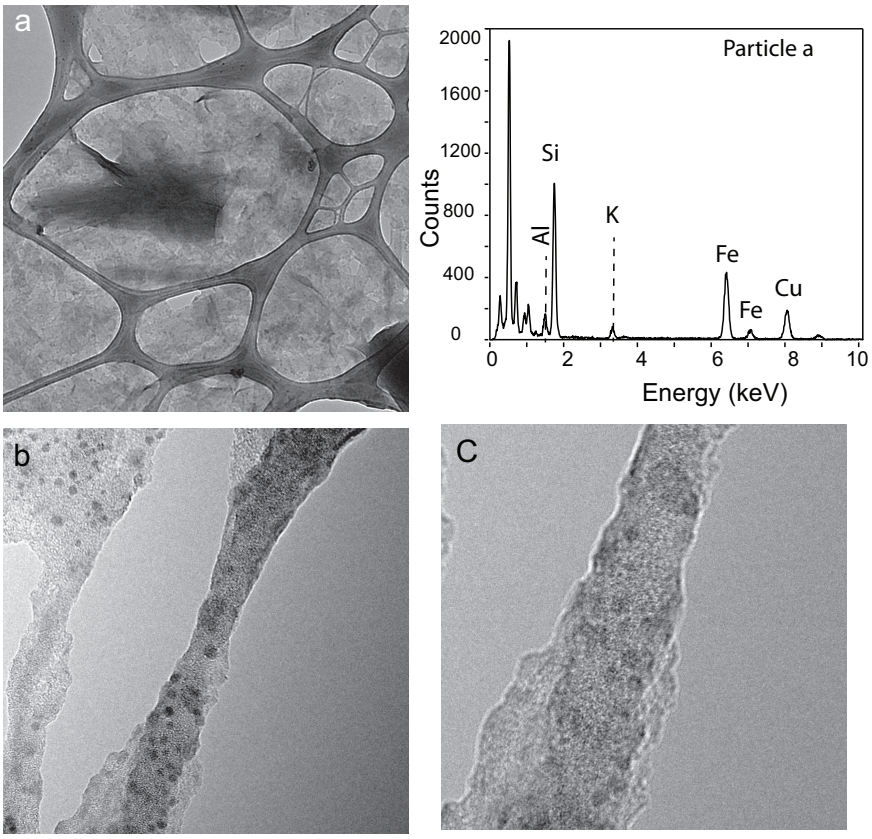

Figure A.5: TEM images of clay particles in nontronite sample with a EDS pattern of particle (a).

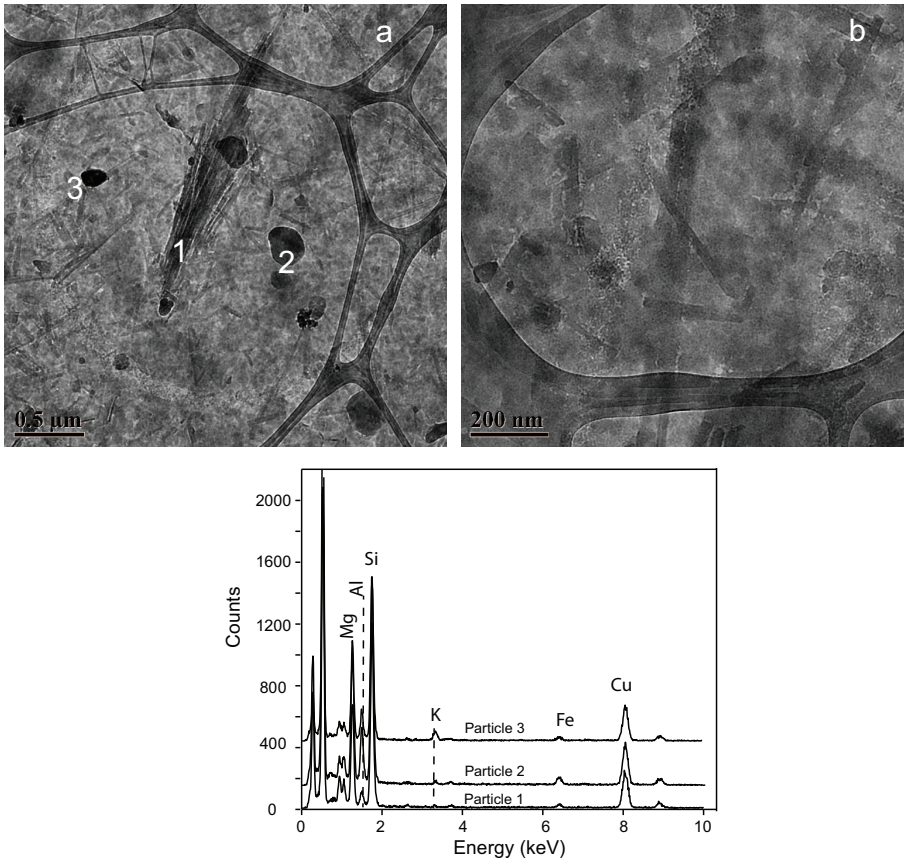

Figure A.6: TEM images of clay particles in Australia saponite sample.

APPENDIX B

ADDITIONAL MINERAL AND CHEMICAL CHARACTERIZATION OF THE TEXAS BENTONITES

The electrical conductivity (EC) and pH were obtained from the unfractionated samples. The d001 values in Table 3.2 are for the powder unfractionated samples.

Table B.1: Characterization of bentonite samples.

Sample	EC (uS)	pH	d001-value Å
Somerville white ash	2686	3.02	15.8
Somerville lower ash	1477	3.03	15.2
Miller mudstone	80.7	6.9	15.3
Miller brown clay	78.8	6.7	15.2
Miller yellow clay	99.6	6.97	15.4
DuBose No.2 Ash	1756	3.99	15.2
DuBose No.2 Bentonite	489	6.81	15.0
DuBose No.3 Upper white	696	4.97	14.7
DuBose No.3 Ash	2048	3.10	14.8
DuBose No.3 Blue Bentonite	762	4.35	14.5
Kennard ash	1606	3.57	14.9
Kennard bentonite	2889	2.92	14.5
Clark hard clay	101.1	5.33	15.0
Clark soft clay	345.4	4.84	14.9
Magdalene Johnson	606	4.56	14.9
Helms upper bentonite	34.8	6.87	14.8
Helms upper ash			15.4
Helms lower ash	508	6.38	15.4
Helms lower bentonite			15.3
HW Johnson upper white	295.8	6.07	15.3
HW Johnson middle blue	657	6.83	15.1
HW Johnson lower white	244.1	6.09	15.1
Smiley outcrop ash	737	5.17	13.3
Smiley outcrop bentonite	130.6	4.96	14.2
Sickenious ash	1935	6.12	15.2

Table B.2: XRF data for the Mn-oxide samples collected from the Helms deposit.

	Wt %												
Sample	Na_2	MgO	Al_2O_3	SiO_2	P_2O_5	S	Cl	K_2O	CaO	TiO_2	MnO_2	Fe_2O_3	BaO
Mn-oxide piles	0.18	1.59	8.54	24.7	0.22	<0.05	0.12	0.59	3.40	0.18	29.1	1.55	1.20
Mn-oxides lower	0.21	1.56	9.96	28.2	0.23	<0.05	<0.02	0.64	1.63	0.19	22.9	2.24	1.82
	ppm												
	V	Cr	Co	Ni	W	Cu	Zn	As	Sn	Pb	Mo	Sr	U
Mn-oxides piles	<100	<50	839	643	100	<50	7470	<50	396	124	101	221	<50
Mn-oxides lower	<100	<50	796	501	183	<50	6740	50	303	57	85	685	73